The Dissertation Committee for Jennie Melinda Baier certifies that this is the approved version of the following dissertation:

Hyaluronic Acid Hydrogel Biomaterials for Soft Tissue Engineering Applications

Committee:

Christine E. Schmidt, Supervisor

George Georgiou, Co-Chair

Rama Akella

Roger T. Bonnecaze

Jennifer L. West

Hyaluronic Acid Hydrogel Biomaterials for Soft Tissue Engineering Applications

by

Jennie Melinda Baier, B.S.ChE.

Dissertation

Presented to the Faculty of the Graduate School of

The University of Texas at Austin

in Partial Fulfillment

of the Requirements

for the Degree of

Doctor of Philosophy

The University of Texas at Austin

August, 2003

Dedication

This dissertation is dedicated to my husband, Tom,

and my extended Baier and Leach families.

Acknowledgements

For their love, wisdom, and never-ending support, I gratefully thank my parents, Kathy and Ken Baier. For being my fellow childhood scientist-engineer and the best brother ever, I thank Ed. For his sense of humor and wholehearted love, I gratefully thank my grandpa, Opa. For their caring support and inspiration for craft breaks, I thank my sister, Jodi, and my home-away-from-home "sisters", Melanie and Beth. For warmly welcoming me into my new family and always making me feel at home, I thank the Leach family. For always reminding me of the importance of family, I thank my Aunt Ginny, Uncle Dick, Sue, Rick, and Steve, and their families. For his corny jokes and help with polymers, I thank Tim. For always being my best friend through it all, I thank Laura.

For her constant reassurance and enthusiastic mentorship, I sincerely thank my dedicated advisor, Christine Schmidt. For their countless influential discussions, I thank my doctoral committee, George Georgiou, Rama Akella, Roger Bonnecaze, and Jennifer West. For his technical insights, generosity, and positive attitude, I am grateful to Charles Patrick. For helpful discussions about the theory and experimental aspects of polymer chemistry, I gratefully acknowledge C.P. Pathak and Brent Iverson. For assistance with histology, I

thank Carol Johnston. For their outstanding encouragement, I thank Jeff Gray, Todd Przybycien, Georges Belfort, and Philippe Lam.

For their vital experimental advice and big-brotherly support, I thank Tyrell and Terry. For their helpful discussions about HA, the coolest biopolymer in the world, I thank Kate and Scott. For her kind and gentle spirit, I thank my "lab mom", Hyma. For their comedic, therapeutic, gastronomic, and sometimes alcoholic relief in and out of the lab, I sincerely thank Archit, Jessica, Curt, Eric, and the rest of the Schmidt and Patrick graduate students. For her logistical help with carrying out experiments at M.D. Anderson, I thank Cindy. For their experimental assistance and their fresh enthusiasm for research, I thank my undergraduate researchers Erik, Gwang-Yi, Nabilla, Kate, and Chelsea. For the countless number of times he patiently helped me with computer issues, I gratefully thank Randy. For help with maneuvering through the UT bureaucracy with a smile, I thank T, Kay, Donna, Joni, Jimmy, EO, EI, Tammy, and Kevin.

For sharing in the blood, sweat, and tears of graduate school, for picking me up when I didn't know the way, for holding my hand, and taking care of my heart, I thank my true inspiration, Tom.

Hyaluronic Acid Hydrogel Biomaterials for Soft Tissue Engineering Applications

Publication No._____

Jennie Melinda Baier, PhD

The University of Texas at Austin, 2003

Supervisors: Christine E. Schmidt and George Georgiou

The primary focus of this work was to develop new naturally derived hydrogel scaffolds for soft tissue engineering applications such as peripheral nerve repair. Ideal implants for soft tissues are degradable, porous, highly permeable, able to maintain a desired shape, and able to specifically modulate biological responses. Naturally derived materials are particularly suitable for these applications because they are degradable and intrinsically bioactive. As presented in this dissertation, we have made significant steps towards meeting these aims by creating new hydrogel scaffolds from crosslinked hyaluronic acid (HA).

As a biomaterial candidate, HA presents a unique combination of advantages. Specifically, HA is a naturally derived, enzymatically degradable, non-immunogenic, non-adhesive, bioactive glycosaminoglycan that has been

associated with several cellular processes, including angiogenesis, extracellular matrix homeostasis, and the regulation of inflammation.

In our first studies, we developed a novel hydrogel tissue engineering scaffold from photocrosslinkable glycidyl methacrylate-modified HA (GMHA). The GMHA hydrogels were found to be enzymatically degradable, biocompatible, and the degradation products of GMHA retained a similar level of bioactivity as unmodified HA fragments. Further development of these GMHA hydrogels focused on methods to attach peptides (e.g., the fibronectin-derived cell adhesion sequence RGD or arg-gly-asp). Such sequences could provide a versatile method to control several adhesion-related cellular processes, including migration and proliferation. Finally, we explored GMHA-based hydrogels for controlled protein release. Localized delivery of bioactive proteins such as growth factors provides an additional level of versatility for modulating specific cellular behaviors involved in tissue repair. We believe that these novel GMHA-based biomaterials offer unique advantages over synthetic and non-degradable scaffolding biomaterials and provide a solid foundation for further modification and use in a variety of soft tissue engineering applications.

Table of Contents

List of Tables

List of Figures

Chapter 1: Introduction

1.1 Surgical Treatments for Tissue Loss and Organ Failure

Annually, several million Americans are afflicted with tissue loss or organ failure due to trauma or disease, resulting collectively in the most common and expensive challenge to today's health care system [1]. To treat this loss, surgeons have several options. They may transplant organs from one individual to another, such as the case with kidney, heart, liver, and corneal transplants. Surgeons also may reconstruct tissues (e.g., breast or intestinal reconstruction), graft tissue within one patient from one site to another (e.g., coronary artery bypass with a saphenous vein graft derived from the lower leg), replace the biological function with drug treatments (e.g., insulin and hormone therapies), or replace the mechanical function of a tissue with a prosthetic implant (e.g., heart valve and hip replacements; **Figure 1.1**). Finally, physicians may treat organ loss with mechanical devices, such as kidney dialyzers or liver assist devices, which are located outside of the body.

These surgical treatments have saved many lives and can be effective organ and tissue replacements; however, these therapies have significant drawbacks. For example, donor shortages severely limit the availability of transplant organs. Surgical reconstruction is limited by the availability of "spare" tissue within the patient and can result in loss of function at the donor site or other long-term problems [2].

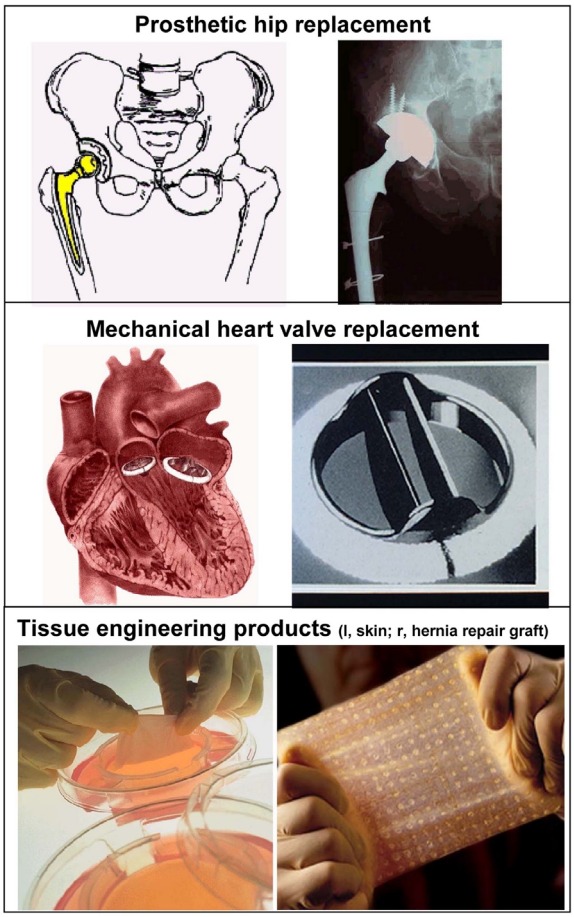

Figure 1.1 Mechanical prosthetics and tissue engineering products

In addition to transplantation and reconstructive surgery, mechanical devices can be used to replace or restore certain lost tissue function. For example, prosthetic devices constructed of metals and hard plastics are used to replace broken hips and heart valves. Unfortunately, these non-degradable devices have drawbacks: the prosthesis is subject to mechanical failure, and often long-term drug intervention is required to prevent blood clotting. To address these drawbacks, the field of tissue engineering aims to utilize the principles of engineering and the life sciences to develop new biological substitutes. Examples of tissue engineering products under recent development are Organogenesis' Apligraf skin replacement (third row, left) and Cook Biotech's Surgisis Gold Hernia Repair Graft (third row, right).

Prosthetic implants and mechanical devices, however, offer distinct advantages because they are composed of synthetic materials (e.g., metals, ceramics, plastics, glasses), which are practically unlimited in supply. Within the past 50 years, work in the biomedical engineering field has developed new materials to extend the functionality, biocompatibility, and lifespan of innovative device designs. Unfortunately, mechanical devices and prosthetics cannot replace the long-term function of a biological tissue or a complex organ and therefore do not completely prevent further patient deterioration.

1.2 TISSUE ENGINEERING

Building on the successful elements of the above-mentioned surgical therapies, a new field has emerged. Tissue engineering is an interdisciplinary field that melds the knowledge of the clinical and life sciences with engineering design principles to create novel methods to repair tissues, facilitate natural healing, or replace organ function [1,3-5]. Four general tissue engineering strategies have emerged: 1) transplanting cells to form new tissues at the damaged site, 2) implanting "bioengineered" or "bioartificial" tissues that were constructed in a laboratory, 3) stimulating healing or regeneration from surrounding healthy tissues, and 4) blocking an undesirable biological or pathological process. **Table 1.1** outlines examples of each tissue engineering strategy.

1.3 SCAFFOLDING BIOMATERIALS AND HYDROGELS

Each of the four tissue engineering strategies critically relies on biomaterial scaffolds. Scaffolds are biocompatible materials that can be porous and sponge-like, hydrated gels, or complex structures with aligned micron-sized

Table 1.1 Tissue engineering strategies

Cell Transplantation	**Disease or injury addressed**	**Ref.**
Dopamine neurons	Parkinson's disease	[6]
Pancreatic islet cells	Diabetes	[7-9]
"Bioengineered" or "Bioartificial" Tissues		
Blood vessels	Atherosclerosis, aneurysm	[10,11]
Heart valves	Malfunctioning valve	[12]
Skin	Burns, diabetic ulcers, chronic wounds	[13-15]
Bladder	Disease, cancer	[16]
Bones	Fractures, tumor removal	[17,18]
Cartilage	Arthritis	[19,20]
Tendons	Injury	[21,22]
Ligaments	Injury	[23]
Ophthalmic	Macular degeneration, cataracts	[24,25]
Techniques to Stimulate Healing or Regeneration		
Peripheral nerve regeneration	Severing or crush injuries	[26-28]
Spinal cord repair	Crush injuries	[29,30]
Wound healing	Burns, diabetic ulcers, chronic wounds	[31]
Bone repair	Fractures, tumor removal	[32]
Methods to Block an Undesirable Biological or Pathological Response		
Coated stents and angioplasty balloons	Prevent atherosclerosis	[33,34]
Anti-adhesive hydrogel barriers	Prevent post-operative adhesions	[35,36]

* This list is illustrative rather than exhaustive.

channels or grooves [37] (see **Figure 1.2**). Such biomaterials must be specifically designed to meet the demands for each application. For example, bone scaffolds must be strong and stiff, blood vessel scaffolds need to be elastic and tubular, and scaffolds for liver regeneration must be soft and porous (**Figure 1.3**).

Given such detailed criteria, it is clear that the success of each tissue engineering scaffold depends on the choice of the implanted biomaterial [38-42]. To meet the needs of demanding applications such as the guided growth of nerve, or the construction of a complex organ such as the heart, the scaffold material must provide cells with a very specific set of instructions. Therefore, an intricate knowledge of both the precise application as well as more general biological processes (e.g., inflammation, tissue rejection, and scar tissue formation) is required. The ideal biomaterial scaffold would promote the desired cellular response while minimizing any unwanted signals from the wound or disease site.

In addition to invoking the appropriate cellular response, three dimensional scaffolding biomaterials must have the following physicochemical characteristics: (1) a high porosity to allow cell growth and the transport of nutrients and cellular byproducts, (2) biodegradable and bioresorbable components, (3) mechanical properties to match the implant site, and (4) a versatile and reproducible manufacturing process to allow a variety of sizes and shapes [41]. It is likely that no one material will satisfy all of the design parameters in all applications. Rather, a wide range of materials will be appropriate to meet the various tissue engineering applications.

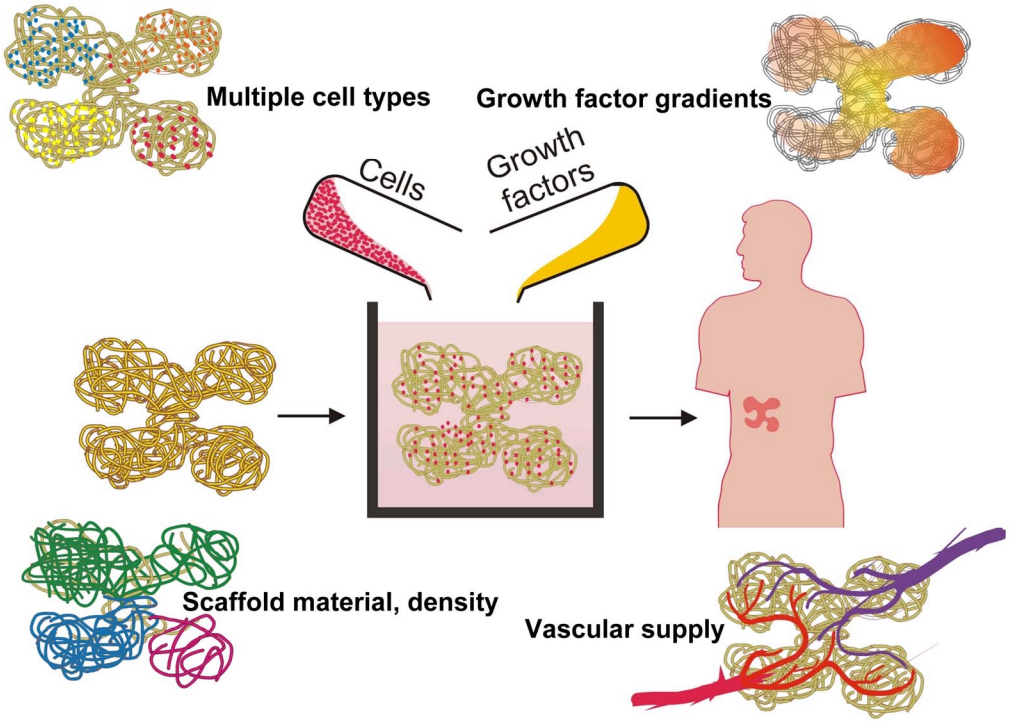

Figure 1.2 Tissue engineering scaffolds for creating bioartificial organs

To create a bioartificial organ, one must first design a scaffold biomaterial. The scaffold can be porous and sponge-like, hydrated gels, or highly complex structures with aligned micron-sized channels or grooves. In a laboratory, the scaffold is combined with cells and a mixture of essential nutrients, including specialized proteins called growth factors. The cells attach to and remodel the scaffold by degrading the polymer and replacing it with its own extracellular matrix. When the desired biological and mechanical properties are achieved, the bioartificial organ can be implanted into a patient. Examples of parameters that can affect the final organ include scaffold material and density, the presence of multiple cell types, growth factor gradients, and a pre-established vascular supply.

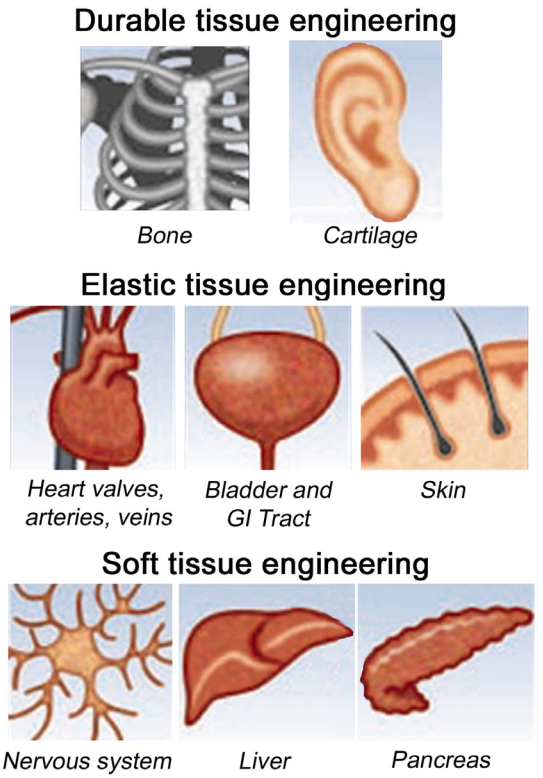

Figure 1.3 Classes of tissue engineering applications as a function of biomechanics

Unique scaffolding biomaterials must be designed to meet the demands for each individual tissue application. For example, durable tissues, such as bone and cartilage, require strong and stiff biomaterials. Elastic tissues, such as those in the cardiovascular, urinary, and gastrointestinal (GI) systems as well as skin, require strength in addition to flexibility, and the ability to recoil following the release of stress. Soft tissue engineering applications, such as nerve, liver, and pancreas, require non-brittle, hydrated materials that are soft and yet can maintain a desired shape. Drawings are adapted from [43].

In our work, we are specifically targeting soft tissue engineering applications, such as nerve regeneration (**Figure 1.4**). In such systems, the scaffolds must be soft, highly hydrated, porous, and degradable. In addition to meeting these needs, hydrogels inherently present several distinct advantages as a scaffolding material (outlined in **Table 1.2**). Hydrogels are three dimensional, water-swollen polymeric structures that have structural similarity to human extracellular matrix [44-46]. Hydrogels are formed by the physical or chemical crosslinking of hydrophilic polymers. These crosslinks provide a mesh-like structure and can be used to specifically tune the physicochemical properties of the scaffold. Furthermore, because hydrogels are highly hydrophilic, they are generally considered to be biocompatible. For all of these reasons, hydrogels have found a number of applications in tissue engineering (see **Table 1.3**).

1.4 NATURAL HYDROGEL BIOMATERIALS

Hydrogels from natural polymers have been widely used for tissue engineering applications [41,44]. Generally, naturally derived polymers (e.g., proteins such as collagen, gelatin and fibrin, and carbohydrates such as agarose, alginate, hyaluronic acid and heparin) are more biocompatible than their synthetic counterparts (e.g., polyethylene glycol, polyhydroxyethyl methacrylate, polyvinyl alcohol) because they more closely resemble native tissues. Furthermore, most natural polymers are biodegradable through hydrolysis or an enzymatically mediated process.

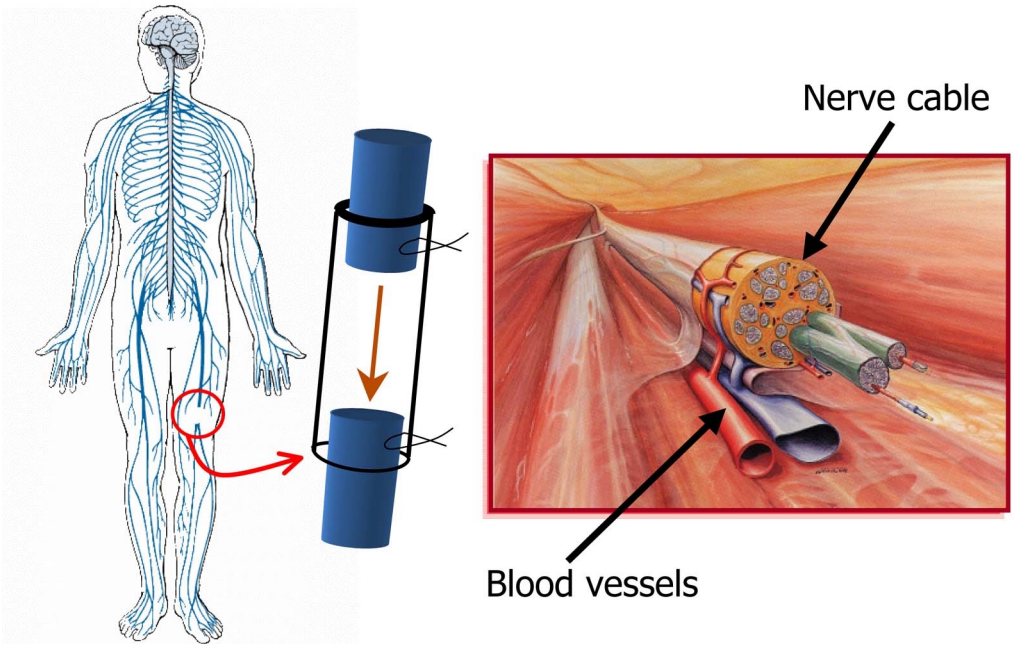

Figure 1.4 Peripheral nerve tissue engineering

Most of the current research in our laboratory is applied to the peripheral nervous system, which is composed of the nerves that innervate muscle tissue and transmit sensory and excitatory input to and from the spinal column. We are analyzing various biomaterials that can be used to specifically stimulate, and guide, nerves to regrow their severed axons. Ultimately, nerve guidance channels (shown in the figure middle) could be used to aid the repair of damaged peripheral nerves, such as would be required for facial and hand reconstruction, and ultimately, could be used to aid the regeneration of damaged spinal cord. A peripheral nerve is shown in cross-section (figure adapted from [47]) and depicts the bundles of individual nerve fibers that make up the entire nerve cable. Peripheral nerves are well vascularized by capillaries within the support tissue of the nerve cable or by vessels that penetrate the nerve from surrounding arteries and veins.

Table 1.2 Advantages and disadvantages of hydrogels as scaffolding biomaterials

Advantages
Hydrated environment can protect cells and some drugs (peptides, proteins, DNA)
Good transport of nutrient to cells and biproducts away from cells
May be easily modified to promote cell adhesion
Can be injected as a liquid that subsequently gels or crosslinks
Usually biocompatible
Disadvantages
Can be hard to handle
Usually mechanically weak
May be difficult to load drugs and cells and then crosslink as a prefabricated scaffold
May be difficult to sterilize

Adapted from [46].

Table 1.3 Applications of hydrogels as tissue engineering scaffolds

Scaffolding Application	Hydrogel Material	Reference
Liver	Alginate	[48]
	Chitosan	[49]
Skin	Collagen	[14,15]
	Gelatin-hyaluronic acid	[50]
	Polyethylene glycol	[31]
Blood vessel	Collagen	[10]
Neural	Polyhydroxypropyl methacrylamide	[30]
	Agarose	[26]
	Chitosan-collagen	[51]
	Fibrin	[29]
Soft tissue augmentation	Alginate	[52]
	Hyaluronic acid	[53]
Pancreatic islet encapsulation	Alginate	[7]
	Polyethylene glycol	[9]
	Polyvinyl alcohol	[8]

Table 1.4 Vertebrate biomaterials

	Proteins	***Glycosaminoglycans***
Examples:	Fibronectin	Hyaluronic acid
	Fibrin	Dermatan sulfate
	Elastin	Chondroitin sulfate
	Collagen/Gelatin	Keratan sulfate
	Keratin	Heparin sulfate/Heparin
Repeat unit:	Amino acids	Carbohydrates
Bioactivity:	High	(Current area of research)
Stability:	Fair to poor	Good
Solubility:	Varies	High
Immunogenicity:	Possible	Generally low

Natural polymers are derived from vertebrate and non-vertebrate sources, each of which has unique advantages and disadvantages. For example, vertebrate derived biomaterials (**Table 1.4**) are less likely to invoke an acute immune response, but are limited in supply or may carry pathogenic viruses (e.g., human immunodeficiency virus or HIV) or prions (e.g., bovine spongiform encephalopathy or Mad Cow Disease). Non-vertebrate natural polymers (e.g., the sea-weed derived polymers agarose and alginate) are available in a larger supply, but may provoke a strong immune response.

In our work, we chose to focus on hyaluronic acid (HA), a naturally derived glycosaminoglycan whose relatively simple sugar-like structure is nearly ubiquitous throughout all organisms. As a candidate biomaterial, HA presents a unique combination of advantages; specifically, HA is a naturally derived,

enzymatically degradable, non-immunogenic, non-adhesive, bioactive polymer that plays key roles in a variety of cellular processes (described in more detail below). A brief overview of HA and the HA-based hydrogel work presented in this dissertation follows.

1.5 OVERVIEW OF DISSERTATION

This dissertation is organized into six chapters. In **Chapter 2**, we give a detailed description of the foundation of our hydrogel biomaterial, HA. This unique biopolymer plays a vital role in embryonic development, extracellular matrix homeostasis, wound healing, and tissue regeneration. Biomaterials made from derivatized and crosslinked HA have received a great deal of attention in the bioengineering community and have been used in a wide variety of applications. HA has great potential for creative application in biomedical engineering as it is naturally derived, non-immunogenic, inherently bioactive, and has multiple sites for modification. This chapter reviews HA's natural structure and function, biomaterials made from derivatized and crosslinked HA as well as a number of clinical, surgical, and bioengineering applications of HA.

In **Chapter 3**, we present the synthesis and characterization of our hydrogel scaffolding material, photocrosslinked glycidyl methacrylate-modified HA (GMHA). A range of hydrogel degradation rates was achieved as well as a corresponding, modest range of material properties. Increased amounts of conjugated methacrylate groups corresponded with increased crosslink densities and decreased degradation rates and yet had an insignificant effect on human aortic endothelial cell cytocompatibility and proliferation. Rat subcutaneous

implants of the GMHA hydrogels showed good biocompatibility, little inflammatory response, and similar levels of vascularization at the implant edge compared with those of fibrin positive controls. Through the work presented in this chapter, we concluded that these novel GMHA hydrogels were promising biomaterials suitable for further optimization.

In **Chapter 4**, we describe studies that further tune the material and biological properties of the GMHA hydrogels for soft tissue engineering applications. We conjugated GMHA with acrylated forms of polyethylene glycol (PEG) and PEG-peptides to yield GMHA-PEG-peptide composite hydrogels. By varying the reactant concentrations, we created solid hydrogels with high peptide conjugation efficiencies, controllable peptide concentrations, and defined physicochemical properties. Furthermore, when modified with a peptide containing the adhesive peptide sequence RGD, the GMHA-PEG-peptide composites are able to support increased levels of human fibroblast adhesion compared to GMHA-PEG hydrogels alone. In summary, we demonstrated that the GMHA hydrogels could be modified to increase cellular adhesion while also maintaining the ability to fine-tune the hydrogel physicochemical properties.

In **Chapter 5**, we present a series of studies that characterize the release of a model protein, bovine serum albumin, from GMHA and GMHA-polyethylene glycol (PEG) hydrogels. Though BSA was released rapidly, increased GMHA and PEG concentrations were correlated with decreased protein release rates. To lengthen the duration of release, poly(lactic-co-glycolic acid) (PLGA) microspheres containing encapsulated BSA were suspended within the hydrogel

matrix. We found that this approach was suitable for extending the duration of BSA release to several weeks. These initial studies indicated that the GMHA and GMHA-PEG hydrogels and hydrogel-microsphere composites are tunable systems for delivering stable proteins in soft tissue engineering applications.

In **Chapter 6**, we summarize the results from our studies, draw conclusions, and recommend areas for future work.

1.6 REFERENCES

1. Langer R, Vacanti JP. Tissue engineering. *Science* 1993;260:920-6.
2. Kusama K, Donegan WL, Samter TG. An investigation of colon cancer associated with urinary diversion. *Dis Colon Rectum* 1989;32:694-7.
3. Skalak R, Fox CF, Eds. *Tissue Engineering*. 1988, Liss: New York.
4. Nerem RM. Cellular engineering. *Ann Biomed Eng* 1991;19:529-45.
5. Stocum DL. Regenerative biology and engineering: strategies for tissue restoration. *Wound Repair Regen* 1998;6:276-90.
6. Lindvall O, Brundin P, Widner H, Rehncrona S, Gustavii B, Frackowiak R, Leenders KL, Sawle G, Rothwell JC, Marsden CD, et al. Grafts of fetal dopamine neurons survive and improve motor function in Parkinson's disease. *Science* 1990;247:574-7.
7. Soon-Shiong P, Heintz RE, Merideth N, Yao QX, Yao Z, Zheng T, Murphy M, Moloney MK, Schmehl M, Harris M, et al. Insulin independence in a type 1 diabetic patient after encapsulated islet transplantation. *Lancet* 1994;343:950-1.

8. Burczak K, Gamian E, Kochman A. Long-term in vivo performance and biocompatibility of poly(vinyl alcohol) hydrogel macrocapsules for hybrid-type artificial pancreas. *Biomaterials* 1996;17:2351-6.
9. Cruise GM, Hegre OD, Lamberti FV, Hager SR, Hill R, Scharp DS, Hubbell JA. In vitro and in vivo performance of porcine islets encapsulated in interfacially photopolymerized poly(ethylene glycol) diacrylate membranes. *Cell Transplant* 1999;8:293-306.
10. Huynh T, Abraham G, Murray J, Brockbank K, Hagen PO, Sullivan S. Remodeling of an acellular collagen graft into a physiologically responsive neovessel. *Nat Biotechnol* 1999;17:1083-6.
11. Niklason LE, Gao J, Abbott WM, Hirschi KK, Houser S, Marini R, Langer R. Functional arteries grown in vitro. *Science* 1999;284:489-93.
12. Fabiani JN, Dreyfus GD, Marchand M, Jourdan J, Aupard M, Latremouille C, Chardigny C, Carpentier AF. The autologous tissue cardiac valve: a new paradigm for heart valve replacement. *Ann Thorac Surg* 1995;60:S189-94.
13. Bell E, Ehrlich HP, Buttle DJ, Nakatsuji T. Living tissue formed in vitro and accepted as skin-equivalent tissue of full thickness. *Science* 1981;211:1052-4.
14. Kuroyanagi Y, Kenmochi M, Ishihara S, Takeda A, Shiraishi A, Ootake N, Uchinuma E, Torikai K, Shioya N. A cultured skin substitute composed of fibroblasts and keratinocytes with a collagen matrix: preliminary results of clinical trials. *Ann Plast Surg* 1993;31:340-9.

15. Black AF, Berthod F, L'Heureux N, Germain L, Auger FA. In vitro reconstruction of a human capillary-like network in a tissue-engineered skin equivalent. *Faseb J* 1998;12:1331-40.
16. Oberpenning F, Meng J, Yoo JJ, Atala A. De novo reconstitution of a functional mammalian urinary bladder by tissue engineering. *Nat Biotechnol* 1999;17:149-55.
17. Muzzarelli RA, Zucchini C, Ilari P, Pugnaloni A, Mattioli Belmonte M, Biagini G, Castaldini C. Osteoconductive properties of methylpyrrolidinone chitosan in an animal model. *Biomaterials* 1993;14:925-9.
18. Taguchi T, Kishida A, Akashi M. Apatite formation on/in hydrogel matrices using an alternate soaking process: II. Effect of swelling ratios of poly(vinyl alcohol) hydrogel matrices on apatite formation. *J Biomater Sci Polym Ed* 1999;10:331-9.
19. Stading M, Langer R. Mechanical shear properties of cell-polymer cartilage constructs. *Tissue Eng* 1999;5:241-50.
20. Schreiber RE, Ilten-Kirby BM, Dunkelman NS, Symons KT, Rekettye LM, Willoughby J, Ratcliffe A. Repair of osteochondral defects with allogeneic tissue engineered cartilage implants. *Clin Orthop* 1999;S382-95.
21. Cao Y, Vacanti JP, Ma X, Paige KT, Upton J, Chowanski Z, Schloo B, Langer R, Vacanti CA. Generation of neo-tendon using synthetic polymers seeded with tenocytes. *Transplant Proc* 1994;26:3390-2.

22. Awad HA, Butler DL, Boivin GP, Smith FN, Malaviya P, Huibregtse B, Caplan AI. Autologous mesenchymal stem cell-mediated repair of tendon. *Tissue Eng* 1999;5:267-77.
23. Huang D, Chang TR, Aggarwal A, Lee RC, Ehrlich HP. Mechanisms and dynamics of mechanical strengthening in ligament-equivalent fibroblast-populated collagen matrices. *Ann Biomed Eng* 1993;21:289-305.
24. Hadlock T, Singh S, Vacanti JP, McLaughlin BJ. Ocular cell monolayers cultured on biodegradable substrates. *Tissue Eng* 1999;5:187-96.
25. Germain L, Auger FA, Grandbois E, Guignard R, Giasson M, Boisjoly H, Guerin SL. Reconstructed human cornea produced in vitro by tissue engineering. *Pathobiology* 1999;67:140-7.
26. Borkenhagen M, Clemence JF, Sigrist H, Aebischer P. Three-dimensional extracellular matrix engineering in the nervous system. *J Biomed Mater Res* 1998;40:392-400.
27. Ceballos D, Navarro X, Dubey N, Wendelschafer-Crabb G, Kennedy WR, Tranquillo RT. Magnetically aligned collagen gel filling a collagen nerve guide improves peripheral nerve regeneration. *Exp Neurol* 1999;158:290-300.
28. Hashimoto T, Suzuki Y, Kitada M, Kataoka K, Wu S, Suzuki K, Endo K, Nishimura Y, Ide C. Peripheral nerve regeneration through alginate gel: analysis of early outgrowth and late increase in diameter of regenerating axons. *Exp Brain Res* 2002;146:356-68.
29. Cheng H, Cao Y, Olson L. Spinal cord repair in adult paraplegic rats: partial restoration of hind limb function. *Science* 1996;273:510-3.

30. Woerly S, Pinet E, de Robertis L, Van Diep D, Bousmina M. Spinal cord repair with PHPMA hydrogel containing RGD peptides (NeuroGel). *Biomaterials* 2001;22:1095-111.
31. Masters KS, Leibovich SJ, Belem P, West JL, Poole-Warren LA. Effects of nitric oxide releasing poly(vinyl alcohol) hydrogel dressings on dermal wound healing in diabetic mice. *Wound Repair Regen* 2002;10:286-94.
32. Constantz BR, Ison IC, Fulmer MT, Poser RD, Smith ST, VanWagoner M, Ross J, Goldstein SA, Jupiter JB, Rosenthal DI. Skeletal repair by in situ formation of the mineral phase of bone. *Science* 1995;267:1796-9.
33. Bohl KS, West JL. Nitric oxide-generating polymers reduce platelet adhesion and smooth muscle cell proliferation. *Biomaterials* 2000;21:2273-8.
34. West JL, Hubbell JA. Separation of the arterial wall from blood contact using hydrogel barriers reduces intimal thickening after balloon injury in the rat: the roles of medial and luminal factors in arterial healing. *Proc Natl Acad Sci U S A* 1996;93:13188-93.
35. Hill-West JL, Chowdhury SM, Dunn RC, Hubbell JA. Efficacy of a resorbable hydrogel barrier, oxidized regenerated cellulose, and hyaluronic acid in the prevention of ovarian adhesions in a rabbit model. *Fertil Steril* 1994;62:630-4.
36. Hill-West JL, Chowdhury SM, Sawhney AS, Pathak CP, Dunn RC, Hubbell JA. Prevention of postoperative adhesions in the rat by in situ photopolymerization of bioresorbable hydrogel barriers. *Obstet Gynecol* 1994;83:59-64.

37. Griffith LG, Naughton G. Tissue engineering--current challenges and expanding opportunities. *Science* 2002;295:1009-14.
38. Hubbell JA. Biomaterials in tissue engineering. *Biotechnology (NY)* 1995;13:565-76.
39. Ratner BD. The engineering of biomaterials exhibiting recognition and specificity. *J Mol Recognit* 1996;9:617-25.
40. Kim BS, Mooney DJ. Development of biocompatible synthetic extracellular matrices for tissue engineering. *Trends Biotechnol* 1998;16:224-30.
41. Hutmacher DW, Goh JC, Teoh SH. An introduction to biodegradable materials for tissue engineering applications. *Ann Acad Med Singapore* 2001;30:183-91.
42. Hench LL, Polak JM. Third-generation biomedical materials. *Science* 2002;295:1014-7.
43. *Business Week*. The new era of regenerative medicine. July 27, 1998.
44. Lee KY, Mooney DJ. Hydrogels for tissue engineering. *Chem Rev* 2001;101:1869-79.
45. Lowman AM, Peppas NA. Hydrogels. In: Mathiowitz E, Editor. *Encyclopedia of Controlled Drug Delivery*. New York: John Wiley & Sons; 1999. p. 397-418.
46. Hoffman AS. Hydrogels for biomedical applications. *Adv Drug Deliv Rev* 2002;54:3-12.
47. Mackinnon SE, Dellon AL. *Surgery of the Peripheral Nerve*. New York: Thieme Medical Publishers; 1988.

48. Joly A, Desjardins JF, Fremond B, Desille M, Campion JP, Malledant Y, Lebreton Y, Semana G, Edwards-Levy F, Levy MC, Clement B. Survival, proliferation, and functions of porcine hepatocytes encapsulated in coated alginate beads: a step toward a reliable bioartificial liver. *Transplantation* 1997;63:795-803.
49. Yagi K, Michibayashi N, Kurikawa N, Nakashima Y, Mizoguchi T, Harada A, Higashiyama S, Muranaka H, Kawase M. Effectiveness of fructose-modified chitosan as a scaffold for hepatocyte attachment. *Biol Pharm Bull* 1997;20:1290-4.
50. Choi YS, Hong SR, Lee YM, Song KW, Park MH, Nam YS. Studies on gelatin-containing artificial skin: II. Preparation and characterization of cross-linked gelatin-hyaluronate sponge. *J Biomed Mater Res* 1999;48:631-9.
51. Eser Elcin A, Elcin YM, Pappas GD. Neural tissue engineering: adrenal chromaffin cell attachment and viability on chitosan scaffolds. *Neurol Res* 1998;20:648-54.
52. Marler JJ, Guha A, Rowley J, Koka R, Mooney D, Upton J, Vacanti JP. Soft-tissue augmentation with injectable alginate and syngeneic fibroblasts. *Plast Reconstr Surg* 2000;105:2049-58.
53. Duranti F, Salti G, Bovani B, Calandra M, Rosati ML. Injectable hyaluronic acid gel for soft tissue augmentation. A clinical and histological study. *Dermatol Surg* 1998;24:1317-25.

Chapter 2: Hyaluronic Acid

Hyaluronic acid (HA, also called hyaluronan or hyaluronate), a high molecular weight glycosaminoglycan found in all mammals, is a unique and highly versatile biopolymer. HA plays a vital role in embryonic development, extracellular matrix homeostasis, wound healing, and tissue regeneration. Although it is clear that HA is critically involved in these processes, a detailed understanding of the exact mechanisms by which it influences cellular behavior is unresolved. Additional complications arise when considering that the behavior and cellular influence of HA is highly dependent on concentration and molecular weight. For all of these reasons, the biology and chemistry of HA is a current area of extensive scientific research.

Biomaterials made from derivatized and crosslinked HA have received a great deal of attention in the bioengineering community and have been used in a wide variety of applications (e.g., orthopaedic, cardiovascular, ophthalmology, and dermatology, as well as general applications in tissue engineering, surgery, and drug delivery). HA has great potential for creative application in biomedical engineering because this unique polymer is naturally derived, non-immunogenic, inherently bioactive, and has multiple sites for modification. This chapter reviews HA's natural structure and function, biomaterials made from derivatized and crosslinked HA as well as a number of clinical, surgical, and bioengineering applications of HA.

2.1 THE NATURAL STRUCTURE AND FUNCTION OF HA

2.1.1 Physicochemical and Structural Properties

Hyaluronic acid, an extracellular matrix (ECM) component, is a high molecular weight glycosaminoglycan composed of disaccharide repeats of glucuronic acid and N-acetylglucosamine (**Figure 2.1**). This relatively simple structure is completely conserved through almost all mammals, suggesting that HA is a biomolecule of considerable importance [1]. In the body, HA occurs in the salt form, hyaluronate, and is found in high concentrations in several soft connective tissues, including skin, umbilical cord, synovial fluid, and vitreous humor. Notable amounts of HA are also found in lung, kidney, brain, and muscle tissues. In commercial production, HA is commonly extracted from rooster comb and human umbilical cord or manufactured in large quantities by bacterial fermentation [2].

The cellular synthesis of HA is a unique and highly controlled process [3]. Most glycosaminoglycans are made in the cell's Golgi networks. HA, however, is synthesized at the plasma membrane and immediately extruded out of the cell and into the ECM. This process is carried out by a group of proteins called HA synthases, which are located in the cell membrane. For a review of HA synthases, see Lee & Spicer [3].

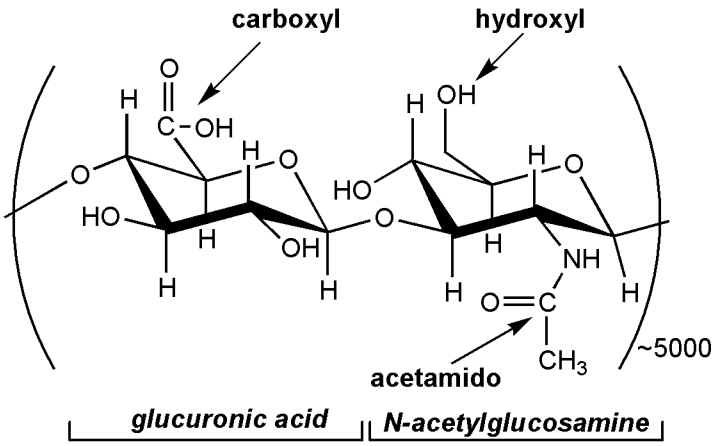

Figure 2.1 The structure of native HA.

HA is a naturally derived polymer composed of disaccharide repeats of glucuronic acid and N-acetylglucosamine. The molecular weight of native HA is typically several million. Each disaccharide repeat of HA contains three possible modification sites: the hydroxyl, carboxyl, and acetamido groups.

HA's structure imparts unique physicochemical and biological properties that depend on molecular weight [2]. When extracted from tissues, HA is polydisperse in size, with an average molecular weight of several million. In physiological solution, HA conforms to a stiffened random coil with a contour length of about 2.5 μm for a 1 x 10^6 molecular weight chain of about 2650 disaccharide repeats. Secondary hydrogen bonds form along the axis of HA, imparting stiffness and creating hydrophobic patches that allow the formation of ordered structures. HA solutions are shear-thinning; in other words, when shear rate is increased, the HA chains align in the direction of flow, resulting in a decreased solution viscosity. This shear thinning effect can be seen when delivering HA through a syringe.

HA is a highly hydrophilic polymer. Each glucuronic acid unit contains one carboxyl group, giving rise to HA's polyanionic character at physiological pH. In the presence of water, HA molecules can expand in volume up to 1000 times and form loose hydrated matrices [4]. Because of this property, HA is thought to play several roles in the ECM, including space filler, lubricant, and osmotic buffer [4]. By forming a hydrated polymer network, HA can act as a sieve, restricting the movement of pathogens, plasma proteins, and proteases [1,4]. In addition, HA's polyionic structure is able to scavenge free radicals, which mediates inflammation by imparting an antioxidant effect [1]. For a thorough review of HA's structural and physicochemical properties, see Lapcik, et al [2].

2.1.2 Roles in the Extracellular Matrix and Interactions with Hyaladherins

HA plays several important organizational roles in the ECM by binding with cells and other components through specific and non-specific interactions. For example, HA interacts with several proteoglycans (e.g., aggrecan, versican) through HA-binding motifs [2], and modulates the organization of fibrin, fibronectin, and collagen networks [5]. In addition to contributing to the homeostasis of ECM structure and hydration, HA is also involved in a number of more complex signaling events relating to cell migration, adhesion, and metastasis. Such processes are mediated through a group of proteins called hyaladherins. These proteins can be categorized into three types: those that are soluble, those that bind HA to other ECM molecules, and those that act as cellular receptors for HA.

Two hyaladherins, CD44 and RHAMM (Receptor for HA-Mediated Mobility), have been extensively studied. CD44 has been implicated as the major cell surface receptor for HA, and is expressed on a variety of cell types (e.g., leukocytes, fibroblasts, epithelial cells, keratinocytes, and some endothelial cells) [6]. The CD44 receptor is associated with various cellular processes, including adhesion, migration, proliferation, and activation as well as HA degradation and uptake [1,4]. (See **Figure 2.2** for a schematic of the signaling mechanisms associated with CD44.) In a number of cell types, the RHAMM hyaladherin has been found on the cell surface, as well as in the cytosol and nucleus [7]. RHAMM

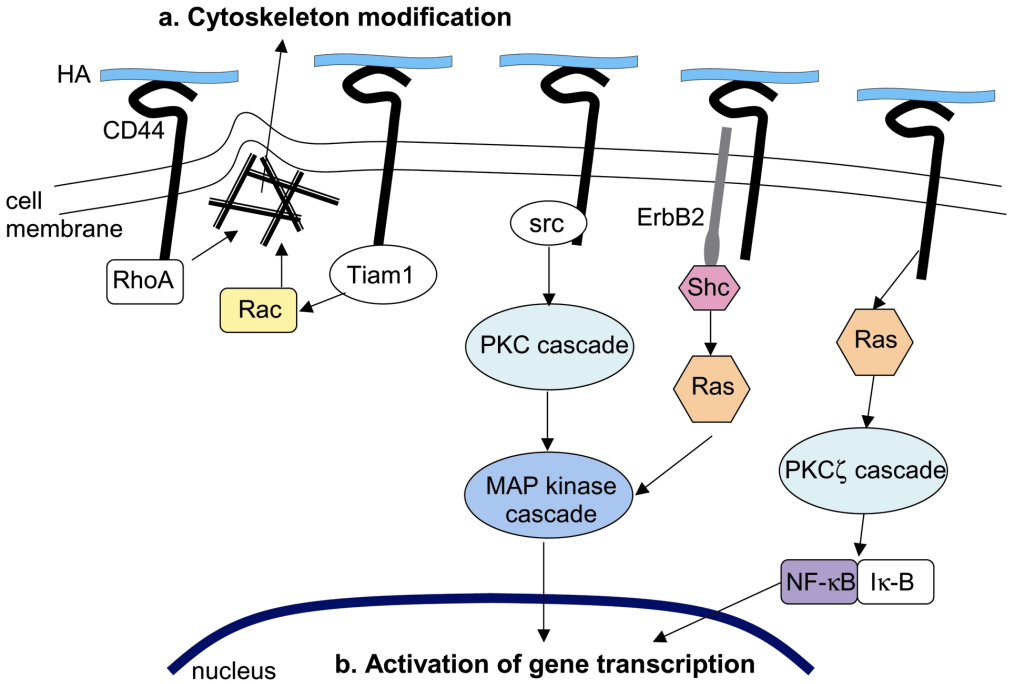

Figure 2.2 Signaling pathways of the HA receptor CD44.

The binding of HA and CD44 can result in signaling cascades that effect (a) the modification of cytoskeletal proteins, leading to changes in cell migration, and (b) the activation of gene transcription, resulting in changes in cell proliferation. Cytoskeletal assembly may be modified through signaling involving Rac and RhoA. The protein kinase C (PKC) and MAP kinase cascades may be involved in altering gene expression inside the nucleus. Figure adapted from [3].

has been implicated in regulating cellular responses to growth factors and plays a role in cell migration, particularly for fibroblasts and smooth muscle cells [7,8]. For a comprehensive review of hyaladherins, see Toole [8].

2.1.3 HA's Complex Influence on Cell Migration

As mentioned above, HA may influence cellular behavior not only through direct mechanisms (e.g., specific binding with cellular hyaladherins), but also by indirect means (through altering the physical properties of the ECM). HA's effect on cell migration is a remarkable illustration of this complexity. For instance, the binding of cellular hyaladherins to HA is involved in migration for a variety of cell types [5]. Yet, it is evident that HA may also indirectly aid cell migration by contributing to more open and hydrated spaces in the ECM or by otherwise remodeling the environment through interactions with collagen and fibrin [3]. Furthermore, as the main component of pericellular coats (matrices that are formed around migrating and proliferating cells), HA non-specifically facilitates the detachment of cells from the ECM [8]. In fact, as a highly hydrophilic polymer, HA is commonly referred to as a non-adhesive substrate (reviewed in [5]). Given such complexity, distinguishing between the effects of HA's biological activity and physicochemical properties is not straightforward.

2.1.4 HA Degradation

In mammals, the enzymatic degradation of HA results from the action of three types of enzymes: hyaluronidase (hyase), β-D-glucuronidase, and β-N-acetyl-hexosaminidase. Throughout the body, these enzymes are found in various forms, intracellularly and in serum. In general, hyase cleaves high molecular weight HA into smaller oligosaccharides while β-D-glucuronidase and β-N-acetyl-hexosaminidase further degrade the oligosaccharide fragments by removing non-reducing terminal sugars. Besides the degradation reaction, testicular hyase can catalyze the reverse reaction, transglycosylation. Therefore, HA is not simply degraded by this enzyme into disaccharide fragments. On the contrary, incubation of HA in a testicular hyase solution yields a mixture of fragment sizes, primarily made up of tetrasaccharides with smaller quantities of hexa-, octa-, and disaccharides [9]. The cell types primarily responsible for hyase synthesis are macrophages, fibroblasts, and endothelial cells; consequently, each of these cell types have been associated with HA degradation in the body [10]. In addition to enzymatic degradation, HA can also be degraded by reactive oxygen intermediates, a mechanism that has been implicated as a source of HA fragments at sites of inflammation [11]. For a review of other non-enzymatic means of HA degradation (e.g., degradation induced by free radicals, ultrasound, pH, and temperature treatments), see Lapcik, et al. [2].

2.1.5 HA in Wound Repair and Angiogenesis

High concentrations of HA can be found in many tissues undergoing remodeling, regeneration, and morphogenesis [8]. Furthermore, in the early stages of wound healing, a matrix composed largely of fibrin and HA is formed, which aids in fibroblast and endothelial cell migration into the injury site. This matrix also supports granulation tissue formation, particularly in fetal tissue, where HA has been implicated in aiding scar-free wound healing [1]. For this reason, exogenous HA has been investigated in wound healing applications and has been found to be effective even in challenging conditions such as chronic wounds [1].

The exact role of HA in wound healing is very complicated. In a comprehensive review of HA and wound repair, Chen and Abatangelo suggest that HA plays a "multifaceted" role in each wound healing stage (i.e., inflammation, granulation tissue formation, reepithelization, and remodeling) [1]. For example, HA aids in launching the early stages of inflammation, initiating the wound healing response, and also moderates the later stages of this potentially damaging process. Furthermore, the granulation tissue that forms remains rich in HA, aiding cell migration, proliferation, and organization of the ECM.

Perhaps one of the most interesting roles of HA in wound healing is the ability of HA oligosaccharides to promote angiogenesis [10]. Degradation products of 4-20 disaccharide units have been shown to stimulate in vivo capillary growth and induce in vitro endothelial proliferation, migration, and tube

formation. The complex nature of HA, however, is again demonstrated: although low molecular weight HA promotes angiogenesis, high molecular weight HA has been shown to inhibit new blood vessel growth. Researchers have attempted to gain a better understanding of the direct and indirect effects of HA molecular weight on angiogenesis, but an exact understanding of this process remains to be elucidated. For a review of the role of HA in angiogenesis, see West and Fan [10].

2.1.6 The Role of HA in Pathological Processes

Factors such as HA concentration and molecular weight have been correlated with the development of certain pathological conditions and can be used as diagnostic markers for disease. Increased serum concentrations of HA can be associated with the progression of certain inflammatory processes, such as rheumatoid arthritis, and have been used to evaluate the success of kidney and liver transplants [4]. Changes in the properties of HA have also been associated with certain vascular diseases, including atherosclerosis and restenosis [12]. Furthermore, high concentrations of HA have been linked to tumor growth and in some cases can be used as a negative predictor of cancer patient survival [12]. Presumably, a role of HA in cardiovascular disease and tumor growth is to increase the fluidity of the ECM, allowing increased cell proliferation and migration. In most cases, it is not clear whether the altered properties of HA directly cause disease or whether these changes are a symptom of the pathology; thus, a detailed understanding of HA's role in these conditions is incomplete [12].

2.2 DERIVATIZED AND CROSSLINKED HA BIOMATERIALS

HA offers many unique advantages as a building block for biomedical devices. Specifically, HA is enzymatically degradable, naturally derived, and non-immunogenic. Unlike proteins, which are easily denatured, HA is a carbohydrate polymer and can withstand demanding chemical modification procedures without losing its biological activity. Purified HA has found clinical uses in ophthalmology, osteoarthritis, and wound healing applications [2]. HA has many other potential applications, particularly as a biomaterial to deliver cells or proteins, but its use is limited because of its high water solubility and rapid degradation in the body. Thus, researchers have investigated methods to prolong the residence time of HA, using chemical modifications to yield materials with greater in vivo stability. Two main approaches for creating HA biomaterials have been utilized: derivatization and crosslinking (summarized in **Figure 2.3**). Both approaches are used to chemically modify one or more of HA's three available reactive groups (hydroxyl, carboxyl, and acetamido; **Figure 2.1**), while attempting to maintain biocompatibility and biological activity. This section provides an overview of several HA derivatization and crosslinking methods; however, this discussion is not comprehensive. For further information on modification strategies, including HA composites and blends, see references [2,13].

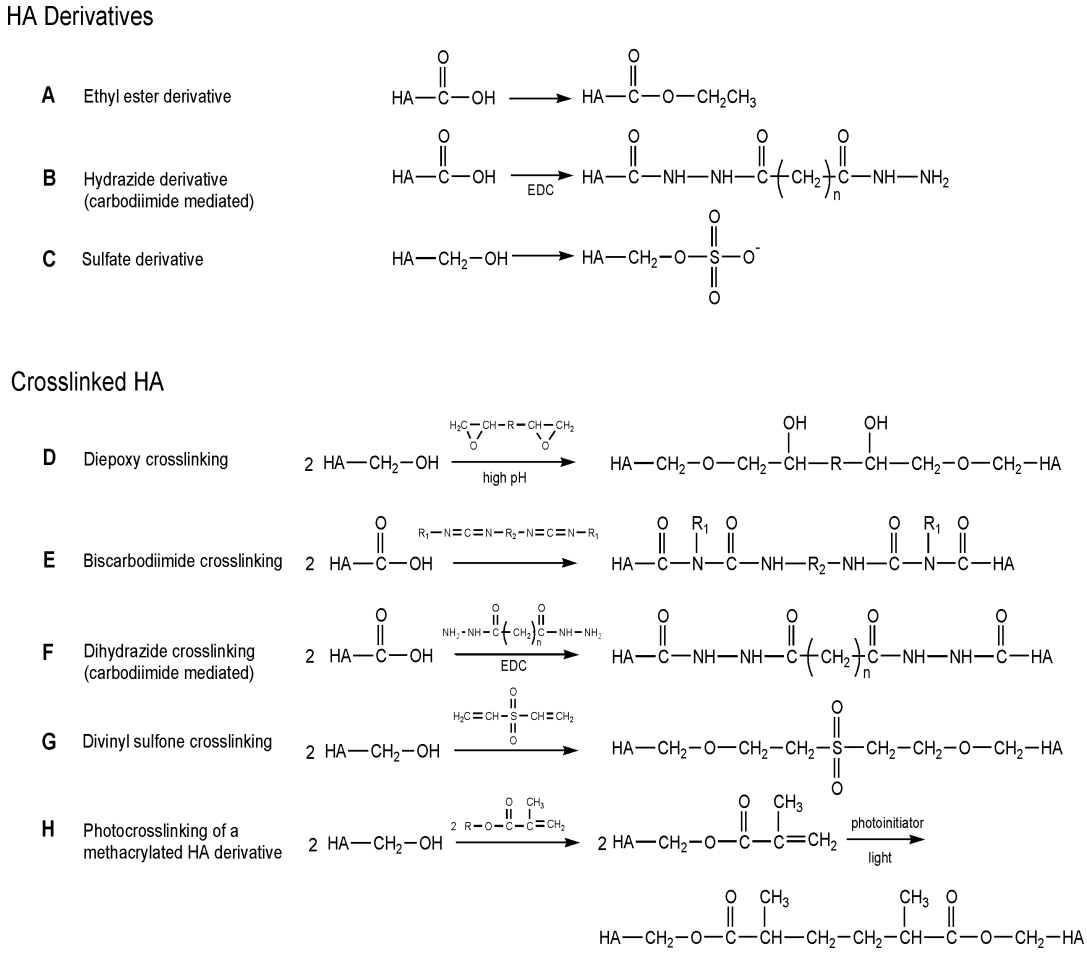

Figure 2.3 Derivatized and crosslinked HA biomaterials.

To tune HA's physicochemical properties for specific applications, HA has been modified in several ways. Un-crosslinked HA derivatives, including modifications based on (a) esterification [14], (b) carbodiimide-mediated reactions [15], and (c) sulfation [16,17] have been created. Crosslinked HA has also been produced using several crosslinking agents, including (d) diepoxies [18,19], (e) biscarbodiimides [20], (f) bifunctional amine crosslinkers [21], and (g) divinyl sulfone [22,23], as well as (h) photocrosslinking methods [24,25].

2.2.1 HA Derivatives

Many studies focus on three main types of HA derivatization strategies: esterification, carbodiimide-mediated modification, and sulfation (**Figure 2.3a-c**). These simple modification strategies can be used to create HA derivatives that are suitable for direct application or for subsequent crosslinking procedures. This section will describe uncrosslinked HA derivatives and Section 2.2.2 ("Crosslinked HA Biomaterials") will include a discussion of crosslinking methods for these materials.

2.2.1.1 Ester Derivatives

To create more hydrophobic forms of HA that have added rigidity and are less susceptible to enzymatic degradation, researchers have esterified HA's carboxyl groups [14]. The modification is carried out through an alkylation step of HA with an alkyl halide, yielding derivatives with 0-100% modifications of the available carboxyl groups. As the percent of HA esterification increases, these materials become more rigid and more hydrophobic. Increased hydrophobicity means that the HA derivatives are less soluble in water and less susceptible to enzymatic degradation. Fidia Advanced Biopolymers have created a range of HA esters, including ethyl esters (Hyaff-7; **Figure 2.3a**) and benzyl esters of HA

(Hyaff-11). Through a variety of processing steps, these HA esters can be shaped into fibers, membranes, sponges, and microspheres.

2.2.1.2 Carbodiimide-Mediated Derivatives

Reactions mediated by carbodiimides (e.g., EDC or 1-ethyl-3-(3'-dimethylaminopropyl)carbodiimide) are a common means of covalently binding the carboxyl group of one bioactive molecule with an amine of another (e.g., reactions between amino acids during peptide synthesis). However, carbodiimide reactions are very sensitive to pH and often result in the formation of an unreactive intermediate, acylurea, from carboxyl groups. Therefore, depending on the reaction conditions, carbodiimide-mediated reactions on HA can result in very low coupling yields. (For excellent discussions of the challenges to carbodiimide-mediated modification of HA, see references [15,20,21]). Pouyani and Prestwich gained a detailed understanding of these reactions, and as a result, chose hydrazide derivatization (**Figure 2.3b**) as a means of increasing the utility of carbodiimide in HA modifications [15]. Prestwich and co-workers have continued to develop a wide variety of HA-hydrazide derivatives for use as drug delivery devices, cellular probes, and HA-protein conjugates [13].

2.2.1.3 Sulfated Derivatives

To create a blood-compatible molecule that mimics heparin, researchers have modified HA with sulfate groups [16] (**Figure 2.3c**). The sulfation is

completed through a reaction of sulfur trioxide pyridine with HA's hydroxyl groups, yielding a range of sulfation from 1 to 4 sulfur groups incorporated per HA disaccharide [17]. This sulfation modification creates HA derivatives that are structurally and chemically similar to heparin [16,17]; cardiovascular applications of these materials are described in more detail below (see Section 2.3 "Applications of HA Biomaterials").

2.2.2 Crosslinked HA Biomaterials

As already mentioned, HA presents many inherent advantages as a candidate biomaterial. In addition to derivatization, crosslinking (**Figure 2.3d-h**) is another means of engineering HA's physicochemical properties. Depending on the crosslinking molecule and reaction chemistry, a wide variety of HA materials can be created, ranging from films with relatively low water content to highly swelling hydrogels. Most HA crosslinking methods fall into either of two general schemes: a one-step procedure consisting of the exposure of HA to a crosslinker, or a two-step procedure where a highly reactive HA derivative is first synthesized and then crosslinked in a subsequent reaction. Below is a brief listing of common HA crosslinking techniques; see references [2,13] for more detail.

2.2.2.1 Diepoxy Crosslinking

Almost 40 years ago, Laurent and co-workers created diepoxy crosslinked HA hydrogels using polyethylene glycol diglycidyl ether [18]. Others have

extended the diepoxy chemistry to other crosslinkers, including ethyleneglycol diglycidylether (a bifunctional crosslinker) and polyglycerol polyglycidylether (a trifunctional crosslinker) [19]. Interestingly, detailed studies of this chemistry have shown that at low pH, diepoxy compounds form ester linkages between carboxyl groups, while at high pH, they form ether linkages between hydroxyl groups [26] (**Figure 2.3d**). Thus, researchers have used diepoxyoctane to crosslink HA in a two-step double-crosslinking treatment: HA is reacted with diepoxyoctane at low pH, forming ester crosslinks, and then a second diepoxyoctane step is then carried out at high pH, forming ether crosslinks [26].

2.2.2.2 Carbodiimide-Mediated Crosslinking

As discussed above, carbodiimide-mediated reactions are commonly used for reactions between carboxylic acids and amines. These reactions, however, are sensitive to pH and readily form an unreactive acylurea from HA's carboxylates; therefore, the applications for which carbodiimides can be used with HA are somewhat limited. Fortunately, several researchers have found specific conditions under which carbodiimide-mediated reactions can allow HA crosslinking.

The simplest of these methods uses solely carbodiimide to induce inter- and intramolecular crosslinks on HA [27]; in other words, these materials can be synthesized without the use of exogenous crosslinkers. To form crosslinks, the carbodiimide-mediated reaction is performed on films of at least 70 weight percent HA in acetone- or ethanol-water solutions. Similar reactions carried out

with HA in solution did not yield crosslinked materials, perhaps as a result of the formation of unreactive acylureas. Challenged by this tendency of carbodiimide-mediated reactions to form unreactive acylureas on HA, Kuo, et al. created a biscarbodiimide crosslinking technique [20] (**Figure 2.3e**). Several biscarbodiimides were synthesized and covalently bound to HA through a mechanism similar to the carbodiimide-mediated creation of an acylurea, producing aromatic or aliphatic crosslinks between HA molecules.

Finally, several efforts have utilized carbodiimides to mediate reactions between HA's carboxyl groups and the amines of bifunctional crosslinkers (**Figure 2.3f**). Bullpitt and Aeschlimann made use of reactions mediated with carbodiimide and 1-hydroxybenzotriazole (HOBt) to couple activated amines ($pK_a < 8.0$; e.g., adipic dihydrazide) to HA's carboxyl groups; carbodiimide and N-hydroxysulfosuccinimide (sulfo-NHS) were used for coupling reactions between HA and simple primary amines ($pK_a > 9.0$; e.g., 1,4-diaminobutane dihydrochloride) [21]. Similarly, Vercryusse and co-workers have synthesized a wide variety of polyvalent hydrazide crosslinkers (2-6 hydrazides per crosslinker) for use in carbodiimide-mediated crosslinking reactions [28].

2.2.2.3 Aldehyde Crosslinking

Formaldehyde and glutaraldehyde have long been used to crosslink proteins for tissue preservation. Formaldehyde is used to create Biomatrix's Hylan-A, a water-soluble form of crosslinked HA that is more viscous and elastic

than native HA [22]. Glutaraldehyde has been used to crosslink HA to yield materials with high resistance towards degradation. Tomihata and Ikade used glutaraldehyde in acidic acetone-water solutions to create crosslinked HA films of low water content [29]. Hu, et al. compared glutaraldehyde and carbodiimide-mediated reactions and found that glutaraldehyde yielded more highly crosslinked materials suitable for use as three-dimensional tissue scaffolds [30].

2.2.2.4 Divinyl Sulfone Crosslinking

Insoluble HA hydrogels can be formed by crosslinking HA with divinyl sulfone (**Figure 2.3g**), yielding materials such as Biomatrix's Hylan-B gel [22,23]. At high pH, divinyl sulfone creates sulphonyl-bis-ethyl crosslinks between HA's hydroxyl groups. Depending on the reaction conditions, materials ranging from soft gels to firm solids (e.g., membranes and tubes) can be formed. Compared to native HA, Hylan-B has an extended residence time in vivo, particularly in sites where low mechanical force is imposed on the implant.

2.2.2.5 Photocrosslinking

While the crosslinking methods discussed above yield a wide variety of stabilized materials, most of these techniques proceed under physiologically incompatible conditions. Furthermore, many of these methods crosslink immediately upon mixing of the HA with the crosslinker. Because HA forms highly viscous solutions, it is often difficult to obtain homogenous materials in

this manner. Photocrosslinking, however, is a method that only reacts upon exposure to the appropriate wavelength of light; therefore, the reactants can be thoroughly mixed before crosslinking is initiated [31]. Furthermore, photocrosslinking methods are capable of proceeding under physiological conditions without detrimental effects to copolymerized bioactive molecules or encapsulated cells. To this end, HA has been modified with several photocrosslinkable groups, including cinnamoyl, coumarin, and thymine [32]; methacrylic anhydride [24]; glycidyl methacrylate [25]; and styrene [33]. (See **Figure 2.3h** for a general schematic of photocrosslinking methacrylated HA derivatives; **Chapters 3-5** detail several studies focusing on the development of photocrosslinkable glycidyl methacrylate-modified HA hydrogels.) Finally, sulfated HA has been modified with 4-azidoaniline, yielding an HA derivative suitable for patterning features as small as 100 μm [34], which may be useful for directing cell growth or adhesion in new biomaterials.

2.3 APPLICATIONS OF HA BIOMATERIALS

HA's intrinsic physicochemical and biological properties suggest that this distinctive polymer is suitable for application in clinical therapies, diagnostics, tissue engineering, and drug delivery. For comprehensive reviews of medical applications of HA, see references [2,13]. **Table 2.1** provides a list of HA products currently approved by the FDA for clinical use.

Table 2.1 FDA approved HA products.

Application	Tradename	Company
Osteoarthritis	Hyalgan	Fidia
	Synvisc	Biomatrix/Genzyme
	Supartz	Seikagaku
	Hylashield	Biomatrix
Ophthalmology	Healon	Pharmacia
	Amvisc	Bausch & Lomb
	Coease, Shellgel, Staarvisc	Anika Therapeutics
	Amo Vitrax, Vitrax	Allergan/Medtronic
	Provisc, Viscoat	Alcon Laboratories
Wound healing	Bionect	Fidia
	Ialuset	IBSA
Postsurgical adhesions	Adcon	Gliatech
	Intergel	LifeCore Biomedical
	Seprafilm	Genzyme
Surgical scaffolding	Hyalomatrix	Fidia
	Hylasine	Biomatrix
Gastrourology	Deflux	Q-Med

Adapted from [2,13,35]

2.3.1 Orthopaedic Applications

Native HA plays a vital role in the development of cartilage, the maintenance of the synovial fluid, and the regeneration of tendons [8]. High concentrations of HA can be found in the ECM of all adult joint tissues, including the synovial fluid and the outer layer of cartilage [36]. In part because of its viscoelastic nature and ability to form highly hydrated matrices, HA acts in the joint as a lubricant and a shock absorber [37]. In diseases such as osteoarthritis, the concentration and molecular weight of the HA naturally present in the joint are decreased, contributing to stiffness and pain. Viscosupplementation treatments aim to treat these conditions, and to this end, a variety of HA materials have been successfully applied as clinical therapies [36,37].

Researchers have also investigated modified HA as a cell delivery scaffold for cartilage and bone tissue engineering. Esterified HA (Hyaff, Fidia Advanced Biopolymers) supports the growth of chondrocytes [38] and the differentiation of bone marrow-derived mesenchymal progenitor cells into chondrocytes and osteoblasts [39]. In fact, when compared to one well-characterized delivery vehicle (porous calcium phosphate ceramic), Hyaff materials allowed greater amounts of bone and cartilage to be formed in vivo (as determined from the image analysis of stained tissue sections) [39].

2.3.2 Anti-Adhesion Applications

As HA is highly hydrophilic, it is a polymer that is well suited for applications requiring minimal cellular adhesion. Postoperative adhesions, which form between adjacent tissue layers following surgery, impede wound healing and often require additional surgical procedures to repair successfully. Barriers made from crosslinked HA have been effectively used to prevent such adhesions from forming [32]. Furthermore, the adhesion of bacteria onto biomaterials can induce infections and great risk to the patient; with this in mind, esterified HA has also been used to prevent bacterial adhesion to dental implants, intraocular lenses, and catheters [40].

2.3.3 Cardiovascular Applications

HA has also proven to be effective for increasing the blood compatibilities of cardiovascular implants such as vascular grafts and stents. For example, biomaterial surfaces treated with crosslinked HA have been associated with reduced platelet adhesion and thrombus formation [22,34,41]. Furthermore, sulfated HA derivatives can act as heparin mimics [16,17]; in fact, HA derivatives with higher degrees of sulfation are associated with increased abilities to prevent blood coagulation (as measured by longer times required for whole blood clotting) [17].

Crosslinked HA is also a promising biomaterial for cardiac tissue engineering. In the embryo, HA is required for the normal development of the valves and chambers within the heart [42]. Building upon this information, studies by Masters and Anseth have indicated that photopolymerized HA hydrogels are suitable materials for constructing tissue engineered heart valves (K.S. Masters and K.S. Anseth, Department of Chemical Engineering, The University of Colorado at Boulder, 2003, personal communication). Valvular interstitial cells, which are the primary cell type found in heart valves, were shown to adhere to and proliferate upon the HA hydrogels. Furthermore, the hyaladherins CD44 and RHAMM are present on the valvular interstitial cells and these receptors were thought to be involved in promoting cellular proliferation in response to degraded HA hydrogel fragments.

2.3.4 Ophthamology

HA, a natural component of the vitreous humor of the eye, has been used for many successful applications in ophthalmologic surgery [2]. In part because it forms viscoelastic and highly hydrated matrices, HA is particularly useful as a space-filling matrix in the eye; thus, intraocular injection of HA during surgery is used to maintain the shape of the anterior chamber. Furthermore, HA solutions also serve as a viscosity-enhancing component of eye drops and an adjuvant to eye tissue repair.

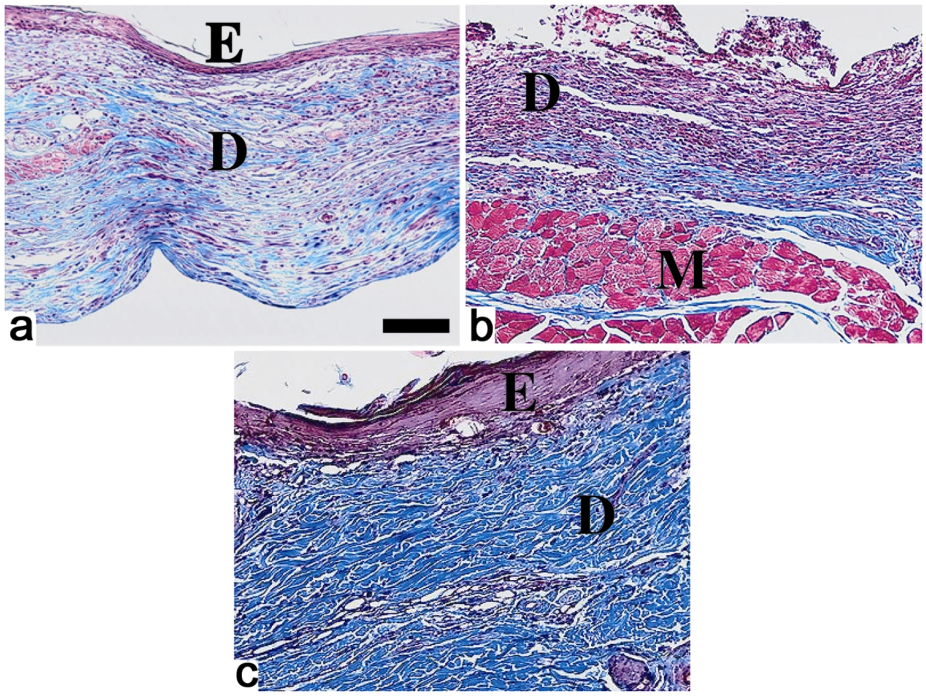

Figure 2.4 Crosslinked HA hydrogel films to assist wound healing.

Full-thickness wounds were created in the skin of Balb/c mice and (a) treated with a crosslinked HA hydrogel film (adipic dihydrazide modified HA that was crosslinked with polyethylene glycol dialdehyde) and covered with a wound dressing (Tegaderm, a thin polyurethane membrane dressing that is impermeable to microorganisms, 3M Health Care, St. Paul, MN), or (b) covered with the wound dressing alone. After 10 days, the HA films were completely degraded and 4 out of 6 of the HA treated wounds were associated with the formation of an epithelial layer and a collagen-rich dermal layer. The tissues treated with the wound dressing alone were less consistent and had reduced re-epithelialization. Tissue extracted from an area peripheral to the wound is shown in (c) as a normal tissue control. The sections are stained with Masson's Trichrome. D = dermis, E = epidermis, M = muscle. Scale bar = 100 μm. Images reprinted from [43].

2.3.5 Dermatology and Wound Healing Applications

HA is naturally present in high concentrations in the skin and soft connective tissues. Therefore, HA is an appropriate choice for a matrix to support dermal regeneration and augmentation. For example, Prestwich and co-workers found that crosslinked HA hydrogel films accelerate the healing of full-thickness wounds (**Figure 2.4**), presumably by providing a highly hydrated and non-immunogenic environment that is conducive to tissue repair [43]. Hyaff scaffolds cultured in vitro with keratinocytes and fibroblasts have been used to create materials similar to skin, including two distinct epidermal and dermal-like tissue layers [38]. Moreover, as a result of its ability to form hydrated, expanded matrices, HA has also been successfully used in cosmetic applications such as soft tissue augmentation [45].

2.3.6 Neural and Glial Applications

HA treatments have also been associated with improved peripheral nerve regeneration. Injections of unmodified HA into a nerve guide have been associated with increased levels of physiological and functional regeneration [46]. Furthermore, when strands of crosslinked HA are coated with polylysine, Schwann cells are able to attach and proliferate on these materials [30]. It is possible that the presence of HA enables increased glial cell migration, more rapid neurite outgrowth or a more easily remodeled ECM between the nerve

stumps. However, the exact mechanism by which HA may aid this process is not well understood.

2.3.7 General Tissue Engineering and Surgical Applications

HA's unique biological properties have inspired the development of a variety of novel therapies for general surgical applications. For example, our laboratory has previously used HA as a dopant during the synthesis of polypyrrole [44], an electrically conductive polymer that alone can promote repair in a variety of systems. When compared to polypyrrole films without HA, composite films of HA and polypyrrole were associated with higher levels of vascularization in subcutaneous implants (**Figure 2.5**). Therefore, HA-polypyrrole materials could be suitable for tissue engineering applications that may benefit from electrical stimulation and enhanced angiogenesis. Other researchers have also utilized HA's antioxidant properties to assist in the prevention of inflammation. In vitro studies have indicated that several materials, including unmodified HA, Hyaff, and a steroid-ester of HA, possess antioxidant activities [47,48]. Such materials could aid in healing conditions such as chronic wounds and rheumatoid arthritis.

2.3.8 Drug Delivery

Because of its biocompatibility, biodegradability, and readily modified chemical structure, HA has been extensively investigated in drug delivery applications. A variety of commercially available preparations of HA derivatives

and crosslinked HA materials have been developed for drug delivery; these materials are created in forms such as films, microspheres, liposomes, fibers, and hydrogels. For excellent reviews on applications of HA in drug delivery, see references [2,13].

2.4 CONCLUSIONS AND FUTURE DIRECTIONS

Through multidisciplinary discoveries about the structure, properties, biological activity, and chemical modification of this unique polymer, HA has found success in an extraordinarily broad range of biomedical applications. Future clinical therapies of HA-derived materials critically rely on a more detailed understanding of the effects of HA molecular weight and concentration and how this biomolecule specifically interacts with cells and ECM components in the body. Future directions of these materials will require finely tuned and controllable interactions between HA and its environment. Work in these areas are underway; for example, adhesive peptide sequences have been covalently bound to HA materials [49]. Also, environmentally responsive materials have been synthesized from HA. These materials can be created to swell or degrade in response to inflammation [19], electrical stimulation [50], and heat [51]. For an excellent online resource regarding the biology, modification chemistries, and various applications of HA, see the Glycoforum website [52].

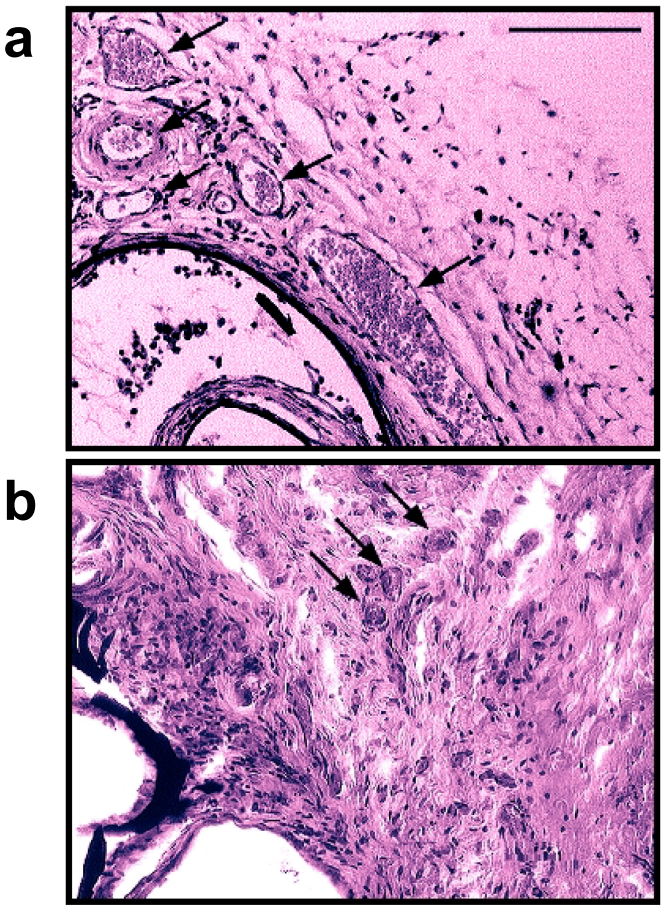

Figure 2.5 Polypyrrole-HA composite films for tissue engineering applications.

(a) Polypyrrole-HA and (b) polypyrrole-polystyrene sulfonate (negative control) films were implanted subcutaneously in rats for two weeks. The tissue sections were stained with hematoxylin and eosin. The heavy black lines in both images are the films. Blood vessels are denoted by arrows. The polypyrrole-HA films were associated with roughly a two-fold enhancement in blood vessel area compared the polypyrrole-polystyrene sulfonate films. Scale bar = 100 μm. Images reprinted from [44].

2.5 REFERENCES

1. Chen WY, Abatangelo G. Functions of hyaluronan in wound repair. *Wound Repair Regen* 1999;7:79-89.
2. Lapcik L, Jr., Lapcik L, De Smedt S, Demeester J, Chabrecek P. Hyaluronan: Preparation, Structure, Properties, and Applications. *Chem Rev* 1998;98:2663-2684.
3. Lee JY, Spicer AP. Hyaluronan: a multifunctional, megaDalton, stealth molecule. *Curr Opin Cell Biol* 2000;12:581-6.
4. Laurent TC, Fraser JR. Hyaluronan. *Faseb J* 1992;6:2397-404.
5. Nehls V, Hayen W. Are hyaluronan receptors involved in three-dimensional cell migration? *Histol Histopathol* 2000;15:629-36.
6. Isacke CM, Yarwood H. The hyaluronan receptor, CD44. *Int J Biochem Cell Biol* 2002;34:718-21.
7. Cheung WF, Cruz TF, Turley EA. Receptor for hyaluronan-mediated motility (RHAMM), a hyaladherin that regulates cell responses to growth factors. *Biochem Soc Trans* 1999;27:135-42.
8. Toole BP. Hyaluronan in morphogenesis. *Semin Cell Dev Biol* 2001;12:79-87.
9. Roden L, Campbell P, Fraser JR, Laurent TC, Pertoft H, Thompson JN. Enzymic pathways of hyaluronan catabolism. *Ciba Found Symp* 1989;143:60-76.

10. West DC, Fan T-PD. Hyaluronan oligosaccharides promote wound repair. In: Fan T-PD and Kohn EC, editor. *The New Angiotherapy*. Totowa, N. J.: Humana Press; 2002. p. 177-88.
11. Noble PW. Hyaluronan and its catabolic products in tissue injury and repair. *Matrix Biol* 2002;21:25-9.
12. Toole BP, Wight TN, Tammi MI. Hyaluronan-cell interactions in cancer and vascular disease. *J Biol Chem* 2002;277:4593-6.
13. Vercruysse KP, Prestwich GD. Hyaluronate derivatives in drug delivery. *Crit Rev Ther Drug Carrier Syst* 1998;15:513-55.
14. Campoccia D, Doherty P, Radice M, Brun P, Abatangelo G, Williams DF. Semisynthetic resorbable materials from hyaluronan esterification. *Biomaterials* 1998;19:2101-27.
15. Pouyani T, Prestwich GD. Functionalized derivatives of hyaluronic acid oligosaccharides: drug carriers and novel biomaterials. *Bioconjug Chem* 1994;5:339-47.
16. Barbucci R, Magnani A, Casolaro M, Marchettini N, Rossi C, Bosco M. Modification of hyaluronic acid by insertion of sulfate groups to obtain a heparin-like molecule. Part I. Characterization and behavior in aqueous solution towards H+ and Cu2+ ions. *Gazzetta Chimica Italiana* 1995;125:169-80.

17. Magnani A, Albanese A, Lamponi S, Barbucci R. Blood-interaction performance of differently sulphated hyaluronic acids. *Thromb Res* 1996;81:383-95.

18. Laurent TC, Hellsing K, Gelotte B. Crosslinked gels of hyaluronic acid. *Acta Chem Scand* 1964;18:274-5.

19. Yui N, Okano T, Sakurai Y. Inflammation responsive degradation of crosslinked hyaluronic acid gels. *J. Controlled Release* 1992;22:105-16.

20. Kuo J-W, Swann DA, Prestwich GD. Chemical modification of hyaluronic acid by carbodiimides. *Bioconjug Chem* 1991;2:232-241.

21. Bulpitt P, Aeschlimann D. New strategy for chemical modification of hyaluronic acid: preparation of functionalized derivatives and their use in the formation of novel biocompatible hydrogels. *J Biomed Mater Res* 1999;47:152-69.

22. Balazs EA, Bland PA, Denlinger JL, Goldman AI, Larsen NE, Leshchiner EA, Leshchiner A, Morales B. Matrix engineering. *Blood Coagul Fibrinolysis* 1991;2:173-8.

23. Band PA. Hyaluronan derivatives: chemistry and clinical applications. In: Laurent TC, editor. *Chemistry, Biology and Medical Applications of Hyaluronan and Its Derivatives*. London: Portland Press; 1998. p. 33-42.

24. Smeds KA, Pfister-Serres A, Hatchell DL, Grinstaff MW. Synthesis of a novel polysaccharide hydrogel. *J Macromolec Sci Pure Appl Chem* 1999;A36:981-989.

25. Baier Leach J, Bivens KA, Patrick Jr CW, Schmidt CE. Photocrosslinked hyaluronic acid hydrogels: Natural, biodegradable tissue engineering scaffolds. *Biotechnol Bioeng* 2003;82:578-89.

26. Zhao XB, Fraser JE, Alexander C, Lockett C, White BJ. Synthesis and characterization of a novel double crosslinked hyaluronan hydrogel. *J Mater Sci Mater Med* 2002;13:11-6.

27. Tomihata K, Ikada Y. Crosslinking of hyaluronic acid with water-soluble carbodiimide. *J Biomed Mater Res* 1997;37:243-51.

28. Vercruysse KP, Marecak DM, Marecek JF, Prestwich GD. Synthesis and in vitro degradation of new polyvalent hydrazide cross-linked hydrogels of hyaluronic acid. *Bioconjug Chem* 1997;8:686-94.

29. Tomihata K, Ikada Y. Crosslinking of hyaluronic acid with glutaraldehyde. *J Polym Sci A: Polym Chem* 1997;35:3553-3559.

30. Hu M, Sabelman EE, Tsai C, Tan J, Hentz VR. Improvement of Schwann cell attachment and proliferation on modified hyaluronic acid strands by polylysine. *Tissue Eng* 2000;6:585-93.

31. Anseth KS, Burdick JA. New directions in photopolymerizable biomaterials. *MRS Bulletin* 2002;27:130-6.

32. Matsuda T, Moghaddam MJ, Miwa H, Sakurai K, Iida F. Photoinduced prevention of tissue adhesion. *Asaio J* 1992;38:M154-7.
33. Matsuda T, Magoshi T. Preparation of vinylated polysaccharides and photofabrication of tubular scaffolds as potential use in tissue engineering. *Biomacromolecules* 2002;3:942-50.
34. Chen G, Ito Y, Imanishi Y, Magnani A, Lamponi S, Barbucci R. Photoimmobilization of sulfated hyaluronic acid for antithrombogenicity. *Bioconjug Chem* 1997;8:730-4.
35. http://www.fda.gov/cdrh. *(accessed December 2002)*.
36. Pozo MA, Balazs EA, Belmonte C. Reduction of sensory responses to passive movements of inflamed knee joints by hylan, a hyaluronan derivative. *Exp Brain Res* 1997;116:3-9.
37. Peyron JG. A new approach to the treatment of osteoarthritis: viscosupplementation. *Osteoarthritis Cartilage* 1993;1:85-7.
38. Brun P, Abatangelo G, Radice M, Zacchi V, Guidolin D, Daga Gordini D, Cortivo R. Chondrocyte aggregation and reorganization into three-dimensional scaffolds. *J Biomed Mater Res* 1999;46:337-46.
39. Solchaga LA, Dennis JE, Goldberg VM, Caplan AI. Hyaluronic acid-based polymers as cell carriers for tissue-engineered repair of bone and cartilage. *J Orthop Res* 1999;17:205-13.

40. Pavesio A, Renier D, Cassinelli C, Morra M. Anti-adhesive surfaces through hyaluronan coatings. *Med Device Technol* 1997;8:20-1, 24-7.
41. Kito H, Matsuda T. Biocompatible coatings for luminal and outer surfaces of small-caliber artificial grafts. *J Biomed Mater Res* 1996;30:321-30.
42. Camenisch TD, Schroeder JA, Bradley J, Klewer SE, McDonald JA. Heart-valve mesenchyme formation is dependent on hyaluronan-augmented activation of ErbB2-ErbB3 receptors. *Nat Med* 2002;8:850-5.
43. Kirker KR, Luo Y, Nielson JH, Shelby J, Prestwich GD. Glycosaminoglycan hydrogel films as bio-interactive dressings for wound healing. *Biomaterials* 2002;23:3661-71.
44. Collier JH, Camp JP, Hudson TW, Schmidt CE. Synthesis and characterization of polypyrrole-hyaluronic acid composite biomaterials for tissue engineering applications. *J Biomed Mater Res* 2000;50:574-84.
45. Duranti F, Salti G, Bovani B, Calandra M, Rosati ML. Injectable hyaluronic acid gel for soft tissue augmentation. A clinical and histological study. *Dermatol Surg* 1998;24:1317-25.
46. Seckel BR, Jones D, Hekimian KJ, Wang KK, Chakalis DP, Costas PD. Hyaluronic acid through a new injectable nerve guide delivery system enhances peripheral nerve regeneration in the rat. *J Neurosci Res* 1995;40:318-24.

47. Cortivo R, Brun P, Cardarelli L, O'Regan M, Radice M, Abatangelo G. Antioxidant effects of hyaluronan and its alpha-methyl-prednisolone derivative in chondrocyte and cartilage cultures. *Semin Arthritis Rheum* 1996;26:492-501.

48. Moseley R, Leaver M, Walker M, Waddington RJ, Parsons D, Chen WY, Embery G. Comparison of the antioxidant properties of HYAFF-11p75, AQUACEL and hyaluronan towards reactive oxygen species in vitro. *Biomaterials* 2002;23:2255-64.

49. Glass JR, Dickerson KT, Stecker K, Polarek JW. Characterization of a hyaluronic acid-Arg-Gly-Asp peptide cell attachment matrix. *Biomaterials* 1996;17:1101-8.

50. Tomer R, Dimitrijevic D, Florence AT. Electrically controlled release of macromolecules from cross-linked hyaluronic acid hydrogels. *J Control Rel* 1995;33:405-13.

51. Ohya S, Nakayama Y, Matsuda T. Thermoresponsive artificial extracellular matrix for tissue engineering: hyaluronic acid bioconjugated with poly(N-isopropylacrylamide) grafts. *Biomacromolecules* 2001;2:856-63.

52. http://www.glycoforum.gr.jp/science/hyaluronan/hyaluronanE.html. (accessed December 2002).

Chapter 3: Glycidyl Methacrylate-Hyaluronic Acid Hydrogels

Ideally, rationally designed tissue engineering scaffolds should promote natural wound healing and regeneration. Therefore, we sought to synthesize a biomimetic hydrogel specifically designed to promote tissue repair and chose hyaluronic acid (HA; also called hyaluronan) as the material from which to start.

We prepared a range of glycidyl methacrylate-HA (GMHA) conjugates, which were subsequently photopolymerized to form crosslinked GMHA hydrogels. A range of hydrogel degradation rates was achieved as well as a corresponding, modest range of material properties (e.g., swelling, mesh size). Increased numbers of conjugated methacrylate groups corresponded with increased crosslink densities and decreased degradation rates and yet had an insignificant effect on human aortic endothelial cell cytocompatibility and proliferation. Rat subcutaneous implants of the GMHA hydrogels showed good biocompatibility, little inflammatory response, and similar levels of vascularization at the implant edge compared with those of fibrin positive controls. Therefore, these novel GMHA hydrogels are suitable for modification with adhesive peptide sequences (e.g., RGD) and use in a variety of soft tissue engineering applications.

3.1 INTRODUCTION

As discussed in **Chapter 1**, future biomaterials applications will rely on scaffolds and drug delivery devices that interact with living systems in a specifically designed manner. A number of recent review articles have stated that such materials will be "biomaterials that heal": that is, biomimetic materials that are designed to promote natural healing and regeneration [1-3]. Therefore, several criteria are required: 1) the design of the biomaterial must incorporate the natural wound healing biology; 2) nonspecific adsorption of proteins should be inhibited; and 3) the biomaterial surface should present biomimetic molecules like those that are present in a wound [2].

To this end, numerous researchers have created and tested in vivo scaffolds composed of polysaccharides [4-7], proteins [8,9] and synthetic molecules [10-12]. These materials have found various degrees of success, but few have met all the requirements described above for "healable biomaterials." Additionally, candidate materials should be nonimmunogenic and have controlled biodegradability, biocompatible polymerization chemistry, and versatile modification strategies (e.g., multiple different reaction sites) [2,3,13]. One naturally derived polymer, hyaluronic acid (HA, **Figure 3.1**), inherently meets many of the above requirements and when crosslinked via photopolymerization, has the potential to provide an ideal wound healing scaffold.

As mentioned in **Chapter 2**, HA is a naturally derived, nonimmunogenic, nonadhesive glycosaminoglycan that plays a prominent role in various wound healing processes, as it is inherently angiogenic when degraded to small fragments [14]. HA promotes early inflammation, which is critical for initiating wound healing, but then moderates later stages of this process, allowing matrix stabilization and reduction of long-term inflammation [14] (**Table 3.1**). Furthermore, immunohistochemical analysis reveals that the environments around the migrating and proliferating fetal cells and adult tissues involved in regeneration and wound healing are enriched with HA [14]. As a mimic of the embryonic environment, exogenous HA supplementation promotes faster and more extensive regeneration in adult injuries [14]. This cumulative evidence suggests that HA is an ideal candidate material for modulating wound healing.

Several physiochemical aspects of HA are advantageous for biomaterial fabrication and application. For example, HA can be easily and controllably produced in large quantities through microbial fermentation, enabling the scale-up of HA-derived products [15] and avoiding the risk of animal-derived pathogens. Nascent HA is highly hydrophilic and thus inherently nonadhesive to proteins and cells [16], valuable properties for preventing scar tissue [17] and capsule formation [2].

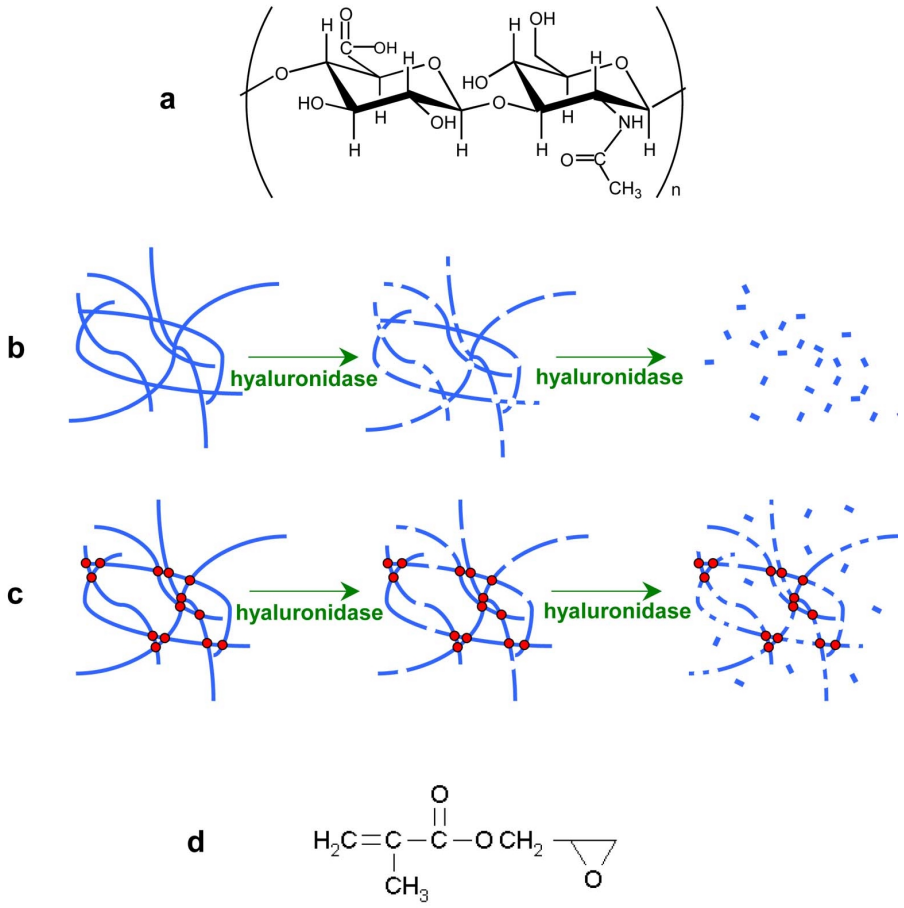

Figure 3.1 Native and crosslinked HA.

(a) HA is a polymer composed of disaccharide repeats of glucuronic acid and acetylglucosamine and has a molecular weight in the millions (n ≅ 5000). (b) Native HA (shown schematically) is quickly degraded in vivo by the enzyme hyaluronidase. (c) Crosslinking the HA chains forms an insoluble hydrogel matrix that is more resistant to enzymatic degradation. (d) Glycidyl methacrylate (GM), a source of photopolymerizable methacrylate, reacts covalently with HA to form GMHA conjugates.

Table 3.1 HA and the wound healing process

Wound Healing Phase	Contributing Role of HA
Inflammation	- Activation of macrophages and neutrophils - Production of proinflammatory cytokines - Moderation of inflammation through free radical scavenging, antioxidant properties, inhibition of inflammatory proteinases
Granulation	- Cellular differentiation, proliferation, and migration - Angiogenesis
Remodeling	- Reduced scar formation

Adapted from Chen and Abatangelo [14]

HA is enzymatically degraded by hyaluronidase and is completely resorbable through multiple metabolic pathways [18]. Although HA is quickly broken down in vivo, crosslinking individual HA polymer chains together decreases their degradation rates (**Figure 3.1b,c**). Many strategies exist for crosslinking HA [18], and of these, we chose photopolymerization—a technique that provides advantages such as increased spatial and temporal control over crosslinking and biocompatibility with in situ polymerization [13,19].

The goal of the work presented in this chapter was to create unique HA hydrogels designed to support wound healing. We characterized several hydrogel physiochemical parameters, including swelling ratio, stiffness, and in vitro enzymatic degradation. Furthermore, human aortic endothelial cell studies and rat subcutaneous implants were used to analyze the possible deleterious effects of the synthesis and polymerization reactions. We synthesized GMHA hydrogels in a controlled manner to yield biocompatible materials that generally retain the desirable wound healing properties of nascent HA.

3.2 MATERIALS AND METHODS

3.2.1 Synthesis and Crosslinking of GMHA Conjugates

We first added photopolymerizable methacrylate groups to HA to yield glycidyl methacrylate-HA (GMHA) conjugates (for a detailed protocol, see **Appendix A.1**). Briefly, we prepared a series of GMHA polymers by treating a

1% w/v solution of fermentation-derived HA (~2 x 10^6 molecular weight, Clear Solutions Biotech, Inc., Stony Brook, NY) in distilled water with a 6-, 10-, or 20-fold molar excess of glycidyl methacrylate (GM; **Figure 3.1d**) in the presence of excess triethylamine and tetrabutyl ammonium bromide overnight at room temperature, followed by a 1-h incubation at 60°C. For example, GMHA synthesized with a 6-fold molar excess GM was made as follows: 1.0 g HA was dissolved in 100 ml distilled water; 2.2 ml triethylamine, 2.2 ml GM, and 2.2 g tetrabutyl ammonium bromide were added separately and thoroughly mixed before the next component was added. After the reaction, the solution was precipitated in acetone (20 times the volume of the reaction solution) and dissolved in distilled water twice to remove excess reactants. The GMHA solution was lyophilized and stored desiccated at 4°C. ^{1}H-NMR spectroscopy was used to verify the methacrylation reaction on HA. GMHA conjugates were dissolved in D_2O and the spectra were recorded using a Varian Inova-500 spectrophotometer.

Next we synthesized the photocrosslinked hydrogels by exposing GMHA (0.5-2.0% w/v in phosphate-buffered saline) to UV light (365 nm, ~22 mW/cm^2, 0.5-5 minutes exposure) in the presence of the photoinitiator Irgacure 2959 (0.01-3% w/v, Ciba Specialty Chemicals, Basel, Switzerland) and N-vinyl pyrrolidinone (0.03-12% v/v).

3.2.2 Swelling Experiments and Flory-Rehner Calculations

To analyze the GMHA hydrogel structure (e.g., relative degrees of crosslinking), we performed a number of swelling experiments (for a detailed protocol, see **Appendix A.2**). The hydrogel swelling ratio based on mass (Q_M) was calculated by dividing the gel mass after swelling (M_s) by the dry gel mass (M_d). A Perkin-Elmer (Wellesley, MA) thermogravimetric analyzer (TGA) was used to measure M_s and M_d. The hydrogels were preswollen in phosphate-buffered saline (PBS) overnight, cut into small pieces (10-20 mg), and placed in the TGA weighing pan. The initial swollen mass was recorded as M_s, and the sample was heated slowly to 90-100°C or until a constant mass was achieved. The final mass obtained was recorded as M_d.

We then used Flory-Rehner calculations to determine the crosslink density and mesh size of the GMHA hydrogels. The average molecular weight between crosslinks, $\overline{M}_c$, was calculated using a simplification of the Flory-Rehner equation [20,21]:

$$Q_v^{5/3} \cong \frac{\overline{\upsilon}\overline{M}_c}{V_1}\left(\frac{1}{2}-\chi\right) \qquad (3.1)$$

where Q_v is the volumetric swelling ratio, $\overline{\upsilon}$ is the specific volume of the dry polymer, $\overline{M}_c$ is the average molecular weight between crosslinks, V_1 is the molar volume of the solvent (18 mol/cm^3 for water), and χ is the Flory polymer-solvent interaction parameter.

Q_v was determined from the degree of mass swelling, Q_M [22]:

$$Q_v = 1 + \frac{\rho_p}{\rho_s}(Q_M - 1) \tag{3.2}$$

where ρ_p is the density of the dry polymer (1.229 g/cm^3) and ρ_s is the density of the solvent (1 g/cm^3 for water). Q_M and ρ_p values were determined experimentally and used to calculate Q_v.

The value of χ for HA was estimated to be 0.473, based on several assumptions. First, it was assumed that χ for HA is comparable to that for dextran, a well-studied polysaccharide, because HA and dextran have similar chemical structures. In addition, χ estimates for HA that were based on an analysis similar to those published by Gekko [23,24] gave values within 2% of the value of χ for dextran. Finally, differences between soluble, unmodified polysaccharides and crosslinked polymers were assumed to be negligible.

The effective crosslink density, ν_e, was calculated as follows [25]:

$$\upsilon_e = \frac{\rho_p}{\overline{M}_c} \tag{3.3}$$

The swollen hydrogel mesh size, ξ, was determined with the following equation [26,27]:

$$\xi = Q_v^{1/3}\sqrt{\bar{r}_o^{\,2}} \tag{3.4}$$

where $\sqrt{\bar{r}_o^{\,2}}$ is the root-mean square distance between crosslinks and depends on the molecular weight between crosslinks. For HA, the following root-mean-square end-to-end distance value was previously reported [28]:

$$\left(\frac{\bar{r}_0^{\,2}}{2n}\right)^{1/2} \cong 2.4\,\text{nm} \tag{3.5}$$

where n is the number of disaccharide repeat units for HA with a given molecular weight. For HA with the molecular weight (M_n) 2 x 10^6, n is 5305, and therefore,

$$\sqrt{\bar{r}_0^{\,2}} = 0.1748\sqrt{M_n} \quad \text{(nm)} \tag{3.6}$$

A combination of (3.4) and (3.6) and a substitution of $\overline{M}_c$ for M_n gives

$$\xi = 0.1748\sqrt{\overline{M}_c}\,Q_v^{1/3} \quad \text{(nm)} \tag{3.7}$$

Because approximations were made in the Flory-Rehner calculations, the values determined (e.g., $\overline{M}_c$, ν_e, ξ) were considered approximations. However, these values were useful for making order-of-magnitude comparisons of the GMHA chemistries for biologically relevant features, such as mesh size.

3.2.3 Rheological Experiments

To further characterize the crosslinking of the GMHA hydrogels, we performed rheological oscillatory shear stress experiments. Degree of crosslinking relates to gel stiffness, which is represented by the experimentally determined complex modulus (G*). A Paar Physica (Ashland, VA) MRC 300 modular

compact rheometer was used in the parallel plate geometry, with a 25-mm plate and a gap size of 1 mm. Constant values of deformation, 0.1-10 mrad, were maintained throughout each frequency sweep of 1-10 Hz. G* was obtained at 3 Hz oscillation and 1 mrad deformation for each sample and was used to compare the relative mechanical stiffness of the hydrogels.

3.2.4 In Vitro Degradation By Hyaluronidase

In vitro enzymatic degradation of the hydrogels was measured as a function of time by incubating the gels in hyaluronidase and monitoring the mass of the hydrogel (for a detailed protocol, see **Appendix A.3**). First, the gels were synthesized in 8-mm diameter, 2-mm deep rubber perfusion chamber molds (Sigma-Aldrich, St. Louis, MO). The hydrogels were carefully transferred to 24-well plates with Teflon-coated cover glass forceps and were soaked in citrate buffer (0.15 M NaCl, 0.15 M Na_2HPO_4-$7H_20$, 0.03 M citric acid, pH 5.3) overnight to reach swelling equilibrium. The gels were removed from the citrate buffer, excess liquid was blotted from the surface with filter paper, and the gel masses were determined. Bovine testicular hyaluronidase (Sigma-Aldrich) in citrate buffer (0.5 ml of 5, 50, or 500 U/ml) was added to each gel and then incubated for various times at 37°C with mild mixing on a platform shaker. Every 1-2 h, the solution was removed, the gels were blotted, and the masses were carefully determined. The gels were then returned to the 24-well plate and

replenished with fresh hyaluronidase solution for the remainder of the degradation study. Gels with little crosslinking (and therefore those that could be easily damaged) were used only for a single time point. Crosslinked GMHA hydrogels in citrate buffer were used as a negative control.

3.2.5 HAEC Cytocompatibility Studies

We investigated the cytocompatibility of human aortic endothelial cells (HAECs) with crosslinked and uncrosslinked 11% methacrylated GMHA hydrogels using an indirect contact method adapted from Trudel and Massia [29] (for a detailed protocol, see **Appendix A.4**). Transwell inserts (Costar; 6.5 mm, 0.4-μm pore size polyester membrane filter, Corning Costar Corp., Acton, MA) were used to hold the hydrogel in indirect contact (1 mm separation distance) with the HAECs, which were seeded in the wells of the 24-well plates. The HAECs (Clonetics, Walkersville, MD) were obtained at passage 3, used at passage 6-8, and maintained in Clonetics' endothelial growth media-2: modified MCDB-131 supplemented with growth factors (EGM-2). All HA and GMHA solutions were sterilized with a syringe filter (0.8/0.2 μm Supor Acrodisc PF (prefilter) syringe filter, Pall Gelman, Ann Arbor, MI).

First, we compared the cytocompatibilities of HA and uncrosslinked GMHA. HAECs were seeded in a 24-well plate, 6250 cells in 1 ml EGM-2 per well. After the cells had adhered, the wells were dosed with 0.1 ml of 1% GMHA

in PBS, 1% HA in PBS or PBS alone (EGM-2 positive control). The final dilutions were approximately 0.1% GMHA and 0.1% HA. After 24 h, the cell viabilities were measured using the CellTiter 96 non-radioactive cell proliferation assay (Promega, Madison, WI) according to the manufacturer's instructions. The CellTiter assay is a colorimetric method for measuring the number of viable cells; therefore, the absorbance of the colored product is proportional to the number of living cells. At least three wells were treated, and the experiment was performed twice. Cell numbers were normalized versus the EGM-2 control.

Next, the cytocompatibility effects of crosslinked GMHA hydrogels were examined. A 0.1 ml GMHA solution with 1% Irgacure 2959 and 0.3% N-vinyl pyrrolidinone was dispensed in each Transwell insert and exposed to UV light for 1 min in a laminar flow hood. The gels were washed in EGM-2 (twice for 1 min and once for 5 min). Solutions of 1% GMHA with either 1% Irgacure 2959 or 0.3% N-vinyl pyrrolidinone were also tested to examine the effects of each component alone. After dilution by the medium, the final dilutions were 0.1% GMHA (crosslinked or uncrosslinked), 0.1% Irgacure 2959, and 0.03% N-vinyl pyrrolidinone. Finally, the experiment was repeated with crosslinked GMHA hydrogels made with 10-fold lower concentrations of Irgacure 2959 and N-vinyl pyrrolidinone.

3.2.6 HAEC Proliferation Response to Degraded GMHA

Degraded HA promotes angiogenesis and endothelial cell proliferation [30]. However, this response can be altered by the addition of methacrylate groups to HA. Therefore, the proliferation response of HAECs was determined in the presence of degraded HA and degraded GMHA in 96-well plates (for a detailed protocol, see **Appendix A.5**). HA and GMHA (5, 7, 11% methacrylation) were degraded in 50 U/ml hyaluronidase in citrate buffer for 4 h at 37°C, and then the hyaluronidase was inactivated by incubation at 56°C for 30 min. The HA and GMHA fragments were diluted to 1.5 μg/ml (this concentration of purified HA fragments increases the proliferation of bovine microvascular endothelial cells [30]) in "starvation medium" (Clonetics' endothelial basal media-2: modified MCDB-131 (EBM-2) with 1% heat-inactivated fetal bovine serum at pH 7.4).

The HAECs were seeded at 10,000 cells per well in EGM-2 and allowed to adhere for 2 h. The EGM-2 was removed and the cells were incubated overnight in the starvation medium. Next, the medium was replaced with the HA or GMHA fragment solutions and incubated for 48 h. Additional wells were also treated with EGM-2 (the positive control) or the starvation medium with heat-inactivated hyaluronidase (the negative control). The cell viabilities were determined using Promega's CellTiter 96 non-radioactive cell proliferation assay. At least three wells were exposed to each treatment, and the experiment was performed three times.

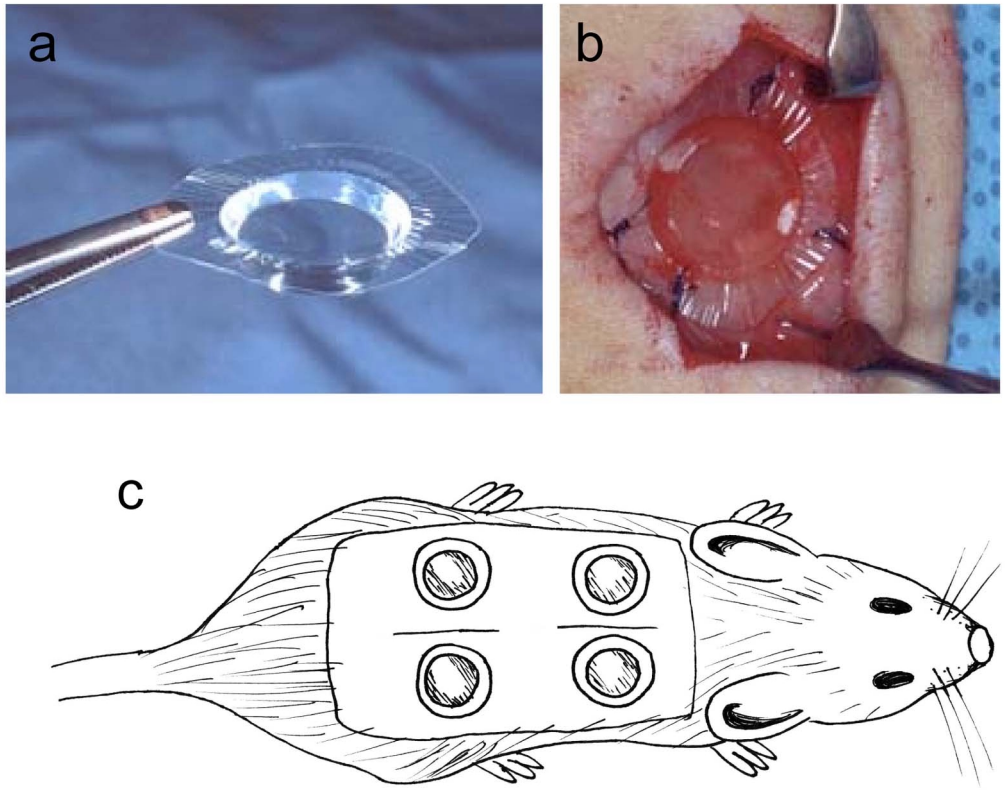

Figure 3.2 TEC subcutaneous implants in rats.

(a) TEC devices filled with the gels were implanted into subcutaneous locations in rats. (b) The TEC devices allow the gels to be localized and easily identified upon explantation. (c) Implantation locations for assessment of in vivo degradation rate.

3.2.7 GMHA Implants

In collaboration with Dr. Charles Patrick, Jr. at The University of Texas M.D. Anderson Cancer Research Center (Houston, TX), we investigated the endothelial cell response to the GMHA hydrogels in subcutaneous implants in rats. We used "tissue engineered construct" (TEC, **Figure 3.2a,b**) devices to identify the location of the implant and to simplify the harvesting procedure [31,32]. Each TEC is 8.5 mm in diameter, 4.0 mm deep, has a sewing cuff that is 5-7 mm wide, and is made from polypropylene film using a custom-made heated die press mold.

Sterile GMHA solutions (7% methacrylation, 1% GMHA, 1% Irgacure 2959, 0.3% N-vinyl pyrrolidinone in PBS; 0.3 ml per TEC) were dispensed in the TECs and exposed to UV light for 1 min. Human fibrin (Tisseel fibrin sealant, Baxter Healthcare Corp., Glendale, CA) was used as a positive control for vascularization [33]. Agarose (1.5% w/v in water; Sigma-Aldrich) was used as a negative control. Four ~250 g male Lewis rats (Harlan, Indianapolis, IN) were anesthetized (0.1 ml/g intramuscular injection of 100 mg/ml ketamine, 20 mg/ml xylazine, 0.4 mg/ml atropine), shaved, and two 2.5-cm incisions were made in the skin along the spine (see **Figure 3.2c**). Blunt dissection was used to form a pocket between the skin and muscle, and the muscle surface was cleared of fascia. The TECs were sutured to the muscle using 5.0 Prolene polypropylene sutures (Ethicon, Inc., Somerville, NJ), with the hydrogel in direct contact with the

muscle surface (**Figure 3.2b**). After implantating four TECs per rat (one fibrin positive control, one agarose negative control, and two HA gels), the skin was closed with 9-mm surgical staples.

At 2 weeks, the TECs and enclosed tissue were explanted, snap-frozen in Tissue-Tek optimal cutting temperature (OCT) compound (Sakura Finetek USA, Torrance, CA), and cryosectioned perpendicular to the muscle surface (6-μm sections). The sections were stained with the CD31 endothelial cell marker and counterstained with Gills #3 hematoxylin (Sigma-Aldrich), according to the methods described in [31] (for a detailed protocol, see **Appendix A.6**). Briefly, the sections were stained with a mouse antirat CD31 primary antibody (Serotec, Raleigh, NC) and a goat antimouse IgG secondary antibody conjugated with horseradish peroxidase (Serotec). CD31-positive cells were visualized using the substrate 3,3-diaminobenzidinetetrahydrochloride (DAB; Research Genetics, Huntsville, AL).

The sections were imaged under brightfield using an Olympus IX-70 inverted microscope (Melville, NY). Images were captured with a Hamamatsu C-5810 color CCD camera (Hamamatsu Corp., Bridgewater, NJ) connected to a Macintosh PowerMac computer, running IPLab image analysis software (Scanalytics, Fairfax, VA). The area of CD31-positive cells was calculated as a percentage of total area viewed per image [31]. The area of DAB stain as well as the total area of the image was quantified using NIH Image software.

3.2.8 Statistical Analysis

We performed Student's t-tests to determine the statistical significance of the differences between results. A significance level of $p < 0.05$ was used as the cutoff (i.e., p values are reported only for cases in which $p < 0.05$).

3.3 RESULTS

3.3.1 GMHA Synthesis and Hydrogel Formation

While the exact reaction mechanism was not confirmed in these studies, it is likely that glycidyl methacrylate reacts with a nucleophilic site on HA, possibly by a transesterification reaction similar to the method described for the glycidyl methacrylate modification of dextran [34]. ^{1}H-NMR spectroscopy confirmed the GMHA reaction, showing acrylate peaks at ~5.6 and ~6.1 ppm and the HA methyl peak at 1.9 ppm (**Figure 3.3**). The spectrum for HA (**Figure 3.3a**) is consistent with published results [35]; the GMHA spectrum (**Figure 3.3b**) is characteristic of the results from multiple reactions (n = 5).

In a comparison of the two spectrum, there are notable differences in the peak heights and shapes. We expect that these differences could be a result of methacrylation, and possibly, degradation of the polymer chains during the modification reaction. (A detailed investigation of the GMHA structure, however, is not within the scope of this study.) Nevertheless, without knowledge of the exact structure, it is possible to approximate percent methacrylation, which is

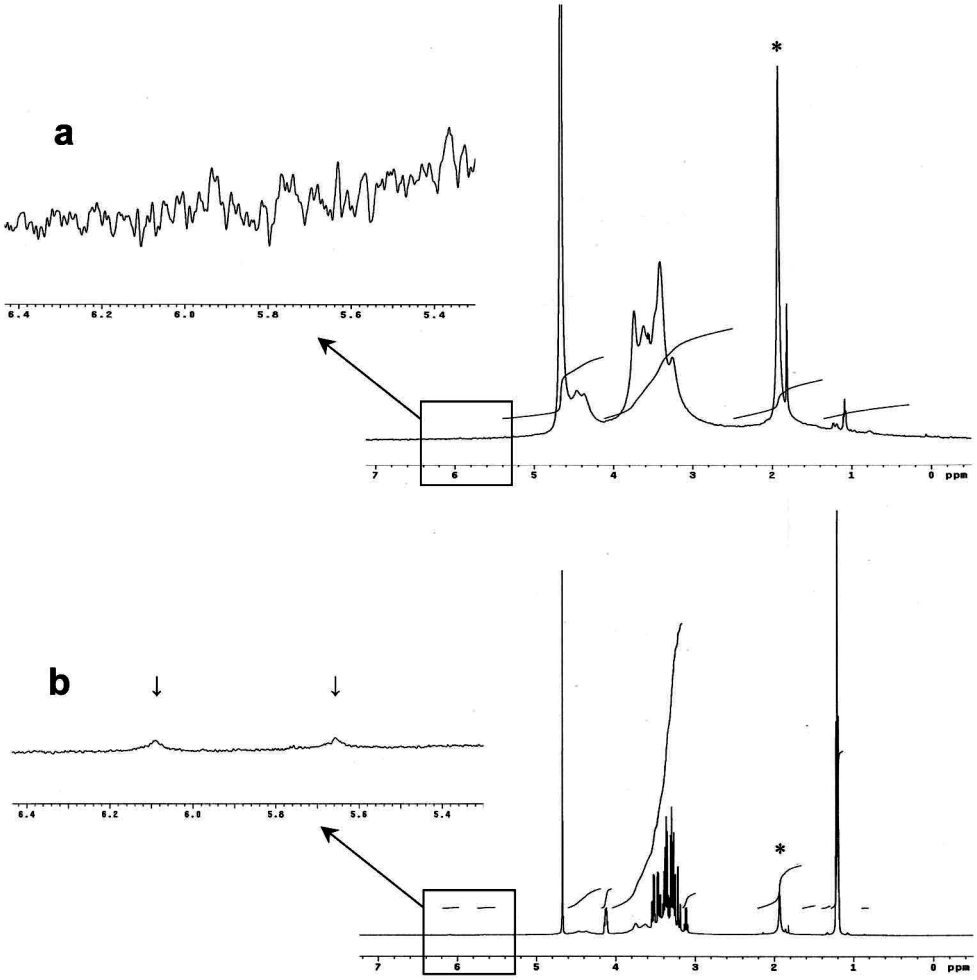

Figure 3.3 ^{1}H-NMR spectroscopy of HA and GMHA.

(a) Native HA (2 x 10^{6} molecular weight); (b) GMHA synthesized with 10-fold molar excess GM, yielding about 7% methacrylation on native HA. Methyl peaks at ~1.9 ppm (denoted by *) are found for native HA and GMHA. Expanded view of ~5.4 to ~6.4 ppm display the appearance of (↓) small peaks in (b), indicative of the presence of GM.

Table 3.2 Minimum concentrations of Irgacure 2959 and N-vinyl pyrrolidinone for GMHA hydrogel formation

% Methacrylation	**1 minute UV exposure**		**5 minutes UV exposure**	
	% Irgacure	*% VP*	*% Irgacure*	*% VP*
5	0.05	0.05	0.05	0.05
7	0.05	0.03	0.03	0.03
11	0.01	0.03	0.01	0.03

Irgacure 2959 is a photoinitiator; N-vinyl pyrrolidinone served as a reaction accelerant and co-monomer.

Table 3.3 Physical properties of GMHA crosslinked hydrogels

% Methacrylation:	**5**	**7**	**11**
Q_M [1]	52.5 ± 1.6	50.1 ± 4.6	42.5 ± 0.3
Q_v	64.3	61.4	51.9
$\overline{M}_c$ (g/mol)	8.45×10^5	7.82×10^5	5.92×10^5
ν_e (mol/cm^3)	1.45×10^{-6}	1.57×10^{-6}	2.07×10^{-6}
ξ (nm)	644	619	539
G* (Pa) [2]	109.4 ± 16.3	131.3 ± 6.4	154.5 ± 28.2

[1] Q_M for 11% methacrylated GMHA is significantly lower than that for 5% and 7% methacrylated GMHA; n = 3.

[2] n = 2 Values for Q_M and G* are mean ± standard deviation.

Abbreviations: glycidyl methacrylate-hyaluronic acid conjugates (GMHA), mass swelling ratio (Q_M), volumetric swelling ratio (Q_v), average molecular weight between crosslinks ($\overline{M}_c$), effective crosslink density (ν_e), mesh size (ξ), complex modulus (G*).

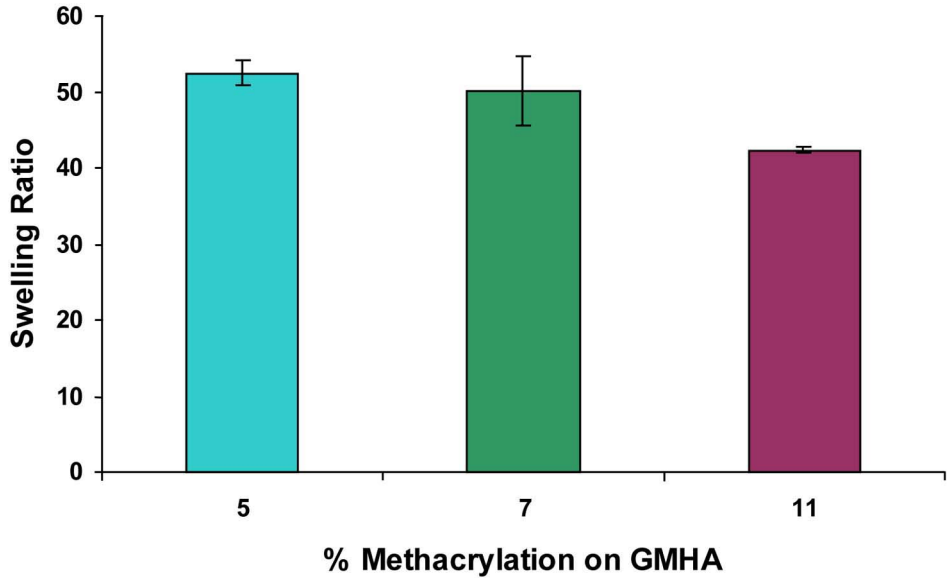

Figure 3.4 Swelling ratios for GMHA hydrogels.

The hydrogel swelling ratio, calculated by dividing the swollen gel mass by the dry gel mass, is an indicator of the degree of crosslinking in the gel. The swelling ratio for 11% methacrylated GMHA hydrogels was significantly lower than that for 5% methacrylated ($p < 0.001$) and 7% methacrylated hydrogels ($p < 0.05$). Each data point represents the average ± SD ($n = 3$).

calculated from the relative integrations of the methacrylate protons and HA's methyl protons [36]. Batches of GMHA made with 6-, 10-, and 20-fold excess GM were found to have approximately 5, 7, and 11% methacrylation, respectively. The ^{1}H-NMR spectra for the uncrosslinked GMHA on their own are not entirely conclusive; thus, further characterizations (e.g., correlate the swelling ratio with percent methacrylation) were conducted to confirm the importance of the varying degrees of methacrylation.

The hydrogels were made by exposing GMHA to UV light in the presence of the photoinitiator Irgacure 2959 and N-vinyl pyrrolidinone (a reaction accelerant and comonomer). The GMHA liquid crosslinked into materials ranging from viscous liquids to brittle solids, depending on the reaction conditions. Increasing the percent methacrylation or increasing the concentrations of GMHA, Irgacure 2959, or N-vinyl pyrrolidinone, yielded gels with increased firmness. **Table 3.2** displays the minimum concentrations of Irgacure 2959 and N-vinyl pyrrolidinone required for each of the chemistries to form hydrogels in 1 or 5 min UV exposure. These minimal concentrations were investigated to confirm that gels could be synthesized under cytocompatible conditions, as discussed later.

3.3.2 GMHA Hydrogel Characterization

Three complementary techniques were used to assess the crosslinking characteristics of the GMHA hydrogels: swelling ratio determination, Flory-Rehner calculations, and rheology. The swelling ratio, which varies inversely with

the number of methacrylate groups present on GMHA (**Figure 3.4**), is used in the Flory-Rehner theory to calculate the molecular weights between crosslinks, effective crosslink densities and mesh sizes (**Table 3.3**). For 5, 7, and 11% methacrylation, the swelling ratios were determined to be 52.5 ± 1.6, 50.1 ± 4.6, and 42.4 ± 0.3, respectively (n = 3 for each case). GMHA with 11% methacrylation had a significantly lower swelling ratio than GMHA with 5% ($p < 0.001$) or 7% ($p < 0.05$) methacrylation. Generally, as percent methacrylation on GMHA increased, the gels showed decreasing swelling ratios, indicating increased levels of crosslinking. However, because a small range of percent methacrylation values was tested, a more complex relationship between methacrylation and the resulting physical properties is not proposed.

The trend of increased crosslinking with increased methacrylation was also apparent in the Flory-Rehner calculations: increased methacrylation corresponded to decreased molecular weights between crosslinks (5%: 8.45×10^5 g/mol, 7%: 7.82×10^5 g/mol, 11%: 5.92×10^5 g/mol), as well as increased effective crosslink density (5%: 1.45×10^{-6} mol/cm^3, 7%: 1.57×10^{-6} mol/cm^3, 11%: 2.07×10^{-6} mol/cm^3) and decreased mesh size (5%: 644 nm, 7%: 619 nm, 11%: 539 nm). Rheological measurement of the complex modulus (G*, **Table 3.3**) further verified this trend: values of G*, while not statistically significant, increased slightly as the percent methacrylation increased (5%: 109.4 ± 16.3 Pa,

7%: 131.3 ± 6.4 Pa, 11%: 154.5 ± 28.2 Pa), again suggesting increased levels of crosslinking.

3.3.3 In Vitro Degradation of GMHA Hydrogels

In vitro degradation rates of the GMHA hydrogels were found by incubating hydrogels in three concentrations of hyaluronidase (5, 50, 500 U/ml in citrate buffer) and determining the gel masses over time. Enzyme concentrations were chosen to approximate endogenous levels (the hyaluronidase concentration in human serum is 2.6 U/ml [37]), as well as concentrations 10- and 100-fold greater to ensure complete gel degradation before hyaluronidase inactivation (hyaluronidase remains active up to 5 h at 37°C) [38].

Degradation rates (**Figure 3.5**) were calculated from the initial linear slope of gel mass versus time plots (data not shown). At 500 U/ml hyaluronidase, the degradation rates of 5% (99.4 ± 8.9 %/h, n = 6) and 7% (105.1 ± 3.6 %/h, n = 6) methacrylated GMHA were not statistically different, indicating that 500 U/ml is far in excess of the concentration required for controlled degradation. Comparisons between hydrogel chemistries were also carried out at 10- to 100-fold lower concentrations of hyaluronidase. At 5 U/ml hyaluronidase, significant differences were measured in the degradation rates: the degradation of 5% methacrylated GMHA gels (10.6 ± 2.0 %/h, n = 6) was significantly faster than that of 7% methacrylated GMHA gels (4.6 ± 0.8 %/h, n = 5; $p < 0.001$), and the

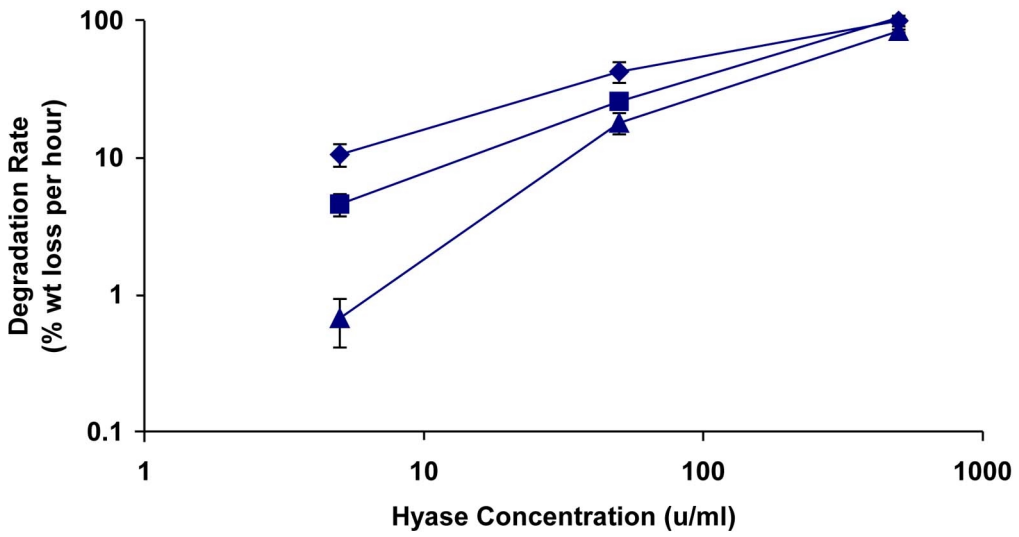

Figure 3.5 In vitro GMHA hydrogel degradation.

Degradation rates of GMHA hydrogels with (◆) 5, (■) 7, and (▲) 11% methacrylation in the presence of 5, 50, and 500 U/ml hyaluronidase. GMHA hydrogels with increased methacrylation show decreased degradation rates. All comparisons between methacrylation conjugates and hyaluronidase concentrations were significantly different ($p < 0.01$), except the comparison of 5% and 7% methacrylated GMHA at 500 U/ml hyaluronidase. Each data point represents the average ± SD ($n > 4$).

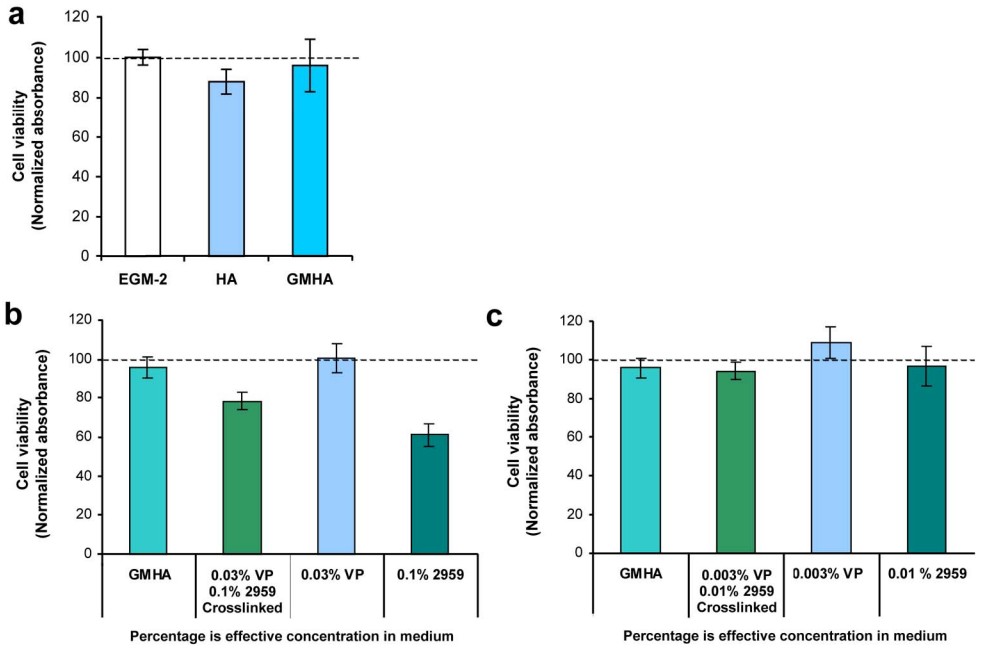

Figure 3.6 HAEC cytocompatibility in the presence of GMHA hydrogels.

HAECs were cultured for 24 h and the cell numbers were measured by a colorimetric cell viability assay. The absorbance for each sample was normalized to the positive control, EGM-2. (a) There was no statistical difference in the cytocompatibility of the 0.1% GMHA solution and either EGM-2 or the 0.1% HA solution. (b) Crosslinked GMHA hydrogels were made with 0.3% N-vinyl pyrrolidinone (VP) and 1% Irgacure 2959 (2959), and placed in indirect contact with the cells; the concentration of VP and 2959 following dilution by the medium was 0.03% and 0.1%, respectively. The hydrogels were associated with a decreased cytocompatibility when compared to 0.1% GMHA in solution. We also tested solutions of 0.1% GMHA with either 0.03% VP or 0.1% 2959. A decreased cytocompatibility was measured for the 0.1% 2959 solution. (c) Next, hydrogels with 10-fold less VP and 2959 were tested (0.03% VP and 0.1% 2959 in the hydrogel; 0.003% VP and 0.01% 2959 in the medium). There was no statistical difference between the cell numbers associated with GMHA solutions and the crosslinked GMHA. Also, statistical decreases in cytocompatibility were not found for solutions of 0.003% VP and 0.01% 2959 compared to GMHA in solution. Each data point represents the mean ± SD ($n > 6$).

degradation of 7% was faster than that of 11% methacrylated GMHA gels (0.7 ± 0.3 %/h, n = 4; $p < 0.0001$). Similarly, at 50 U/ml hyaluronidase, the degradation rate of 5% methacrylated GMHA gels (42.3 ± 7.3 %/h, n = 6) was significantly greater than that of 7% gels (25.7 ± 0.6 %/h, n = 6; $p < 0.001$), and the degradation rate of 7% methacrylated GMHA gels was greater than that of 11% gels (17.9 ± 3.2 %/h, n = 6; $p < 0.001$). Therefore, considering the 5- and 50-U/ml hyaluronidase results, increasing methacrylation on GMHA resulted in a decreased degradation rate, again indicating a correlation between methacrylation and the degree of crosslinking. No significant change in mass was observed in the negative-control GMHA hydrogels, which were incubated in citrate buffer alone.

3.3.4 HAEC Cytocompatibility Response to GMHA Hydrogels

In vitro HAEC cytocompatibility was measured in response to GMHA solutions and crosslinked hydrogels. Cell viabilities were measured after 24 h and normalized versus EGM-2. The concentrations for HA, GMHA, Irgacure 2959, and N-vinyl pyrrolidinone are reported in this section as effective concentrations after dilution by the medium. As shown in **Figure 3.6a**, no statistically significant difference was found between the response to 0.1% GMHA in solution (95.92 ± 5.31, n = 6) and EGM-2 (100.00 ± 3.37, n = 13). This indicates that the GM conjugation chemistry did not have a harsh cytotoxic effect and that the acetone precipitation step after the GM modification reaction adequately removed excess

GM from the product. Interestingly, 0.1% GMHA had a small but statistically significant increase in viability when compared to 0.1% HA (87.83 ± 4.93, n = 6).

The cytocompatibility effects of crosslinked GMHA were also investigated, as shown in **Figure 3.6b**. When compared to 0.1% GMHA in solution, a significant decrease in viability was measured for crosslinked gels (final concentration following dilution of 0.1% Irgacure 2959 and 0.03% N-vinyl pyrrolidinone; 78.42 ± 4.58; $p < 0.001$). Treatments at a final dilution of 0.1% GMHA with either 0.1% Irgacure 2959 or 0.03% N-vinyl pyrrolidinone were also tested. When compared to 0.1% GMHA in solution, no decrease in viability was measured for 0.03% N-vinyl pyrrolidinone (100.44 ± 7.66). However, a statistically significant decrease was measured for 0.1% Irgacure 2959 (61.16 ± 5.77, $p < 0.0001$). These results indicate that Irgacure 2959 may play a role in the decreased cytocompatibility of GMHA hydrogels synthesized under these conditions.

Next, hydrogels with 10-fold less Irgacure 2959 and N-vinyl pyrrolidinone were tested. As shown in **Figure 3.6c**, no statistically significant decrease in viability (compared to GMHA in solution) was measured for hydrogels made with 0.03% N-vinyl pyrrolidinone and 0.1% Irgacure 2959 (concentrations following dilution of 0.003% and 0.01%, respectively; 94.19 ± 4.45). Similar results were found for 0.1% GMHA solutions with 0.003% N-vinyl pyrrolidinone (109.14 ± 8.26) and 0.01% Irgacure 2959 (96.90 ± 10.03).

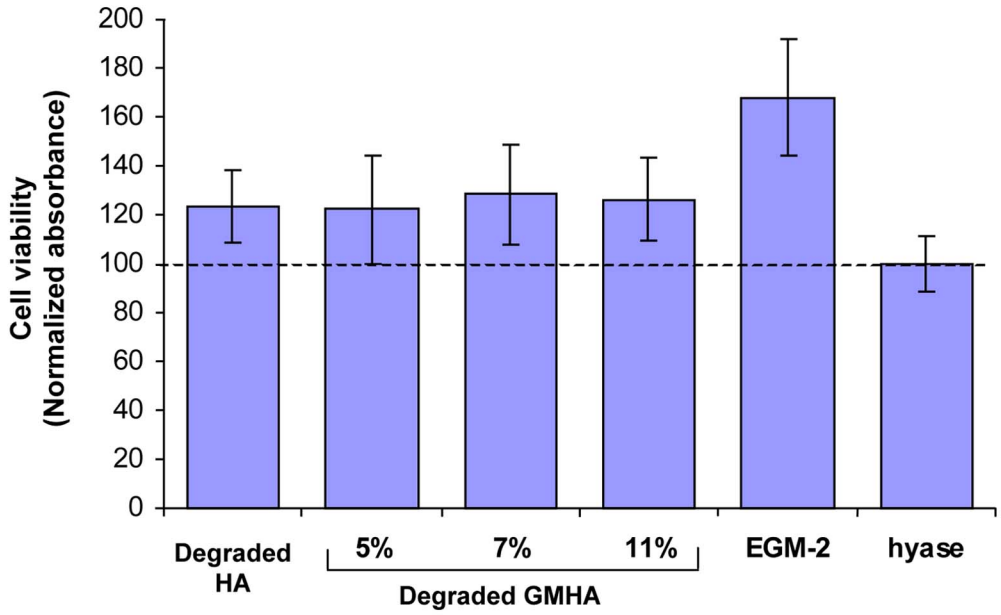

Figure 3.7 HAEC proliferation response to degraded GMHA fragments.

HAECs were cultured in 1.5 μg/ml of HA fragments or GMHA fragments (5, 7, 11% methacrylation) in starvation medium for 48 h. EGM-2 provided a positive control and heat-inactivated hyaluronidase in starvation medium was a negative control. Cell viabilities, which were measured via absorbance in a colorimetric cell viability assay, were normalized to the heat-inactivated hyaluronidase control. No statistical difference was found in the proliferation response to HA fragments and GMHA fragments for all values of methacrylation, indicating that glycidyl methacrylate modification of HA does not significantly reduce its biological activity. The proliferation response to HA and GMHA fragments was significantly greater than the response to hyaluronidase and significantly less than the response to EGM-2 ($p < 0.001$). Each data point represents the mean ± SD ($n > 9$).

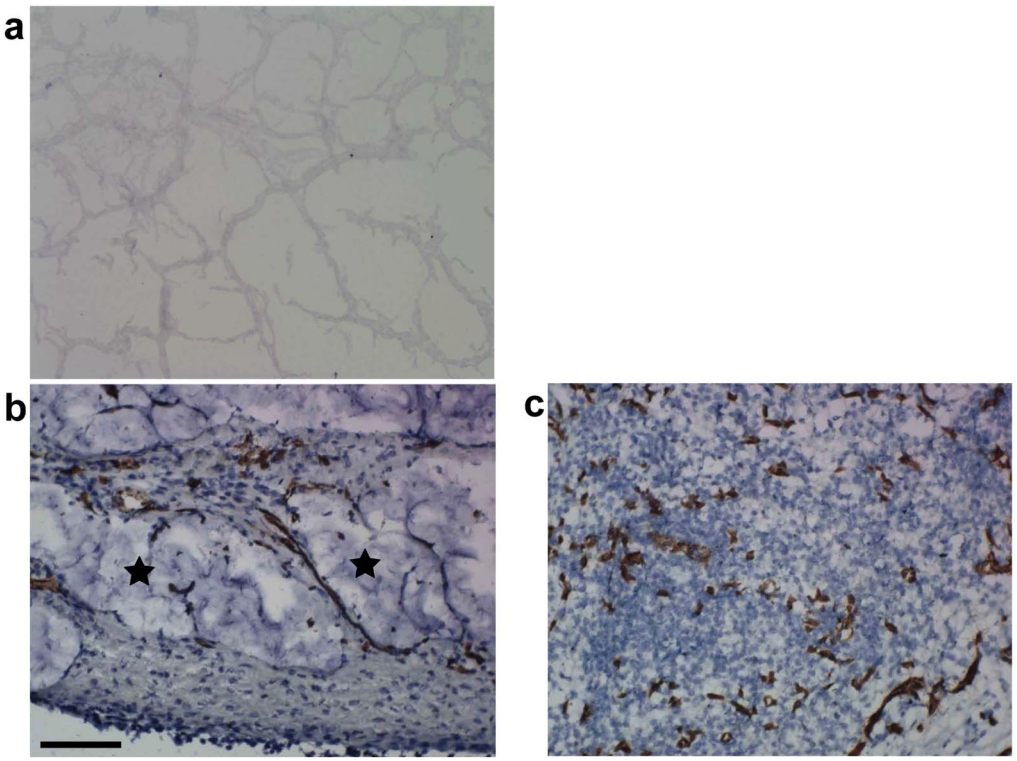

Figure 3.8 GMHA implants in rats.

Hydrogels were implanted subcutaneously in rats for 2 weeks. (a) Agarose negative controls, (b) 7% GMHA hydrogels (★ denotes areas of hydrogel), and (c) fibrin positive controls were stained with hematoxylin and CD31, a marker for endothelial cells. No significant difference was found in the numbers of endothelial cells present in the GMHA (7.06 ± 0.14 % area CD31-positive cells, n = 4) or in the fibrin (6.63 ± 1.10 % area CD31-positive cells, n = 9) hydrogels. No endothelial cells were associated with the agarose controls. Scale bar, 200 μm.

Our findings were similar to those involving the cytotoxicity effects of Irgacure 2959 (also called Darocur 2959) on fibroblasts [39]. At 48 h, Bryant et al. found that fibroblasts treated with 0.01% Darocur 2959 had a survival rate similar to those without treatment and that treatment with 0.1% Darocur 2959 yielded a slight decrease in viability. Although there were marked differences in the experimental procedures (e.g., cell type used), our study verified the general trend of increased cytotoxicity associated with increased Irgacure 2959 concentrations.

3.3.5 HAEC Proliferation Response to GMHA Hydrogels

The HAEC proliferation response to degraded HA and GMHA is reported in **Figure 3.7**. Since we wanted to examine GMHA's ability to promote endothelial cell proliferation relative to unmodified HA, GMHA was not crosslinked, and Irgacure 2959 and N-vinyl pyrrolidinone were not included in the proliferation experiments. We measured relative cell viabilities using methods similar to those in the cytocompatibility studies except that the absorbance values were normalized to the negative control: heat-inactivated hyaluronidase in starvation medium. Values for HA and all GMHA fragments tested were statistically similar to each other and statistically greater than that for the hyaluronidase negative control, indicating that there was an increased proliferation response to HA and that there was no significant loss of activity as a result of the conjugation chemistry. However, proliferation rates in the presence

of HA and GMHA fragments did not increase to the levels of the fully supplemented EGM-2 positive control ($p < 0.001$ in all cases), probably because the HA and GMHA fragments were diluted in the starvation medium and did not contain all of the appropriate factors required for optimal growth. Yet HA and all GMHA conjugates showed HAEC proliferation rates higher than that of the negative control, in general agreement with published studies of HA fragments [30].

3.3.6 GMHA Implants

To investigate the in vivo endothelial cell response to the crosslinked GMHA, we implanted hydrogels of 7% methacrylated GMHA subcutaneously in rats. After 2 weeks, the TECs were removed, and the tissue contained in the construct was harvested, cryosectioned, and stained with CD31-DAB and hematoxylin. Agarose (**Figure 3.8a**) was not infiltrated by cells and thus served as a suitable negative control. Cellular migration into the gel interstices was detected in the GMHA implants (**Figure 3.8b**), indicating that cells were attaching to and degrading the edge of the GMHA hydrogels. Inflammation, which was anticipated because of the biological activity of HA [14] was present but minimal. Although the GMHA hydrogels were not completely degraded at two weeks, the fibrin hydrogels (**Figure 3.8c**) were entirely degraded. The tissues in the fibrin TECs were well infiltrated by cells and highly vascularized. The percent endothelial cells at the edge of the implant measured for GMHA hydrogels (7.1 ± 0.1, $n = 4$)

was statistically indistinguishable from that for fibrin (6.6 ± 1.7, n = 9), indicating that both materials promoted similar levels of interactions with endothelial cells.

3.4 DISCUSSION

HA presents unique advantages for synthesizing healable scaffolds because of its prominent role in wound healing, as well as its natural biodegradability, ease of production and modification, and hydrophilic and nonadhesive character. Furthermore, while most natural and synthetic biomaterials possess relatively few functional side groups, HA has three reaction groups: hydroxyl, carboxyl, and acetamido. These reaction sites lend versatility to HA for modification with chemically crosslinkable groups and bioactive moieties. The aim of the research presented in this chapter was to take advantage of these distinctive properties to create a novel tissue engineering scaffold.

A variety of chemical reactions exist for HA modification (e.g., esterification, nitration, acetylation) and polymerization (based on formaldehyde, epoxide, polyisocyanate, vinyl sulfone, or carbodiimide) [18]. Bulpitt and Aeschlimann (1999) developed an in situ polymerizable HA for articular cartilage applications by synthesizing HA-aldehyde or HA-amine derivatives and crosslinking the derivatives with a variety of commercially available crosslinkers, such as bifunctional esters, and glutaraldehyde. Although this method produces HA hydrogels with a variety of properties and degradation rates, there are disadvantages: the modification procedure involves many synthesis and

purification steps, and the crosslinking reaction occurs immediately upon mixing the solutions of modified HA and crosslinker. Because HA forms highly viscous solutions, we have found that the crosslinking chemistries that occur upon mixing are hard to control and yield inconsistent gels.

Use of photopolymerizable methacrylate groups presents several advantages over other crosslinking methods. Specifically, photopolymerization avoids the disadvantages stemming from reactions that occur immediately upon solution mixing and those that depend on pH, ionic strength, or temperature. With photopolymerization, the solutions can be completely mixed before exposure to the appropriate wavelength of light, yielding a rapid, controllable, and minimally invasive crosslinking method [13,19]. Furthermore, photopolymerization can be performed under physiological conditions, which allows for either the copolymerization of bioactive molecules or the incorporation of cells. Many photopolymerization chemistries are known, but they have primarily been investigated with nondegradable synthetic polymers [13].

Several methods have been introduced for synthesizing methacrylate-modified HA, one using methacrylic anhydride [36] and others with glycidyl methacrylate (GM) [29,40]. We have found that the GM modification consistently yields methacrylate-modified HA, and that the addition of triethylamine and tetrabutyl ammonium bromide, a phase-transfer catalyst, permits a faster reaction of aqueous HA with the nonaqueous GM. We have also used acetone

precipitation to rinse out the unused reactants from GMHA, thereby avoiding the lengthy dialysis procedures used in other methods [29,40]. HAEC cytocompatibility and proliferation studies (discussed later) suggest that the excess glycidyl methacrylate, a known cytotoxic chemical, is adequately rinsed from the GMHA conjugates by the acetone precipitation step.

In our study, physical characterization of the GMHA hydrogels revealed that increasing levels of methacrylation could be used to fine-tune the swelling ratio (**Figure 3.4**), crosslink density, mesh size and complex modulus (**Table 3.3**), and degradation rate (**Figure 3.5**) within a modest range. However, we feel that manipulating any of the system variables (e.g., percent methacrylation, choice and concentration of photopolymerization reactants) will yield gels with a broader range of properties and increased cytocompatibility. For example, the range of degradation rates achieved in vitro could be broadened by variations in the crosslink density, as described above, or by the incorporation of hyaluronidase in the polymerization solution (yielding faster degradation rates).

The cytocompatibility of GMHA hydrogels is critical to the ultimate success of wound healing. We have found no statistically significant decrease in the in vitro HAEC cytocompatibility associated with the GMHA conjugates in solution (**Figure 3.6**). Treatments containing N-vinyl pyrrolidinone and GMHA in solution yielded cytocompatibilities statistically similar to that of EGM-2. However, we did note significant decreases in cell viability associated with

GMHA in the presence of higher concentrations of Irgacure 2959, similar to published work with fibroblasts [39]. Nonetheless, compared with results of a recent in vitro study of smooth muscle cell cytotoxicity in response to photopolymerizable HA [29], the GMHA hydrogels presented here were much more cytocompatible.

Once the range of cytocompatible concentrations of Irgacure 2959 and N-vinyl pyrrolidinone were determined, we sought to reconfirm that hydrogels can indeed be synthesized under such conditions (**Table 3.2**). It should be noted that in the cytotoxicity studies, Irgacure 2959 and N-vinyl-pyrrolidinone are diluted 10-fold by the cell culture medium. Therefore, the gels presented in **Figure 3.6c** were made with 0.1% Irgacure 2959 and 0.03% N-vinyl pyrrolidinone. The minimum amount of Irgacure 2959 and N-vinyl pyrrolidinone required for hydrogel formation was 0.01% and 0.03%, respectively (for 11% methacrylated GMHA, the same percentage used in the cytocompatibility studies). In other words, for the case of 11% methacrylated GMHA, the concentrations found to be cytocompatible were equal to or greater than the concentrations required for hydrogel formation.

To use crosslinked GMHA as a healable biomaterial, HA's intrinsic biological activity and role in wound healing must be retained after the methacrylate modification reaction. In the in vitro HAEC proliferation assay that we used to investigate the biological activities of HA and GMHA fragments, the

proliferation rate was enhanced by 20% in the HA fragments over the negative control (**Figure 3.7**); furthermore, no statistical difference was found in the native HA and the various GMHA methacrylation chemistries. Although this was the only in vitro method used to gauge GMHA's retention of HA's biological activity, it was a promising start for follow-up studies exploring the effects of methacrylation modifications on biologically active polymers.

In the rat subcutaneous implants used to determine the in vivo cellular response to the GMHA hydrogels (**Figure 3.8**), a small inflammatory response was associated with the GMHA implants; this response, however, is expected with high concentrations of HA and is vital for the initiation of wound healing. Also, endothelial cells infiltrated the GMHA gels, and comparable levels of these CD31-positive cells were present in both the fibrin-positive controls and the GMHA hydrogels. Future work in this area includes further modification of GMHA to promote controlled endothelial cell infiltration; for example, binding HA's carboxyl groups to the amino termini of adhesive peptide sequences, extracellular matrix molecules or growth factors via 1-ethyl-(dimethylaminopropyl) carbodiimide-mediated reactions such as those reported for peptide-alginate composites [41].

In conclusion, we report a simple method for synthesizing glycidyl methacrylate-HA conjugates. The resulting GMHA polymers were cytocompatible, photopolymerizable, and biodegradable, and they retained HA's

intrinsic biological activity in promoting endothelial cell proliferation. Furthermore, the GMHA hydrogels were comparable to fibrin in the extent to which the materials promoted interactions with endothelial cells in rat subcutaneous implants. GMHA hydrogels are, we believe, promising candidates for tissue engineering constructs that support wound healing.

3.5 REFERENCES

1. Hubbell JA. Bioactive biomaterials. *Curr Opin Biotechnol* 1999;10:123-9.
2. Ratner BD. Reducing capsular thickness and enhancing angiogenesis around implant drug release systems. *J Control Release* 2002;78:211-8.
3. Stocum DL. Regenerative biology and engineering: strategies for tissue restoration. *Wound Repair Regen* 1998;6:276-90.
4. Weisser J, Rahfoth B, Timmermann A, Aigner T, Brauer R, von der Mark K. Role of growth factors in rabbit articular cartilage repair by chondrocytes in agarose. *Osteoarthritis Cartilage* 2001;9:S48-54.
5. Draget KI, Skjak-Braek G, Smidsrod O. Alginate based new materials. *Int J Biol Macromol* 1997;21:47-55.
6. Suh JK, Matthew HW. Application of chitosan-based polysaccharide biomaterials in cartilage tissue engineering: a review. *Biomaterials* 2000;21:2589-98.

7. Cadee JA, van Luyn MJ, Brouwer LA, Plantinga JA, van Wachem PB, de Groot CJ, den Otter W, Hennink WE. In vivo biocompatibility of dextran-based hydrogels. *J Biomed Mater Res* 2000;50:397-404.
8. Pandit AS, Feldman DS, Caulfield J. In vivo wound healing response to a modified degradable fibrin scaffold. *J Biomater Appl* 1998;12:222-36.
9. Lee CH, Singla A, Lee Y. Biomedical applications of collagen. *Int J Pharm* 2001;221:1-22.
10. Cruise GM, Hegre OD, Lamberti FV, Hager SR, Hill R, Scharp DS, Hubbell JA. In vitro and in vivo performance of porcine islets encapsulated in interfacially photopolymerized poly(ethylene glycol) diacrylate membranes. *Cell Transplant* 1999;8:293-306.
11. West JL, Hubbell JA. Separation of the arterial wall from blood contact using hydrogel barriers reduces intimal thickening after balloon injury in the rat: the roles of medial and luminal factors in arterial healing. *Proc Natl Acad Sci U S A* 1996;93:13188-93.
12. Woerly S, Pinet E, De Robertis L, Bousmina M, Laroche G, Roitback T, Vargova L, Sykova E. Heterogeneous PHPMA hydrogels for tissue repair and axonal regeneration in the injured spinal cord. *J Biomater Sci Polym Ed* 1998;9:681-711.
13. Anseth KS, Burdick JA. New directions in photopolymerizable biomaterials. *MRS Bulletin* 2002;27:130-6.

14. Chen WY, Abatangelo G. Functions of hyaluronan in wound repair. *Wound Repair Regen* 1999;7:79-89.

15. Lapcik L, Jr., Lapcik L, De Smedt S, Demeester J, Chabrecek P. Hyaluronan: Preparation, Structure, Properties, and Applications. *Chem Rev* 1998;98:2663-2684.

16. Nehls V, Hayen W. Are hyaluronan receptors involved in three-dimensional cell migration? *Histol Histopathol* 2000;15:629-36.

17. West JL. Wound healing. In: Patrick Jr. CW, Mikos AG, and McIntire LV, Editor. *Frontiers in Tissue Engineering*. NY: Elsevier Science, Inc.; 1998. p. 138-51.

18. Band PA. Hyaluronan derivatives: chemistry and clinical applications. In: Laurent TC, Editor. *The Chemistry, Biology and Medical Applications of Hyaluronan and Its Derivatives*. London, UK: Portland Press Ltd.; 1998. p. 33-42.

19. Pathak CP, Sawhney AS, Hubbell JA. Rapid photopolymerization of immunoprotective gels in contact with cells and tissue. *J. Am. Chem. Soc.* 1992;114:8311-12.

20. Metters AT, Anseth KS, Bowman CN. Fundamental studies of biodegradable hydrogels as cartilage replacement materials. *Biomed Sci Instrum* 1999;35:33-8.

21. Flory PJ. *Principles of Polymer Chemistry*. Ithaca, NY: Cornell University Press; 1953.

22. Marsano E, Gagliardi S, Ghioni F, Bianchi E. Behavior of gels based on (hydroxypropyl) cellulose methacrylate. *Polymer* 2000;41:7691-7698.

23. Gekko K. Solution properties of dextran and its ionic derivatives. *Am Chem Soc Symp Ser* 1981;150:415-38.

24. Cleland RL, Wang JL. Ionic polysaccharides. III. Dilute solution properties of hyaluronic acid fractions. *Biopolymers* 1970;9:799-810.

25. Huglin MB, Rehab MM, Zakaria MB. Thermodynamic interactions in copolymeric hydrogels. *Macromolecules* 1986;19:2986-91.

26. de Jong SJ, van Eerdenbrugh B, van Nostrum CF, Kettenes-van den Bosch JJ, Hennink WE. Physically crosslinked dextran hydrogels by stereocomplex formation of lactic acid oligomers: degradation and protein release behavior. *J Control Release* 2001;71:261-75.

27. Lowman AM, Peppas NA. Hydrogels. In: Mathiowitz E, Editor. *Encyclopedia of Controlled Drug Delivery*. NY: John Wiley and Sons, Inc.; 1999. p. 397-418.

28. Cleland RL. Ionic polysaccharides. IV. Free-rotation dimensions for disaccharide polymers. Comparison with experiment for hyaluronic acid. *Biopolymers* 1970;9:811-24.

29. Trudel J, Massia SP. Assessment of the cytotoxicity of photocrosslinked dextran and hyaluronan-based hydrogels to vascular smooth muscle cells. *Biomaterials* 2002;23:3299-3307.
30. West DC, Kumar S. The effect of hyaluronate and its oligosaccharides on endothelial cell proliferation and monolayer integrity. *Exp Cell Res* 1989;183:179-96.
31. Brey EM, King TW, Johnston C, McIntire LV, Reece GP, Patrick CW, Jr. A technique for quantitative three-dimensional analysis of microvascular structure. *Microvasc Res* 2002;63:273-294.
32. King TW, Brey EM, Youssef AA, Johnston C, Patrick CW, Jr. Quantification of vascular density using a semiautomated technique for immunostained specimens. *Anal Quant Cytol Histol* 2002;24:39-48.
33. Dvorak HF, Harvey VS, Estrella P, Brown LF, McDonagh J, Dvorak AM. Fibrin containing gels induce angiogenesis. Implications for tumor stroma generation and wound healing. *Lab Invest* 1987;57:673-86.
34. van Dijk-Wolthuis WNE, Kettenes-van den Bosch JJ, van der Kerk-van Hoof A, Hennink WE. Reaction of dextran with glycidyl methacrylate: an unexpected transesterification. *Macromolecules* 1997;30:3411-3413.
35. Bulpitt P, Aeschlimann D. New strategy for chemical modification of hyaluronic acid: preparation of functionalized derivatives and their use in the

formation of novel biocompatible hydrogels. *J Biomed Mater Res* 1999;47:152-69.

36. Smeds KA, Pfister-Serres A, Hatchell DL, Grinstaff MW. Synthesis of a novel polysaccharide hydrogel. *J Macromolec Sci Pure Appl Chem* 1999;A36:981-989.
37. Delpech B, Bertrand P, Chauzy C. An indirect enzymoimmunological assay for hyaluronidase. *J Immunol Methods* 1987;104:223-9.
38. Tung JS, Mark GE, Hollis GF. A microplate assay for hyaluronidase and hyaluronidase inhibitors. *Anal Biochem* 1994;223:149-52.
39. Bryant SJ, Nuttelman CR, Anseth KS. Cytocompatibility of UV and visible light photoinitiating systems on cultured NIH/3T3 fibroblasts in vitro. *J Biomater Sci Polym Ed* 2000;11:439-57.
40. Jin Y, Yamanaka J, Sato S, Miyata I, Yomota C, Yonese M. Recyclable characteristics of hyaluronate-polyhydroxyethyl acrylate blend hydrogel for controlled releases. *J Control Release* 2001;73:173-81.
41. Rowley JA, Madlambayan G, Mooney DJ. Alginate hydrogels as synthetic extracellular matrix materials. *Biomaterials* 1999;20:45-53.

Chapter 4: GMHA-PEG-Peptide Composite Hydrogels

As discussed in **Chapter 3**, we created photocrosslinkable glycidyl methacrylate-hyaluronic acid (GMHA) hydrogel biomaterials that were cytocompatible, biologically active, and resistant to enzymatic degradation by hyaluronidase. The goal of the studies presented in this chapter was to further tune the material and biological properties of the GMHA hydrogels.

We conjugated GMHA with acrylated forms of polyethylene glycol (PEG) and PEG-peptides to yield GMHA-PEG-peptide composite hydrogels. By varying the reactant concentrations, we created solid hydrogels with high peptide conjugation efficiencies (up to 80%), controllable peptide concentrations (in the range of 1 - 6 μmol peptide per ml hydrogel), and defined physicochemical properties (e.g., swelling ratio, enzymatic degradation rate). Furthermore, when modified with a peptide containing the adhesive peptide sequence RGD, the GMHA-PEG-peptide composites are able to support increased levels of human fibroblast adhesion compared to GMHA-PEG hydrogels alone. These composite hydrogels may prove to be a promising scaffolding biomaterial for a variety of soft tissue engineering applications.

4.1 INTRODUCTION

HA, a naturally occurring glycosaminoglycan, offers many unique advantages as a building block for biomaterials [1]. For example, HA is non-immunogenic, enzymatically degradable, and relatively non-adhesive to cells and proteins [2,3]. Physiologically, HA plays a role in several processes, including angiogenesis, extracellular matrix homeostasis, wound healing, and the mediation of long-term inflammation [2]. Furthermore, HA is particularly suitable for biomaterial fabrication as it can be produced in large quantities through bacterial fermentation [3], thus avoiding the risk of the animal-derived pathogens that are possibly associated with naturally derived materials.

As discussed in **Chapter 3**, we have modified HA with glycidyl methacrylate, yielding a photocrosslinkable conjugate, GMHA [4]. The resulting polymers are cytocompatible, biologically active, and can be photocrosslinked to form GMHA hydrogels with tunable material properties (e.g., degradation rate, crosslink density). When implanted subcutaneously in rats, the GMHA hydrogels were associated with similar levels of vascularization at the implant edge as fibrin positive controls. However, in vitro studies of endothelial cell adhesion indicated that the GMHA hydrogels alone do not support cell adhesion and spreading (unpublished data). These in vitro results are in agreement with published work with similar crosslinked HA hydrogels [5], and given HA's highly hydrated and non-adhesive nature, these in vitro results are not unexpected.

A specific goal of the work presented in this chapter was to modify GMHA with peptide sequences, such as the cell adhesive fibronectin-derived sequence RGD (Arg-Gly-Asp). Work with other nonadhesive hydrogels such as polyethylene glycol (PEG) [6,7], and alginate [8] have demonstrated that covalently bound peptide sequences can be used to specifically tune cellular adhesion, migration, and proliferation. Fortunately, GMHA has several possible sites for modification, including carboxyl, hydroxyl, and acetamido groups found naturally on HA in addition to the conjugated photoreactive methacrylate groups.

Other researchers have also created crosslinked HA-RGD conjugates. For example, Glass, et al. [9] reported a periodate oxidation method to conjugate RGD onto HA hydrogel matrices. The RGD-HA matrices were associated with higher levels of osteoscarcoma cell adhesion and proliferation. However, periodate oxidation of HA opens ring structures in the glucuronic acid moieties of the polymer backbone; such changes may result in decreased biological activity or otherwise altered physicochemical properties [10]. Very recently, the Hubbell laboratory published an extensive study of the mechanical properties of HA-based hydrogels for cartilage repair [5]. The hydrogels were reinforced with low molecular weight PEG diacrylate and functionalized with acrylated PEG-RGD conjugates that were created through Michael-type addition chemistry. These examples of crosslinked HA-RGD conjugates demonstrate the growing interest in HA as scaffold materials for tissue engineering applications.

We created GMHA-peptide conjugates for soft tissue engineering applications (e.g., nerve regeneration, wound healing). To conserve cost, the model peptide hexaglycine (Gly-Gly-Gly-Gly-Gly-Gly) was used to develop three methods for GMHA conjugation. The most efficient method yielded a GMHA-PEG-peptide composite hydrogel, which was characterized in terms of its swelling and degradation properties. Finally, GMHA-PEG-RGD composites were preliminarily explored for their ability to support in vitro fibroblast adhesion.

4.2 MATERIALS AND METHODS

All materials were acquired from Sigma-Aldrich (St. Louis, MO), unless otherwise noted.

4.2.1 GMHA Conjugates

We synthesized GMHA conjugates using previously developed methods [4] (see also **Chapter 3** and the detailed protocol in **Appendix A.1**). Briefly, we prepared GMHA with 11% methacrylation by reacting a 1% (w/v) solution of fermentation-derived HA (~2 x 10^6 molecular weight, Clear Solutions Biotech, Stony Brook, NY) in distilled water with 20-fold molar excess of glycidyl methacrylate in the presence of excess triethylamine and tetrabutyl ammonium bromide. The reaction was mixed overnight at room temperature and then for 1 h at 60°C. Finally, the GMHA was precipitated in acetone and dissolved in deionized water twice and then lyophilized.

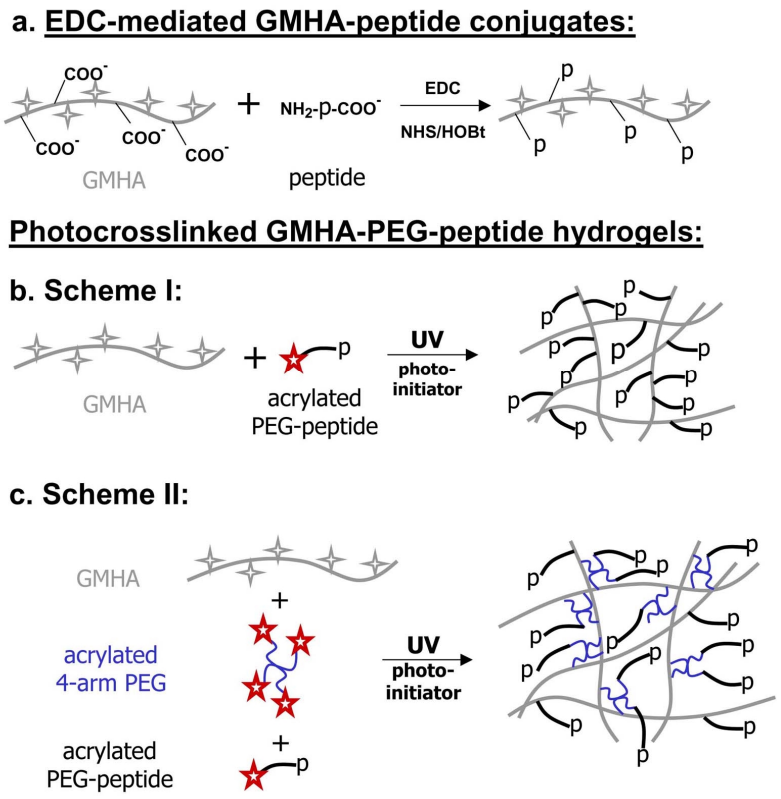

Figure 4.1 Schematic of peptide conjugation chemistries.

Three approaches were evaluated as means of covalently binding peptides (a) to uncrosslinked GMHA and (b, c) during the hydrogel crosslinking reaction. (a) GMHA, drawn schematically to denote the carboxylate groups ($-COO^-$) and methacrylate groups (4-point stars), is conjugated with peptides by a reaction mediated by EDC and an ester-activating agent (either NHS or HOBt). To incorporate peptides during the hydrogel photocrosslinking, acrylated PEG-peptides (acrylate groups are denoted by 5-pointed stars) are mixed with (b) GMHA alone or (c) GMHA and acrylated 4-arm PEG. The acrylated 4-arm PEG increases the total number of photoreactive groups in the hydrogel, effectively increasing the number of available sites for crosslinking and reaction with acrylated PEG-peptides.

4.2.2 EDC-Mediated GMHA-Peptide Conjugation

We conjugated the model peptide hexaglycine onto uncrosslinked GMHA using an EDC-mediated reaction [8,10] (shown schematically in **Figure 4.1a**; for a detailed protocol see **Appendix A.7**). All steps were carried out at room temperature. Solutions of 1% (w/v) GMHA were prepared in buffered pH 4.5 - 7.5 solutions that contained 0.1 M morpholinoethanesulfonic acid (MES) and 0.3 M NaCl. 1-hydroxybenzotriazole hydrate (HOBt; American Peptide, Sunnyvale, CA) or N-hydroxysuccinimide (NHS) was added at a 0.25, 0.5 or 1 molar ratio to GMHA's carboxylates and mixed for 5 min. Next, EDC (0.1, 0.5, 2 or 4 molar ratio to GMHA's carboxylates) was added and mixed for 5 min. Finally, hexaglycine (1.0 - 2.0 molar ratio to GMHA's carboxylates) was added and mixed for 2 h. The reaction was transferred to 7000 molecular weight cut-off dialysis tubing (Pierce, Rockford, IL), dialyzed overnight against distilled deionized water (20 times the volume of the reaction) and lyophilized. The extent of hexaglycine conjugation was determined with a ninhydrin assay as described later.

4.2.3 Photocrosslinked GMHA-PEG-Peptide Hydrogels

We also used an acrylated PEG-peptide method [6] to conjugate hexaglycine to GMHA during the crosslinking reaction. To synthesize the acrylated PEG-hexaglycine, 62 μmol of hexaglycine (2.24 ml of a 10 mg/ml stock solution of hexaglycine in 1 M HCl) was added to 15 ml of 50 mM sodium

bicarbonate buffer, pH 8.5. The pH was readjusted to 8.5 with approximately 2.2 ml of 1 M NaOH. Next, 62 μmol (0.2 g) of dry acryloyl-PEG-NHS (Nektar Therapeutics, Huntsville, AL) was added to the hexaglycine solution and mixed immediately to dissolve. The reaction was mixed for 2 h at room temperature, transferred to 1000 molecular weight cut-off dialysis tubing (Spectrum Laboratories, Rancho Dominguez, CA), and dialyzed overnight against distilled deionized water (20 times the volume of the reaction solution). The product was lyophilized and stored desiccated at -20 °C. The conjugation was verified by determining the mass of the product with Matrix-Assisted Laser Desorption/Ionization Mass Spectrometry (MALDI-MS). For a detailed protocol for conjugating peptides to acryloyl-PEG-NHS, see **Appendix A.8**.

The crosslinked GMHA-PEG-peptide hydrogels were synthesized by two reaction schemes. In the first scheme (Scheme I; shown schematically in **Figure 4.1b**), we exposed a mixture of GMHA (1% w/v or ~2.3 μmol photoreactive sites per ml in phosphate-buffered saline) and acrylated PEG-hexaglycine (approximately 1.0 - 30.0 μmol/ml) to UV light (365 nm, ~22 mW/cm^2, 60 s exposure) in the presence of the photoinitiator Irgacure 2959 (1% w/v, Ciba Specialty Chemicals, Basel, Switzerland) and N-vinyl pyrrolidinone (0.3% v/v). The second scheme (Scheme II; **Figure 4.1c**), is similar to Scheme I, except that we also added acrylated 4-arm PEG (MW 10,000; SunBio, Walnut Creek, CA) to increase the total number of photoreactive sites available in the hydrogel. The

concentrations of acrylated 4-arm PEG were 0.5, 3.5, and 4.6% (w/v), which correspond to approximately 2.1, 13.4, and 17.5 μmol photoreactive sites per ml.

4.2.4 Ninhydrin Assay

To verify the moles of peptide bound to uncrosslinked GMHA (EDC-mediated GMHA conjugation) and crosslinked GMHA-PEG-peptide hydrogels, we used the ninhydrin assay to measure the concentration of free amino acid in hydrolyzed samples [11,12] (for a detailed protocol see **Appendix A.9**). The samples and peptide standards were hydrolyzed at 1 mg/ml in 13.5 M NaOH in an autoclave (at least 40 min at 121-125°C). Next, 12.1 M HCl was carefully added drop-wise to neutralize the base. The volume was measured and the sample concentration was recorded. The hydrolyzed solution was diluted to 50 μg/ml in 0.1 M citric acid buffer, pH 4.7. The pH was measured and adjusted, if necessary.

To prepare the ninhydrin reagent, stock solutions of stannous chloride (100 mg/ml in ethylene glycol) and 4 N acetate buffer (pH 5.5-8.0) are required. The 4 N acetate buffer was made by dissolving 54.4 g sodium acetate in 100 ml acetic acid and then adjusting the total volume to 500 ml with distilled deionized water. The ninhydrin reagent was freshly prepared by dissolving 0.2 g ninhydrin in 7.5 ml ethylene glycol and 2.5 ml 4 N acetate buffer. Then 250 μl of stannous chloride solution was added with mixing. The ninhydrin reagent was only used while it was pale red in color.

In a 96-well plate, 80 µl of the hydrolyzed samples or standards and 80 µl of the ninhydrin reagent were added per well. All samples were prepared in triplicate. The well plate was covered with sealing tape (Corning Costar, Acton, MA) and incubated at 95-100°C in a water bath for 10 min. The absorbance of each well was read at 595 nm using a microplate reader (Biotek Instruments, Winooski, VT) and the amino acid content of each sample was calculated from a standard curve.

4.2.5 Swelling Ratio

To investigate the relative degrees of crosslinking in the hydrogels, we determined the swelling ratio of each sample using published methods [4] (for additional information, see **Chapter 3** and the detailed protocol in **Appendix A.2**). The swelling ratio is inversely related to the extent of crosslinking and was calculated by dividing the gel mass after swelling (M_s) by the dry gel mass (M_d). A Perkin-Elmer (Wellesley, MA) thermogravimetric analyzer (TGA) was used to measure M_s and M_d. The hydrogels were preswollen in phosphate-buffered saline overnight and a small piece (10-20 mg) was placed in the TGA weighing pan. The initial mass was recorded as M_s, and the sample was heated slowly to 100°C until a constant mass was achieved. The final mass obtained was recorded as M_d.

4.2.6 In Vitro Degradation by Hyaluronidase

We determined the enzymatic degradation rate of GMHA-PEG hydrogels using previously developed methods [4] (for a detailed protocol see **Appendix A.3**). Solutions of GMHA (1%, w/v) and acrylated 4-arm PEG (0.3, 0.6, 1.2, or 4.6%, w/v) were photocrosslinked in 8-mm diameter, 2-mm deep perfusion chamber molds (Sigma-Aldrich). The hydrogels were transferred to 24-well plates and soaked in citrate buffer (0.15 M NaCl, 0.15 M Na_2HPO_4-$7H_20$, 0.03 M citric acid, pH 5.3) overnight. The gels were removed and the gel masses were recorded. Bovine testicular hyaluronidase in citrate buffer (1.0 ml of 5 U/ml) was added to each gel and incubated at 37°C with mixing on a shaker. Every 2 h, the solution was removed and the gel masses were determined. GMHA-PEG hydrogels in citrate buffer without hyaluronidase were used as negative controls.

4.2.7 Cell Adhesion

We studied the ability of enzymatically degradable GMHA-PEG-peptide hydrogels (Scheme II; 1% GMHA, 0.5% acrylated 4-arm PEG, 0.1% Irgacure 2959, 0.03% N-vinyl pyrrolidinone) to support in vitro fibroblast adhesion. A composite of GMHA-PEG-GRGDSG (Gly-Arg-Gly-Asp-Ser-Gly; ~90% purity, synthesized by the Institute for Cellular and Molecular Biology Core Facility at The University of Texas at Austin) was compared to two negative control

hydrogels, GMHA-PEG and GMHA-PEG-hexaglycine. Each peptide was examined at 1.5 and 5 μmol/ml hydrogel.

To create a thin, flat hydrogel, 50 μl of gelation solution was placed on an 18 x 18 mm square No. 2 coverslip and covered with a 12 mm diameter circular No. 1 coverslip. The entire assembly was exposed to UV light for 2 minutes and then the coverslips were carefully separated in opposite parallel directions. In most cases, the hydrogel adhered to the top circular coverslip. If the hydrogel was homogeneous in appearance (no bubbles or tearing) and covered approximately 75% of the coverslip, it was placed in a well of a 12-well plate. The hydrogels that were torn or loosely adhered to the coverslip were excluded. The coverslips with adherent hydrogels (three samples of each hydrogel composite type) were sterilized for 10 min under UV light in a laminar flow tissue culture hood and then carefully washed for 5 min each in sterile PBS and Clonetics' fibroblast growth media-2 (FGM-2).

Clonetics adult normal human dermal fibroblasts (Cambrex, Walkersville, MD) were obtained at passage 1, used at passage 4, and maintained in FBM-2. In 1.5 ml of medium, 80,000 cells were seeded per well onto the hydrogels. After 72 hours incubation, the hydrogels were carefully washed with PBS and then the cells were imaged at 10x magnification under phase contrast using an Olympus IX-70 inverted microscope (Melville, NY). Cells adherent to the hydrogels were counted in at least three 6.6 mm^2 views per sample.

4.2.8 Statistical Analysis

We used Student's t-tests to find the statistical significance of the differences between results. A significance of $p < 0.05$ was used as the cutoff.

4.3 RESULTS

Three approaches (**Figure 4.1**) were examined as means of covalently binding peptides to GMHA. To conserve cost, hexaglycine was used as a model peptide and each approach was optimized for maximal conjugation efficiency.

4.3.1 EDC-Mediated GMHA-Peptide Conjugation

An EDC-mediated reaction was used to covalently link hexaglycine onto uncrosslinked GMHA. We investigated five reaction variables: pH, the choice and moles of ester-activating agent (e.g., NHS or HOBt) and the moles of EDC and hexaglycine. The moles of NHS, HOBt, EDC, and hexaglycine used in the reactions were expressed as the molar ratio of the component to the moles of GMHA's carboxylates (designated, for example, as EDC:GMHA $-COO^-$). A ninhydrin assay was used to measure hexaglycine conjugation for at least 2 hydrolyzed samples for each condition.

First, we examined the effect of reaction pH on EDC-mediated reactions in the presence of NHS or HOBt (**Figure 4.2a**). Reactions were carried out with 0.5 EDC:GMHA $-COO^-$, 0.25 NHS:GMHA $-COO^-$ or 0.25 HOBt:GMHA $-COO^-$, 1 hexaglycine:GMHA $-COO^-$, and pH values of 4.5, 5.5, 6.5, and 7.5. Reactions

that were carried out at pH 5.5 had the greatest conjugation efficiencies (NHS: 2.6 ± 0.5%, n = 6; HOBt: 3.0 ± 0.7%, n = 3) and were statistically different than the negative control (no EDC, NHS or HOBt: 0.4 ± 0.3%, n = 3). Reactions with NHS at pH 4.5 (1.5 ± 0.5%, n = 5) and pH 6.5 (1.8 ± 0.8%, n = 6) were also statistically different than the negative control.

Next, the effect of EDC:GMHA-COO^- was investigated (**Figure 4.2b**). Reactions were completed with 0.25 HOBt:GMHA -COO^-, 1 hexaglycine:GMHA -COO^-, and at pH 5.5. All efficiencies were statistically different from the negative control. For EDC:GMHA -COO^- values of 0.l, 0.5, 2, and 4, the respective efficiencies were 4.4 ± 1.2% (n = 4), 3.0 ± 0.7% (n = 3), 2.7 ± 0.5% (n = 4), and 1.4 ± 0.6% (n = 4). For reactions with 0.1 EDC:GMHA -COO^-, the conjugation efficiency is greater, but not statistically distinct from reactions carried out with a 0.5 EDC:GMHA -COO^-. Similarly, for reactions with 0.5 EDC:GMHA -COO^-, the conjugation efficiency is greater, but not statistically different than reactions carried out at 2.0 EDC:GMHA -COO^-. It may seem unexpected that efficiency would decrease with increasing EDC concentrations. However, it should be noted that 0.25 HOBt:GMHA -COO^- was used in each case. When the concentration of EDC is roughly equal to the concentration of HOBt, the efficiencies were higher than when EDC is in excess of HOBt. This trend reinforces published work [10], suggesting the importance of ester-activating agents in EDC-mediated HA modification reactions.

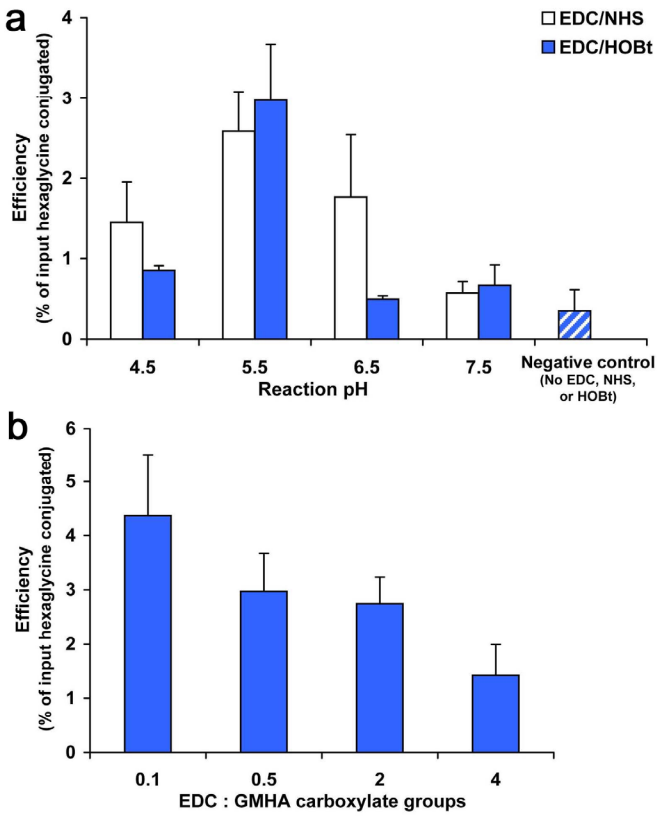

Figure 4.2 Efficiency of EDC-mediated GMHA-peptide conjugations.

The model peptide hexaglycine was conjugated onto uncrosslinked GMHA by EDC-mediated reactions. Shown are the results of three reaction variables: reaction pH, the choice of ester-activating agent (NHS, open bars; HOBt, shaded bars), and the molar ratio of EDC to GMHA's carboxylate groups. (a) Reactions that were carried out at pH 5.5 had the greatest conjugation efficiencies and were statistically greater than the negative control (no EDC, NHS or HOBt; hatched bar). Reactions with NHS at pH 4.5 and pH 6.5 were also statistically greater than the negative control. (b) The effect of the molar ratio of EDC to GMHA's carboxylate groups was investigated for reactions in the presence of HOBt. All efficiencies were statistically different from the negative control. Each bar represents the average plus the standard deviation.

The remaining variables (i.e., moles of ester activating agent and hexaglycine) were investigated at pH 5.5 and with a constant 0.5 EDC:GMHA -COO^-. We found that with 1 hexaglycine:GMHA -COO^- and NHS:GMHA -COO^- or HOBt:GMHA -COO^- varying from 0.25 to 1, the conjugation efficiencies were not statistically different and were all in the range of 1 - 3 % (data not shown). Likewise, with 0.25 HOBt:GMHA -COO^- and hexaglycine:GMHA -COO^- from 0.5 to 2, the differences in conjugation efficiencies were not statistically significant and were in the range of 1 - 3% (data not shown).

4.3.2 Photocrosslinked GMHA-PEG-Peptide Hydrogels

To incorporate the model peptide hexaglycine into GMHA hydrogels during the crosslinking reaction, two general reaction schemes were developed. For each scheme, we sought a chemistry that would yield solid hydrogels and conjugated peptide yields in the range of 1-5 μmol/ml (based on the range found to be optimal for cell adhesion and migration in similar hydrogel systems [7,13,14]).

In Scheme I, the effect of varying acrylated PEG-hexaglycine concentration was evaluated in gelation solutions of 1% (w/v) GMHA, 1% Irgacure 2959, and 0.3% (v/v) N-vinyl pyrrolidinone. For acrylated PEG-hexaglycine input concentrations above 1.4 μmol/ml, solid hydrogels did not form. We presume that in these cases, the number of photocrosslinkable sites

available on GMHA alone is not sufficient to support crosslinking as well as peptide conjugation. In previous work [4], we have found that 11% methacrylation is the highest extent of modification achievable under the chosen reaction conditions. Therefore, we sought another method of increasing the number of available photocrosslinkable sites within the gelation solution.

In Scheme II, we supplemented the total number of available photoreactive groups by adding acrylated 4-arm PEG to the gelation solutions from Scheme I. The hydrogel samples were hydrolyzed and the ninhydrin assay was used to determine the mass of conjugated hexaglycine. From this information, the conjugation efficiency (i.e., the percent of the input hexaglycine that is conjugated to the hydrogel) and yield (i.e., the concentration of peptide conjugated to the hydrogel) were calculated. In **Figure 4.3**, a single data set is shown for three concentrations of total hydrogel reactive sites (4.4, 15.7, and 19.8 μmol/ml), which are plotted versus the hexaglycine concentration in the gelation solution (**Figure 4.3a,c**) and the molar ratio of input hexaglycine to hydrogel reactive sites (**Figure 4.3b,d**). Efficiency was found to vary inversely with the moles of hexaglycine, the total number of reactive sites, and the ratio of hexaglycine to hydrogel reactive sites. Yield, on the other hand, increased with increasing hexaglycine put into the reaction, the total number of reactive sites, and the ratio of hexaglycine to hydrogel reactive sites.

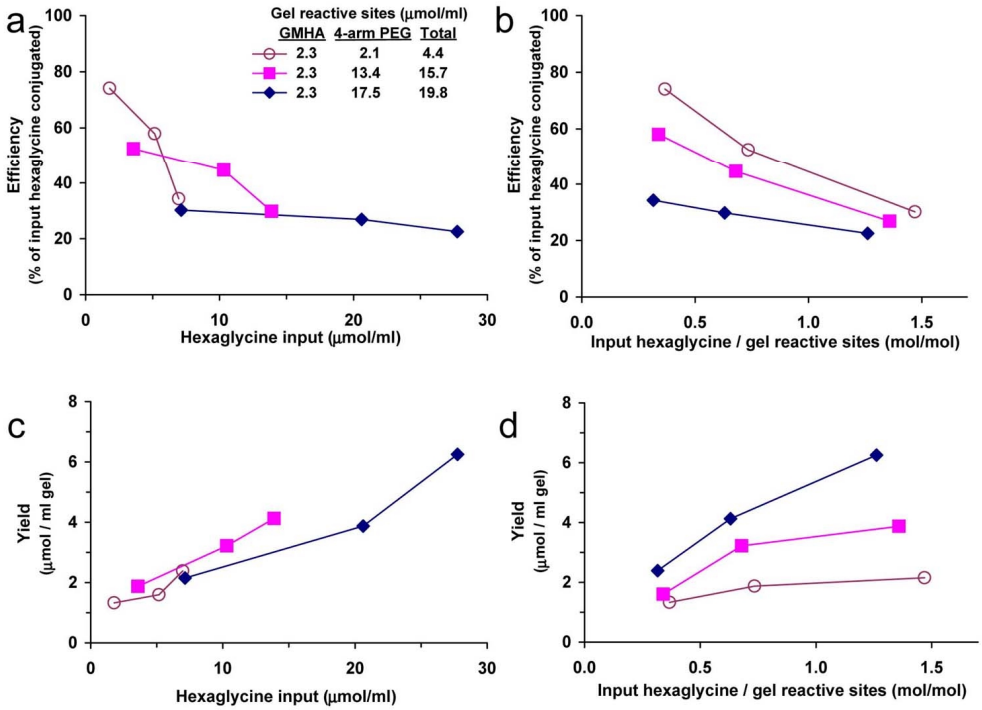

Figure 4.3 Efficiency and yield of GMHA-PEG-peptide conjugate hydrogels.

Composite hydrogels were synthesized with 1% (w/v) GMHA and varying amounts of acrylated 4-arm PEG and acrylated PEG-hexaglycine. The mass of hexaglycine conjugated was determined with the ninhydrin assay and used to calculate conjugation (a,b) efficiency (i.e., the percent of the input hexaglycine that is conjugated to the hydrogel) and (c,d) yield (i.e., the concentration of peptide conjugated to the hydrogel). A single data set is shown for 3 concentrations of hydrogel reactive sites (○, 4.4 µmol /ml; ■, 15.7 µmol /ml; ◆, 19.8 µmol /ml) and are plotted versus (a,c) µmol of hexaglycine input per ml of gelation solution and (b,d) molar ratio of input hexaglycine to hydrogel reactive sites.

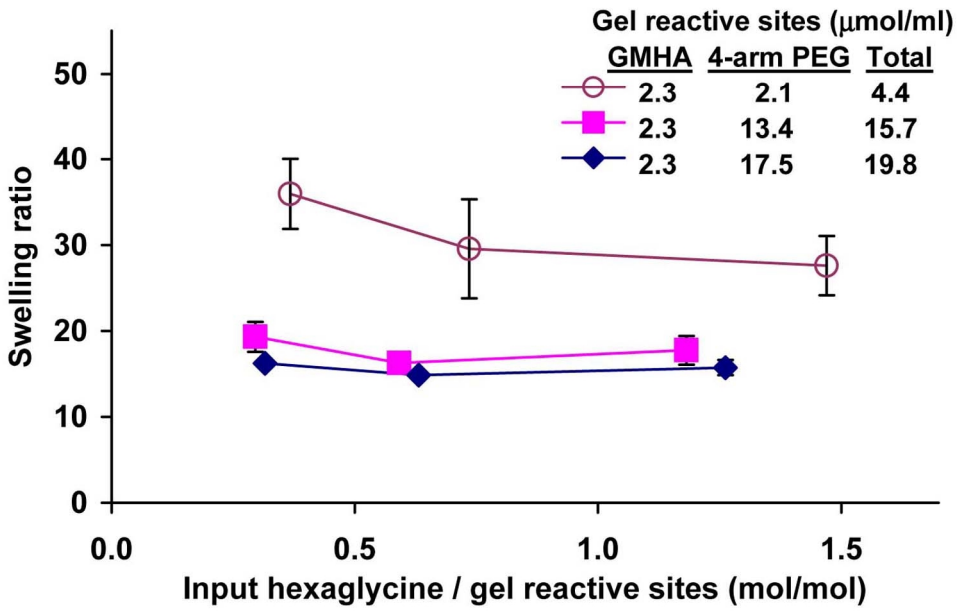

Figure 4.4 Swelling ratio of GMHA-PEG-peptide hydrogels.

The swelling ratio, calculated by the ratio of the swollen mass to the dry mass of a hydrogel, is inversely related to the hydrogel crosslink density. The swelling ratios for hydrogels with 4.4 μmol/ml reactive sites (○) are statistically greater than the hydrogels with either 15.7 (■) or 19.8 (◆) μmol/ml reactive sites. The difference in swelling ratios between the hydrogels with 15.7 μmol reactive sites per ml is not statistically distinct from the hydrogels with 19.8 μmol reactive sites per ml. Within each set of hydrogels with equal numbers of gel reactive sites, the differences in swelling ratios are not statistically significant. Each point represents the average ± standard deviation.

4.3.3 Swelling Ratio

To evaluate the effect of acrylated 4-arm PEG and PEG-hexaglycine on the relative extents of crosslinking, we determined the swelling ratio of the GMHA-PEG-hexaglycine hydrogels (**Figure 4.4**). For gels with 4.4 μmol/ml hydrogel reactive sites and 0.4, 0.7, and 1.5 molar ratios of hexaglycine to hydrogel reactive sites, the swelling ratios were 35.9 ± 4.1 (n = 2), 29.6 ± 5.8 (n = 3), and 27.6 ± 3.4 (n = 3), respectively. Gels with 15.7 μmol/ml hydrogel reactive sites and 0.3, 0.6, and 1.2 molar ratios of hexaglycine to hydrogel reactive sites, had swelling ratios of 19.3 ± 1.7 (n = 2), 16.3 ± 0.1 (n = 2), and 17.8 ± 1.7 (n = 2), respectively. For gels with 19.8 μmol/ml hydrogel reactive sites and 0.3, 0.6, and 1.3 molar ratios of hexaglycine to hydrogel reactive sites, the swelling ratios were 16.2 ± 0.1 (n = 2), 14.9 ± 0.1 (n = 2), and 15.7 ± 0.9 (n = 2), respectively.

When the total number of hydrogel reactive sites was held constant and the moles of hexaglycine put into reaction were increased, the differences in swelling ratios were not statistically different. However, the swelling ratios for hydrogels with 4.4 μmol/ml reactive sites were statistically greater than those for hydrogels with either 15.7 or 19.8 μmol/ml reactive sites. Also, the difference in swelling ratios for the hydrogels with 15.7 μmol/ml reactive sites was not statistically different from those for the hydrogels with 19.8 μmol/ml reactive sites.

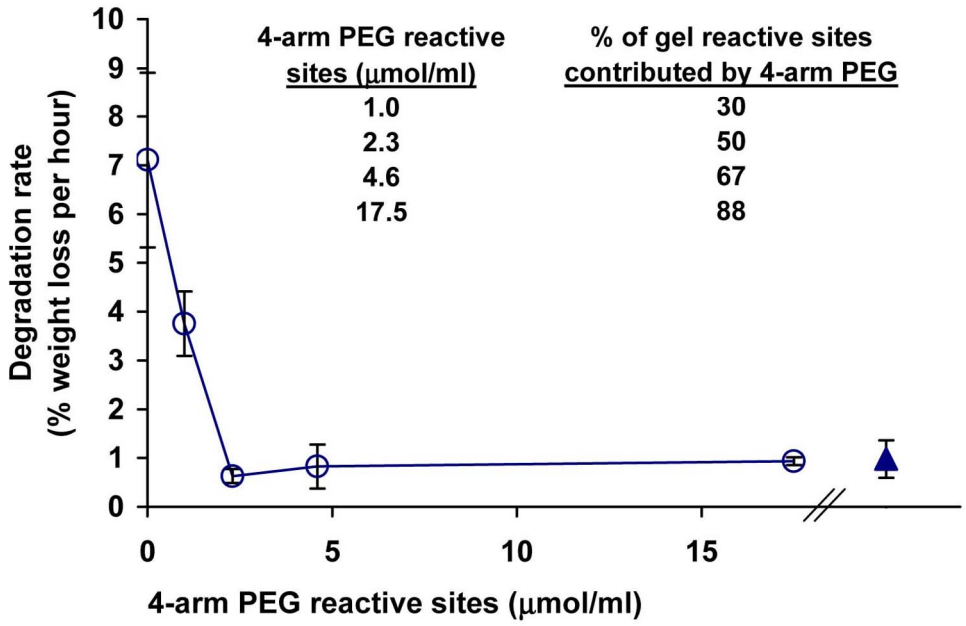

Figure 4.5 Degradation rate of GMHA-PEG hydrogels.

GMHA degrades in the presence of hyaluronidase, but PEG does not. Therefore, we sought to determine the minimum concentration of 4-arm PEG required that would render the hydrogels essentially non-degradable by hyaluronidase. Hydrogels with 1.0 μmol/ml 4-arm PEG reactive sites are degradable, while gels with 2.3 μmol/ml 4-arm PEG reactive sites are not degradable. These data suggest the GMHA-PEG hydrogels are degradable by hyaluronidase when acrylated 4-arm PEG contributes less than 50% of the total number of photoreactive groups. GMHA-PEG hydrogels in the presence of 5 U/ml hyaluronidase, ○; GMHA-PEG hydrogels in the presence of citric acid buffer alone, ▲. Each point represents the average ± standard deviation.

4.3.4 In Vitro Degradation by Hyaluronidase

In vitro degradation rates (**Figure 4.5**) of the GMHA-PEG hydrogels were determined by incubating the gels in 5 U/ml hyaluronidase and monitoring the hydrogel masses over time. GMHA degrades in the presence of hyaluronidase [4], but PEG does not. Thus, we determined the maximum concentration of acrylated 4-arm PEG beyond which the hydrogels are no longer degradable by hyaluronidase. The degradation rates for GMHA hydrogels (7.12 ± 1.80 %/hr, n = 4) and GMHA-PEG hydrogels with 1.0 μmol/ml reactive sites contributed by 4-arm PEG (3.76 ± 0.66 %/hr, n = 4) are statistically distinct and also greater than the degradation rates for the negative control (GMHA-PEG hydrogels incubated in citrate buffer alone; 0.98 ± 0.38 %/hr; n = 3) as well as the GMHA-PEG hydrogels with 2.3 μmol/ml or greater 4-arm PEG. However, hydrogels with 2.3 μmol/ml (0.63 ± 0.15 %/hr; n = 4), 4.6 μmol/ml (0.83 ± 0.45 %/hr; n = 4), and 17.5 μmol/ml (0.94 ± 0.08 %/hr; n = 2) were statistically indistinguishable from the negative control. These data indicate that the GMHA-PEG hydrogels are degradable by hyaluronidase when acrylated 4-arm PEG contributes less than 50% of the total number of photoreactive groups.

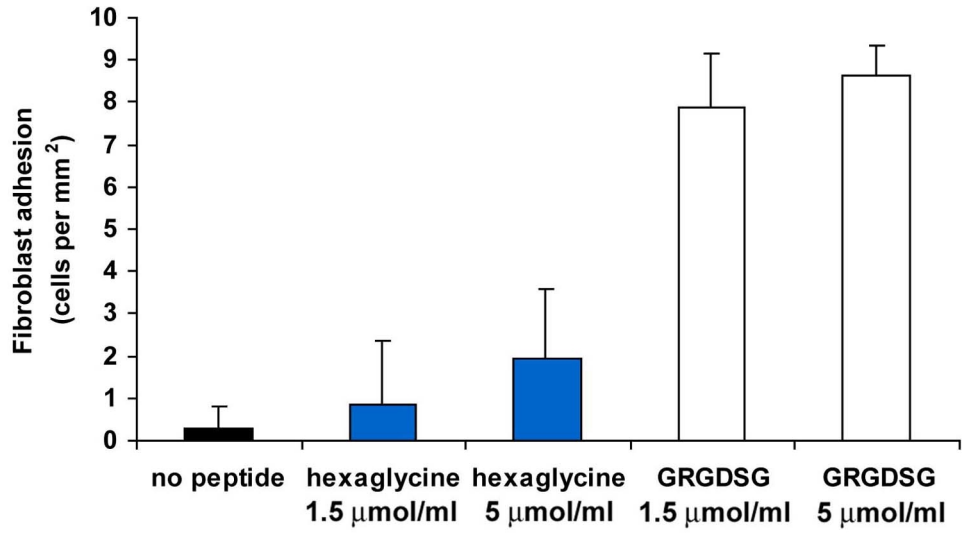

Figure 4.6 Cell adhesion on GMHA-PEG-GRGDSG hydrogels.

As a preliminary study of cell adhesion, normal human dermal fibroblasts were grown for 3 days on GMHA-PEG hydrogels alone (negative control), GMHA-PEG-hexaglycine hydrogels (negative control) and GMHA-PEG-GRGDSG hydrogels. Cell adhesion in response to both the hexaglycine- and GRGDSG-conjugated hydrogels was explored at peptide concentrations of 1.5 and 5 μmol/ml. The number of fibroblasts adhering to hexaglycine-conjugated hydrogels is not statistically different from those adhering to GMHA-PEG hydrogels without peptide. The GMHA-PEG-GRGDSG hydrogels, however, were associated with significantly greater numbers of fibroblasts adhering to their surface than either the GMHA-PEG-hexaglycine composites or the GMHA-PEG hydrogels without peptide. Each bar represents the average plus the standard deviation.

4.3.5 Cell Adhesion

To preliminarily investigate the ability of the GMHA-PEG-peptide composite hydrogels to support cell adhesion, we incubated normal human dermal fibroblasts on the gels for 3 days (**Figure 4.6**). We focused on three types of hydrogels: GMHA-PEG hydrogels (a non-peptide negative control), GMHA-PEG-hexaglycine conjugates (a non-bioactive peptide negative control) and GMHA-PEG-GRGDSG composites. Cell adhesion in response to both the hexaglycine- and GRGDSG-conjugated hydrogels was explored at peptide concentrations of 1.5 and 5 μmol/ml. The cells adhering on all GMHA-PEG hydrogels, regardless of the type of peptide, were fairly rounded in appearance. The number of fibroblasts adhering to the GMHA-PEG hydrogels (0.3 ± 0.5 cells/mm^2) was not statistically distinguishable from the number adhering to the GMHA-PEG hydrogels conjugated with either concentration of hexaglycine (1.5 μmol/ml: 0.9 ± 1.5 cells/mm^2; 5 μmol/ml: 2.0 ± 1.6 cells/mm^2). The GMHA-PEG-GRGDSG hydrogels, however, were associated with statistically greater numbers of adherent fibroblasts (1.5 μmol/ml: 7.9 ± 1.3 cells/mm^2; 5 μmol/ml: 8.6 ± 0.7 cells/mm^2).

4.4 DISCUSSION

The specific goals of the work presented in this chapter were to modify glycidyl methacrylate-HA (GMHA) hydrogels with peptide sequences and to

determine the effects of the peptide conjugation on the hydrogels' physicochemical properties. To conjugate peptides onto GMHA, we investigated three complementary techniques: an EDC-mediated reaction on uncrosslinked GMHA and two photoactivated conjugations that take place during the crosslinking reaction. The three approaches are depicted schematically in **Figure 4.1**. To conserve cost in each case, the conjugation chemistries were carried out with a model peptide, hexaglycine, and the process was optimized to maximize conjugation efficiency. We specifically chose hexaglycine for its simple chemical structure, as we intended for optimization with this peptide to serve as a stepping-stone to conjugations with more functional peptides (e.g., RGD).

First, we investigated an EDC-mediated reaction between the carboxylates of uncrosslinked GMHA and hexaglycine's primary amine (**Figure 4.2**). This seemed to be a sensible approach as EDC-mediated reactions are commonly used for conjugating carboxylates and amines [15]. However, EDC reactions are highly dependent on pH, and an excess of amine is required for high levels of modification [10,15]. Furthermore, EDC-mediated reactions with HA have been found to be particularly challenging, as they readily convert HA's carboxylate to an unreactive N-acylurea [10,16,17]. We examined a variety of reaction conditions (pH, type of ester-activating agent, and concentrations of EDC, ester-activating agent, and peptide) and found that the EDC-mediated GMHA-peptide conjugations resulted in efficiencies of less than 10%. As this low efficiency is in

agreement with other published HA studies [10,16,17], we chose to focus our attention on other conjugation techniques.

Next, we investigated two methods of incorporating peptides during the hydrogel photocrosslinking process. We hypothesized that a photoactivated reaction would allow higher conjugation frequencies as long as there are sufficient numbers of methacrylate or acrylate groups available for crosslinking as well as conjugation with acrylated PEG-peptides. Therefore, we sought to develop a chemistry that would yield solid hydrogels with conjugated peptide yields in the range of 1-5 μmol/ml. This range of peptide densities is based on those found to be optimal for cell adhesion and migration in non-adhesive PEG hydrogel systems [7,13,14].

In Scheme I, acrylated PEG-peptides were mixed in a GMHA solution with a photoinitiator (Irgacure 2959) and a reaction accelerant (N-vinyl pyrrolidinone), and exposed to UV light. The acrylated PEG-peptides are incorporated into the hydrogel as the GMHA chains crosslink together. However, the solutions did not form stable hydrogels, possibly because there was an insufficient number of GMHA methacrylates available to contribute to both crosslinking and peptide modification.

In Scheme II, we supplemented the total number of available photoreactive reactive sites by adding acrylated 4-arm PEG to the Scheme I gelation solutions. By varying the concentrations of acrylated 4-arm PEG and

acrylated PEG-peptides, we were able to synthesize hydrogels with a range of conjugation efficiencies, yields, swelling ratios, and enzymatic degradation rates.

To establish a working range of reactant concentrations, we first focused on conjugation efficiency (**Figure 4.3a,b**) and yield (i.e., the peptide concentration in the hydrogel; **Figure 4.3c,d**). We expected that for a constant peptide input concentration, greater numbers of hydrogel reaction sites available would allow higher conjugation efficiencies. But, while the Scheme II reactions more readily formed solid hydrogel-peptide conjugates than the Scheme I reactions, increased acrylated 4-arm PEG concentration did not always allow higher conjugation efficiencies. We hypothesize that in these cases, the peptide conjugation reaction could have been limited by diffusion because efficiency decreased as the gelation solutions become more concentrated. Regardless, the Scheme II GMHA-PEG-peptide composites had much higher conjugation efficiencies (20-80%, versus less than 10% for the EDC-mediated reactions) and resulted in solid hydrogels with yields within the target range of 1-5 μmol/ml.

In addition to peptide density, the hydrogel molecular structure can greatly impact cellular behavior [14,18,19]. Therefore, we measured the hydrogel swelling ratios (**Figure 4.4**) to determine the effect of varying acrylated 4-arm PEG and acrylated PEG-peptide concentrations. For a constant number of hydrogel reactive sites, increasing the concentration of acrylated PEG-peptide does not have a significant effect on swelling ratio. However, the hydrogels with

the lowest number of reactive sites (4.4 μmol/ml) have statistically greater swelling ratios than the hydrogels with greater moles of hydrogel reactive sites. This makes sense because fewer reactive sites will result in a lower crosslink density, which will be reflected by a relatively higher swelling ratio.

We also explored cell adhesion on GMHA-PEG-peptide hydrogels with human fibroblasts (**Figure 4.6**), a common model for studying cell adhesion in vitro [5,6,13]. The GMHA-PEG hydrogels conjugated with the adhesive peptide sequence GRGDSG supported increased levels of cell adhesion compared to both of the negative control hydrogels. Although the concentrations of GRGDSG used in these studies are similar to the levels used in other investigations of cell adhesion on PEG hydrogels [7,13,14], the fibroblasts adhered to the GMHA-PEG-GRGDSG hydrogels were not fully spread. However, hydrogel compliance can greatly affect cell activity [18], and because the stiffness of GMHA hydrogels [4] is much lower than hydrogels containing low molecular weight PEG [5], we hypothesize that the compliance of the GMHA-PEG hydrogels could be a limiting factor to cell adhesion. Nevertheless, we believe that the increased fibroblast adhesion on the GMHA-PEG-GRGDSG hydrogels compared to the adhesion on GMHA-PEG and GMHA-PEG-hexaglycine hydrogels are promising indications of the potential of these HA-based biomaterials. Thus, work ongoing in our laboratory will explore the possible effect of GMHA-PEG hydrogel stiffness on cell adhesion.

In conclusion, we report a simple method to conjugate adhesive peptide sequences to photocrosslinkable GMHA polymers. The properties of the GMHA-PEG-peptide composites can be tuned by varying acrylated 4-arm PEG and acrylated PEG-peptide concentration. We created solid hydrogels with high conjugation efficiencies and tunable peptide yields, as well as controllable swelling ratios and degradation rates. Furthermore, the GMHA-PEG-GRGDSG composite hydrogels are able to support higher levels of fibroblast adhesion compared to GMHA-PEG hydrogels alone. We believe that these GMHA-PEG-peptide composites provide a promising foundation for further modification and use in specific soft tissue engineering scaffolding applications.

4.5 REFERENCES

1. Baier Leach J, Schmidt CE. Hyaluronan. In: Wnek GE and Bowlin GL, editor. *Encyclopedia of Biomaterials and Biomedical Engineering*. New York, NY: Marcel Dekker; (in press).
2. Chen WY, Abatangelo G. Functions of hyaluronan in wound repair. *Wound Repair Regen* 1999;7:79-89.
3. Lapcik L, Jr., Lapcik L, De Smedt S, Demeester J, Chabrecek P. Hyaluronan: Preparation, Structure, Properties, and Applications. *Chem Rev* 1998;98:2663-2684.

4. Baier Leach J, Bivens KA, Patrick Jr CW, Schmidt CE. Photocrosslinked hyaluronic acid hydrogels: Natural, biodegradable tissue engineering scaffolds. *Biotechnol Bioeng* 2003;82:578-89.
5. Park YD, Tirelli N, Hubbell JA. Photopolymerized hyaluronic acid-based hydrogels and interpenetrating networks. *Biomaterials* 2003;24:893-900.
6. Hern DL, Hubbell JA. Incorporation of adhesion peptides into nonadhesive hydrogels useful for tissue resurfacing. *J Biomed Mater Res* 1998;39:266-76.
7. Mann BK, West JL. Cell adhesion peptides alter smooth muscle cell adhesion, proliferation, migration, and matrix protein synthesis on modified surfaces and in polymer scaffolds. *J Biomed Mater Res* 2002;60:86-93.
8. Rowley JA, Madlambayan G, Mooney DJ. Alginate hydrogels as synthetic extracellular matrix materials. *Biomaterials* 1999;20:45-53.
9. Glass JR, Dickerson KT, Stecker K, Polarek JW. Characterization of a hyaluronic acid-Arg-Gly-Asp peptide cell attachment matrix. *Biomaterials* 1996;17:1101-8.
10. Bulpitt P, Aeschlimann D. New strategy for chemical modification of hyaluronic acid: preparation of functionalized derivatives and their use in the formation of novel biocompatible hydrogels. *J Biomed Mater Res* 1999;47:152-69.
11. Starcher B. A ninhydrin-based assay to quantitate the total protein content of tissue samples. *Anal Biochem* 2001;292:125-9.

12. Gupta RK, Chang AC, Griffin P, Rivera R, Guo YY, Siber GR. Determination of protein loading in biodegradable polymer microspheres containing tetanus toxoid. *Vaccine* 1997;15:672-8.
13. Gobin AS, West JL. Cell migration through defined, synthetic ECM analogs. *FASEB J* 2002;16:751-3.
14. Shin H, Jo S, Mikos AG. Modulation of marrow stromal osteoblast adhesion on biomimetic oligo[poly(ethylene glycol) fumarate] hydrogels modified with Arg-Gly-Asp peptides and a poly(ethyleneglycol) spacer. *J Biomed Mater Res* 2002;61:169-79.
15. Hermanson GT. *Bioconjugate Techniques*. San Diego, CA: Academic Press, Inc.; 1996.
16. Ogamo A, Matsuzaki K, Uchiyama H, Nagasawa K. Preparation and properties of fluorescent glycosaminoglycuronans labeled with 5-aminofluorescein. *Carbohydr Res* 1982;105:69-85.
17. Kuo JW, Swann DA, Prestwich GD. Chemical modification of hyaluronic acid by carbodiimides. *Bioconjug Chem* 1991;2:232-41.
18. Pelham RJ, Jr., Wang Y. Cell locomotion and focal adhesions are regulated by substrate flexibility. *Proc Natl Acad Sci U S A* 1997;94:13661-5.
19. Geiger B, Bershadsky A, Pankov R, Yamada KM. Transmembrane crosstalk between the extracellular matrix--cytoskeleton crosstalk. *Nat Rev Mol Cell Biol* 2001;2:793-805.

Chapter 5: GMHA-PEG Hydrogels for Protein Delivery

As discussed in **Chapter 3**, we have created photocrosslinkable glycidyl methacrylate-HA (GMHA) hydrogel tissue engineering scaffolds that are cytocompatible, biologically active, and resistant to enzymatic degradation by hyaluronidase. The goal of the studies presented in this chapter was to characterize the release of a model protein, bovine serum albumin, from GMHA and GMHA-polyethylene glycol (PEG) hydrogels. Though BSA was released rapidly (>60% within 6 h), increased GMHA and PEG concentrations were correlated with decreased protein release rates. To lengthen the duration of release, poly(lactic-co-glycolic acid) (PLGA) microspheres containing encapsulated BSA were suspended within the hydrogel matrix. We found that this approach was suitable for extending the duration of BSA release to several weeks. These initial studies indicate that the GMHA and GMHA-PEG hydrogels and hydrogel-microsphere composites are tunable systems for delivering stable proteins in soft tissue engineering applications.

5.1 INTRODUCTION

The fields of tissue engineering and biopharmaceutics provide a number of complex opportunities for the design of new implant materials [1-5]. Each individual application relies on rationally designed scaffolds and devices that interact with living systems in a highly controlled manner. For these reasons, it is

likely that no one biomaterial will satisfy all of the design parameters in all applications.

The specific focus of our work has been soft tissue engineering applications, such as peripheral nerve repair. Ideal implants for soft tissues are degradable, porous, highly permeable, able to maintain a desired shape, and capable to specifically modulate biological responses (e.g., through bioactive factors such as covalently bound adhesive peptides or the controlled release of growth factors). In previous work, we made the first steps towards meeting these aims by creating new hydrogel scaffolds from crosslinked hyaluronic acid (HA) [6,7]. In this study, we expanded the HA-based hydrogels to create composite materials that are degradable, permeable, firm and yet pliable, and slowly release a model protein.

As described in **Chapter 3**, we have developed a new biomaterial, glycidyl methacrylate-modified HA (GMHA), which can be photocrosslinked to form a highly hydrated and degradable tissue engineering scaffold [6]. HA presents a unique combination of advantages for biomaterial formulations: it is a naturally derived, enzymatically degradable, non-immunogenic, non-adhesive, bioactive glycosaminoglycan that has been associated with several cellular processes, including angiogenesis, extracellular matrix homeostasis, and the regulation of inflammation [8]. The GMHA hydrogels were found to be enzymatically degradable, cytocompatible, and the degradation products of

GMHA retained a similar level of bioactivity as unmodified HA fragments. Further development of these GMHA hydrogels focused on methods to attach peptides (e.g., the fibronectin-derived cell adhesion sequence RGD or arg-gly-asp) [7]. Such sequences could allow control over several adhesion-related cellular processes, including migration and proliferation [9-11].

In addition to peptide sequences, encapsulated proteins can selectively alter hydrogel biofunctionality. Researchers have reported controlled protein delivery using a variety of hydrogel materials, including degradable and non-degradable forms of synthetic and naturally derived materials [12-19]. Many of these materials are able to deliver proteins over extended periods of time (days to weeks) because the diffusional properties of the hydrogels are under a fine level of control [20]. It is likely that if the release of bioactive proteins is diffusion-limited, that the diffusion of other soluble factors from the implant surroundings is also restricted. Though this design is preferred for the delivery of therapeutic proteins such as insulin [21] or antigenic proteins for vaccination [22], it poses several drawbacks for tissue engineering applications. For example, a number of regenerative processes, such as the guided growth of axons during peripheral nerve regeneration, rely on the diffusion of soluble growth factors and cytokines from the surrounding tissue [23]. Furthermore, regeneration is a highly demanding metabolic process, and the unhindered diffusion of nutrients and metabolic waste is critical for optimal cellular growth.

Aside from hydrogels, most materials designed for controlled release devices (e.g., microspheres, soluble gels, films) have structural or degradation properties that are not suitable for soft tissue scaffolds (e.g., two-dimensional or particulate structure, long degradation rates, or very quick dissolution times). Despite these challenging criteria, we were encouraged by the promising results from other HA-based strategies for controlled delivery [24-31]. Thus, our aim was to investigate protein release from our GMHA hydrogels, which were previously designed for soft tissue applications. Given that the mesh size of GMHA hydrogels is relatively large [6], we expected that protein release from these materials would be rapid. However, some tissue engineering systems, such as peripheral nerve repair, require several weeks to months to fully regenerate [32]. Therefore, we also chose to investigate hydrogel-microsphere composite release devices. Ideally, this composite system would provide greater control over protein activity and stability compared to covalently linking proteins directly to the matrix [13] and also provide advantages over methods relying on fine-tuning the hydrogel structure and diffusivity (as described above).

In this work, we incorporated a model protein, bovine serum albumin (BSA), into GMHA and GMHA-polyethylene glycol (PEG) hydrogels. The diffusional properties of BSA within the hydrogels were examined as well as the effect of the photocrosslinking chemistry on protein aggregation. To extend the duration of protein release, we also created hydrogel-microsphere composite

release systems by dispersing BSA-containing PLGA microspheres within the hydrogel solution prior to crosslinking. These preliminary studies suggest that GMHA-based hydrogels and hydrogel-microsphere composites are tunable systems for delivering stable proteins in soft tissue engineering applications.

5.2 MATERIALS AND METHODS

5.2.1 GMHA Modification and Hydrogel Photocrosslinking

We synthesized GMHA conjugates using previously developed methods [6] (for a detailed protocol see **Appendix 1**). Briefly, we made GMHA with 11% methacrylation by reacting a 1% (w/v) solution of fermentation-derived HA (~2 x 10^6 Da, Clear Solutions Biotech, Stony Brook, NY) in distilled water with 20-fold molar excess of glycidyl methacrylate in the presence of excess triethylamine and tetrabutyl ammonium bromide. The reaction was mixed overnight at room temperature and then for 1 h at 60°C. Finally, the GMHA was precipitated in acetone and dissolved in deionized water twice, and then lyophilized.

To synthesize photocrosslinked hydrogels, we exposed a gelation solution of GMHA (1-2% w/v in phosphate-buffered saline) to UV light (365 nm, ~22 mW/cm^2, 1 min exposure) in the presence of the photoinitiator Irgacure 2959 (1% w/v, Ciba Specialty Chemicals, Basel, Switzerland) and N-vinyl pyrrolidinone (0.3% v/v). To create GMHA-PEG hydrogels, 0.2 - 1.8 % (w/v) acrylated 4-arm PEG (MW 10,000; SunBio, Walnut Creek, CA) was also added to the solution.

5.2.2 Hydrogel Protein Release

To characterize the release of a model protein from the GMHA and GMHA-PEG hydrogels, 2% (w/v) BSA was dissolved in the gelation solutions prior to crosslinking. We crosslinked 50 µl of gelation solution in 8-mm diameter, 2-mm deep rubber perfusion chamber molds (Sigma-Aldrich, St. Louis, MO) and then the hydrogels were carefully transferred to empty 15-ml polypropylene tubes. Once all of the hydrogels were synthesized, 15 ml of 37°C phosphate buffered saline (PBS) with 0.1% methylparaben (a preservative) was added to each tube. The tubes were mixed end-over-end (~10 rpm) at 37°C. At specified sample collection times, 1 ml of solution was transferred to a siliconized 1.5 ml microfuge tube and the 15-ml tube was replenished with 1 ml fresh 37°C PBS. The protein content of each sample was analyzed with the Bio-Rad (Hercules, CA) protein assay using the microassay procedure. Triplicate hydrogels were analyzed in each trial and the experiment was carried out three times. The mass released at time i was calculated from equation 5.1 [28]:

$$M_i = C_i V + \sum C_{i-1} V_s \qquad (5.1)$$

where C_i is the concentration of protein in the release solution at time i, V is the total volume of release solution (15 ml) and V_s is the sample volume (1 ml).

The hydrogels used during the protein release experiments (8 mm diameter, ~1 mm thick) satisfy the infinite slab condition (length at least four

times that of the slab thickness) [33]. The volume of the release solutions was approximately 300 times the volume of the hydrogels, fitting Crank's assumptions for an infinite open system with near-zero concentration boundary conditions (at least 20-fold greater fluid volume than that of the release matrix) [34].

5.2.3 Calculation of D_e

Using the protein release data, the effective protein diffusion coefficient (D_e) was analyzed according to established methods [20,34]. Protein-loaded GMHA and GMHA-PEG hydrogels are homogeneous matrix controlled-release systems, which can be described by the following form of Fick's law of diffusion

$$\frac{\partial c}{\partial t} = D_e \frac{\partial^2 c}{\partial x^2} \qquad (5.2)$$

with the following boundary conditions:

$$c(-\delta < x < \delta, t = 0) = c_o$$
$$c(x = \pm\delta, t \geq 0) = 0$$
$$\frac{\partial c}{\partial x}(x = 0, t \geq 0) = 0$$

where c is the concentration of protein within the hydrogel, x and t are position and time of release, 2δ is the hydrogel of thickness, and c_o is the initial protein concentration in the hydrogel. For short release times ($M_t/M_\infty < 0.6$), equation 5.2 can be solved to give

$$\frac{M_t}{M_\infty} = 2\left[\frac{D_e t}{\delta^2}\right]^{1/2}\left[\frac{1}{\sqrt{\pi}} + 2\sum_{n=1}^{\infty}(-1)^n \text{ierfc}\frac{n\delta}{\sqrt{D_e t}}\right] \qquad (5.3)$$

where M_t is the mass of protein released at time t, M_∞ is the mass released at time infinity, and M_t/M_∞ is the fractional mass of released protein. Equation 5.3 can be further reduced by only using the first term (n = 1) of the summation series to give

$$\frac{M_t}{M_\infty} \cong 2\left[\frac{D_e t}{\pi\delta^2}\right]^{1/2} \qquad (5.4)$$

Therefore, the fractional release of protein released should be proportional to the square root of release time. The concentrations of released proteins at time t and at the end of the experiment (approximation of time infinity) were used to calculate M_t/M_∞, which was in turn used to calculate D_e using equation 5.4.

5.2.4 Size Exclusion Chromatography

To explore the effect of UV exposure on protein stability (i.e., aggregation), we analyzed the released protein solutions using size exclusion chromatography [35-39]. A Shimadzu (Columbia, MD) HPLC system consisted of a LC-10AT vp pump, a SIL-10A autoinjector, an APD-MI10A vp diode array detector and a 7.8 × 300 mm Protein Pak 125 column (Waters, Milford, MA). The mobile phase was a pH 7.4, 50 mM phosphate buffer containing 0.3 M sodium chloride, the flow rate was 0.5 ml/min, the sample concentrations were approximately 5 mg/ml, and the sample volume was 15 µl. The eluent was

detected using absorbance at 214 nm. Triplicate measurements were made for each sample. The amount of soluble monomer and mulitmer aggregates were determined using Peakfit (Systat Software, Richmond, CA).

5.2.5 Microsphere Synthesis

To extend the duration of protein release from the hydrogels, PLGA microspheres containing BSA were suspended in the gelation solution prior to photocrosslinking. This section describes the microsphere synthesis and the next section describes the microsphere-hydrogel protein release experiments. The BSA-PLGA microspheres were synthesized using spray freezing into liquid (SFL) [37,38] and solid-in-oil-in-oil (s/o/o) encapsulation technologies [39].

To create the solid protein phase, BSA was micronized using SFL [37,38]. Briefly, a 5 mg/ml solution of BSA in deionized water was delivered at high pressure (5000 psi) through a 65 μm nozzle. The nozzle was submerged below the surface of 1 L of liquid nitrogen to minimize the exposure of the BSA solution to air during the micronization and freezing steps. The frozen BSA particles were then lyophilized and stored at -70°C prior to encapsulation.

A previously developed s/o/o technique was adapted to encapsulate micronized BSA in PLGA microspheres [39]. To create the solid phase, 145 mg of SFL-processed BSA was placed in a glass scintillation vial and 10 ml of acetonitrile was added to make a protein suspension. A 10% (w/v) suspension of

magnesium hydroxide was passed through a 25 μm sieve and added to the protein suspension to achieve a base:protein mass ratio of 3:5. The protein-base suspension was sonicated on ice using a Branson Sonifer 450 (Branson Ultrasonics, Danbury, CT) with a 102 converter and tip operated at a duty cycle of 6 (~35 W) for 20 min in pulse mode (0.5 s on, 0.5 s off).

To create the solid-in-oil phase, a 2.5 ml aliquot of the sonicated protein suspension was dispensed into a new scintillation vial. A solution of 50% Resomer RG502H PLGA (50:50 lactic acid:glycolic acid, M_w ~7800, M_n ~4500; Boehringer Ingelheim, Ingelheim, Germany) in acetonitrile was added to bring the theoretical protein load to 5%, and the suspension was sonicated (same settings as above) for 2 min to achieve mixing. Excess acetonitrile was evaporated by immersing the vial in a room temperature water bath and blowing dry nitrogen gas over the surface of the suspension until the final concentration of solids (protein, base, and polymer) was 50% (w/v). The vial was weighed periodically during the purge step to ensure an exact reduction, and the total time of evaporation was about 30 min. To counteract potential settling of protein particles, the reduced suspension was sonicated for 20 s prior to the next step.

The microspheres were formed from the solid-in-oil phase by creating an emulsion in 9 ml of paraffin oil containing 0.5% Span 85. The emulsion was mixed and then added to 100 ml cottonseed oil containing 1% Span 85 for solvent extraction (acetonitrile is more miscible in cottonseed oil than paraffin oil). The

paraffin and cottonseed oils were mixed well, the container was sealed, and the microspheres hardened for 1 h with periodic agitation to counteract settling of the microspheres. The spheres were separated from the oil by passing through a steel mesh screen with a 25 μm cutoff, washed with hexanes, and lyophilized for 24 h.

To determine the mass of protein encapsulated in the PLGA microspheres, 5-10 mg of microspheres were added to 1 ml of acetonitrile. The PLGA was allowed to dissolve for 5 h at 37 °C, and then the samples were centrifuged (1500 g for 30 min) to pellet the protein precipitate. The supernatant was discarded and the protein was dissolved in 1 ml PBS containing 0.1% methylparaben. The protein concentration was determined using a bicinchoninic acid (BCA) microassay kit (BCA-1; Sigma-Aldrich).

5.2.6 Hydrogel-Microsphere Composites

To extend the duration of BSA release, hydrogel-microsphere composites were created. Hydrogels containing 1% (w/v) GMHA with and without 1.8% (w/v) acrylated 4-arm PEG were prepared with 2% BSA using three methods: (1) 2% BSA was dissolved in the gelation solutions prior to crosslinking (no microspheres); (2) half of the BSA (1% w/v) was dissolved in the gelation solution and the other half was contributed by BSA-PLGA microspheres, and (3) 2% BSA was provided by BSA-PLGA microspheres (no BSA in the hydrogel bulk). In the hydrogel-microsphere composites, the BSA-PLGA spheres were

suspended in the gelation solution prior to crosslinking. BSA release was determined as above. Fick's law of diffusion does not apply to this heterogeneous system; therefore, D_e was not determined for the composite hydrogels.

5.2.7 Microscopy Analysis

The PLGA microspheres, alone and suspended in the hydrogel matrix, were examined using scanning electron microscopy (SEM) and light microscopy, respectively. For SEM analysis, dry microspheres were mounted on a metal stage using double-sided carbon tape. The mounted microspheres were sputter-coated with ~30 nm of chromium and imaged with a LEO (Thornwood, NY) 1530 scanning electron microscope at 100 - 2000x magnification.

To image the density of the microspheres within the hydrogel matrix, 40 mg of BSA-PLGA microspheres were suspended in 0.1 ml gelation solution and then crosslinked under UV light. Images were captured at 20x magnification under brightfield microscopy using an Olympus IX70 microscope (Melville, NY) and an Optronics Magnafire camera (Goleta, CA).

5.2.8 Statistical Analysis

We performed Student's t-tests to determine the statistical significance of the differences between results. A significance level of $p < 0.05$ was used as the cutoff.

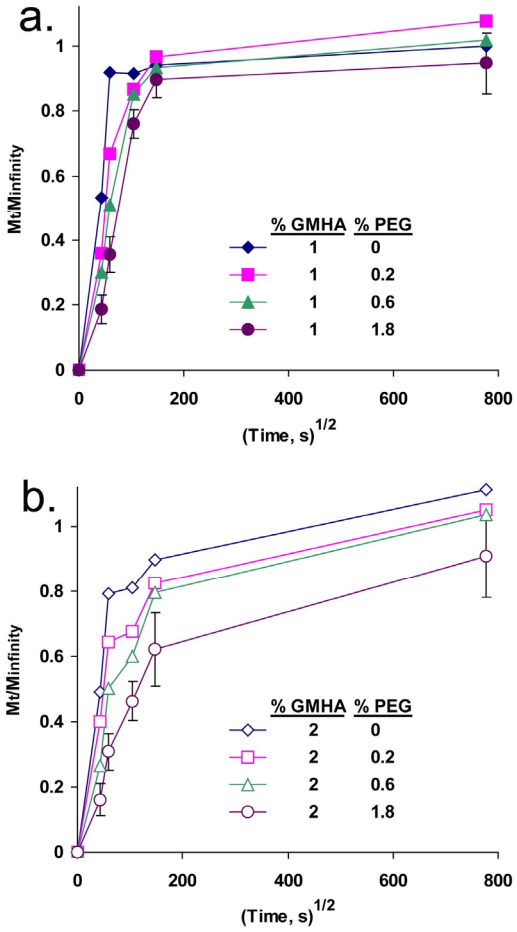

Figure 5.1 Release profiles of BSA from GMHA and GMHA-PEG hydrogels.

Hydrogels (50 µl; 8 mm diameter, ~1 mm thick) containing 2% w/w BSA, various concentrations of acrylated 4-arm PEG and (a) 1% w/w GMHA or (b) 2% GMHA were incubated at 37°C with mixing in 15 ml PBS with 0.1% methylparaben. Although each hydrogel released at least 60% of the BSA within 6 h, hydrogels with increased concentrations of GMHA and PEG were associated with slower release rates. Triplicate hydrogels were analyzed and each data point represents the average fractional release of BSA (M_t/M_∞) at each time, t for one experimental trial. The standard deviations for all data points are less than 0.2 and are arbitrarily shown for the 1.8% PEG hydrogels to indicate a representative level of error for all samples.

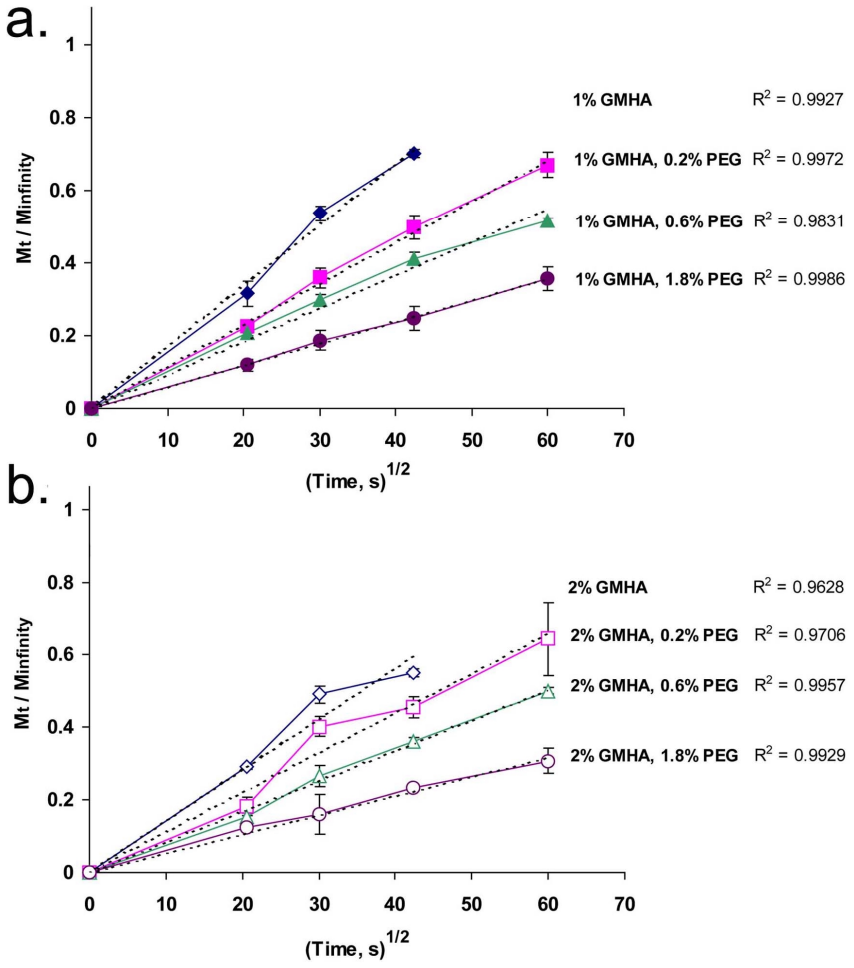

Figure 5.2 Linear fits of the hydrogel release profiles at $M_t/M_\infty < 0.6$.

Hydrogels (50 µl; 8 mm diameter, ~1 mm thick) containing 2% w/w BSA, various concentrations of acrylated 4-arm PEG, and (a) 1% w/w GMHA or (b) 2% GMHA were incubated at 37°C with mixing in 15 ml PBS with 0.1% methylparaben. Triplicate hydrogels were analyzed in each trial and the experiment was repeated three times (total n = 9). Each data point represents the average ± standard deviation of the fractional release of BSA (M_t/M_∞) at each time, t.

5.3 RESULTS

5.3.1 Protein Release From GMHA Hydrogels and D_e Calculations

The release of BSA from GMHA-based hydrogels was determined through two experiments. In all cases, triplicate hydrogels of each type were examined. The goal of the first experiment was to determine the duration of protein release and the total mass that is released in this time period. Samples were taken for up to 1 week, at which time it was assumed that all of the protein had been released. The percent of original BSA mass that was released from the hydrogels was 53.2 ± 5.04% and did not correlate with the concentration of either GMHA or PEG. As shown in **Figure 5.1**, each hydrogel type released >60% of the BSA within 6 h. Notably, hydrogels with increased concentrations of GMHA and PEG were associated with slower release rates.

A second set of experiments was used to determine D_e. Because equations 5.3 and 5.4 only apply for $M_t/M_\infty < 0.6$, we focused on the first 6 h of release. Each trial was repeated three times (n = 9 for each hydrogel). For each trial and hydrogel type, the average M_t/M_∞ was plotted versus the square root of release time ($t^{1/2}$). Linear fits were calculated with Microsoft Excel (Redmond, WA); representative results are shown for one trial in **Figure 5.2**. The slopes from three trials were averaged and used to calculate D_e and the normalized diffusivity, D_e/D_o (**Table 5.1**). The values of D_e ranged from 0.85×10^{-7} to 4.54×10^{-7} cm^2/s and decreased with increasing concentrations of GMHA and PEG (**Figure 5.3**).

Table 5.1 D_e and D_e/D_o of BSA in GMHA and GMHA-PEG hydrogels

Weight % GMHA	Weight % acrylated 4-arm PEG	D_e x 10^7 (cm^2/s)	D_e/D_o*
1	0	4.54 ± 0.42	0.48 ± 0.04
1	0.2	3.38 ± 0.91	0.36 ± 0.10
1	0.6	2.25 ± 1.02	0.24 ± 0.11
1	1.8	1.43 ± 0.93	0.15 ± 0.10
2	0	3.75 ± 0.50	0.40 ± 0.05
2	0.2	2.34 ± 0.55	0.25 ± 0.06
2	0.6	1.88 ± 0.57	0.20 ± 0.06
2	1.8	0.85 ± 0.36	0.09 ± 0.04

*D_o (infinite-dilution diffusion coefficient), BSA in water at 37°C: 9.14 x 10^{-7} cm^2/s [40]

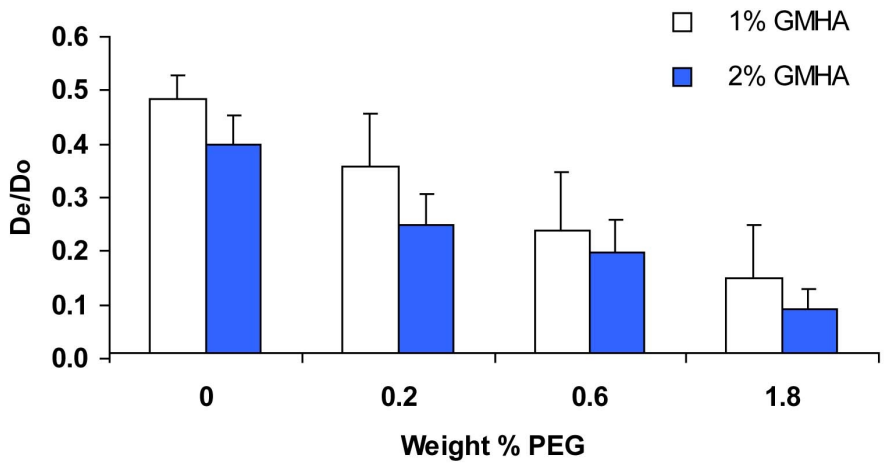

Figure 5.3 Normalized effective diffusion coefficients for BSA in GMHA and GMHA-PEG hydrogels.

Based on the linear fits in **Figure 5.2** and equation 5.4, we calculated the effective diffusion coefficient (D_e) for each type of hydrogel. The normalized diffusivity (D_e/D_o) was obtained by dividing D_e by the infinite-dilution diffusion coefficient of BSA in water (D_o), which is 9.41 x 10^{-7} cm^2/s at 37°C [40]. Each bar represents the mean plus the standard error of the mean.

Table 5.2. Effect of photopolymerization on the physical state of BSA following release from GMHA and GMHA-PEG hydrogels

		% Monomer in Released Protein
Weight % GMHA	**Weight % PEG**	
1	0	93.3 ± 0.04
1	1.8	93.9 ± 0.33
2	0	91.4 ± 0.31
2	1.8	91.7 ± 1.67
BSA Standard		84.7 ± 2.4

5.3.2 Analysis of the Physical State of the Released BSA

Exposure to UV light and crosslinking agents could affect protein structure and stability [41]. Possible effects of this process include protein denaturation, aggregation, hydrolysis, and reaction with the crosslinking agents, all of which could decrease the activity of encapsulated proteins. Therefore, we preliminarily explored the effect of photopolymerization on the physical state of encapsulated BSA using size exclusion chromatography (**Table 5.2**).

The molecular weight of the BSA in the release solutions was determined for a hydrogel sub-set (combinations of 1% and 2% GMHA and 0% and 1.8% PEG) and was compared to the original BSA in solution (i.e., a BSA standard). The BSA in each of the release solutions was >90% monomer (<10% oligomers), while the BSA standard contained 84.7 ± 2.4% monomer (15.3 ± 2.4% oligomers). Therefore, the released BSA was enriched with monomer compared to the original protein. Small fragments were not detected, which indicated that significant amounts of hydrolyzed BSA are not being released from the hydrogels.

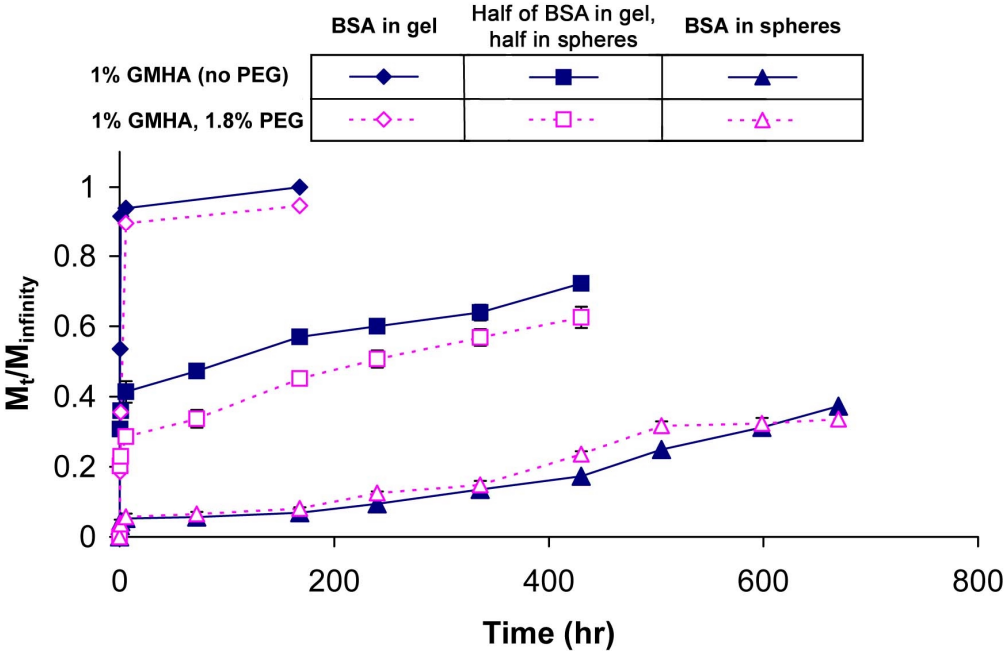

Figure 5.4 Release of BSA from hydrogel-microsphere composite systems.

Hydrogels (50 µl; 8 mm diameter, ~1 mm thick) containing 1% (w/v) GMHA alone (solid symbols) and with 1.8% (w/v) acrylated 4-arm PEG (open symbols), were prepared with 2% (w/v) BSA using three different methods: (1) as in earlier experiments, 2% BSA was dissolved in the gelation solutions prior to photocrosslinking (no microspheres; diamond symbols); (2) half of the BSA (1% w/v) was dissolved in the gelation solution and the other half was contributed by BSA-PLGA microspheres (square symbols), and (3) 2% BSA was provided by BSA-PLGA microspheres (triangle symbols). In the hydrogel-microsphere composites, the BSA-PLGA spheres were suspended in the gelation solution prior to photocrosslinking. Triplicate hydrogels were analyzed and each data point represents the average ± standard deviation of the fractional release of BSA (M_t/M_∞) at each time, t.

5.3.3 BSA Release From Hydrogel-Microsphere Composite Systems

To extend the duration of BSA release from the GMHA and GMHA-PEG hydrogels, PLGA microspheres containing 5% (w/w) BSA were suspended within the gelation solution prior to photocrosslinking. We obtained the release profiles (**Figure 5.4**) for three types of hydrogels: (1) 2% (w/v) BSA dissolved in the hydrogels (no microspheres), (2) half of the BSA (1%) in the hydrogel and half (1%) contained in BSA-PLGA microspheres, and (3) 2% BSA provided by the BSA-PLGA microspheres (no BSA dissolved in the hydrogel). In each case, the original total amount of BSA in the hydrogel or hydrogel-microsphere composite was 2% (weight BSA per total volume of the hydrogel or hydrogel-microsphere composite). Upon gross inspection, the microspheres did not seem to impair the photocrosslinking process and the vast majority of the microspheres remained embedded within the hydrogels for the duration of the release experiment. However, the presence of microspheres during the crosslinking process could affect the hydrogel properties (e.g., degradation rate, crosslink density); further studies would be required to study these effects in detail.

As expected, the hydrogels without microspheres released all of the embedded BSA within 6 h. For the hydrogel-microsphere composites where the entire amount of BSA is provided by the BSA-PLGA microspheres, ~5% of the embedded BSA is released in the first day and then 30-40% of the remaining encapsulated BSA is released within 4 weeks. For the middle case, where half of

the BSA is dissolved in the hydrogel and the other half is encapsulated in the BSA-PLGA microspheres, a rapid release of 30-40% of the BSA is released within the first day, and then 60-70% of the remaining BSA is released within 18 days.

5.3.4 Microscopy

SEM analysis (**Figure 5.5a,b**) verified that the average size of the BSA-PLGA microspheres is ~10-25 μm in diameter and also showed that the surface of the microspheres is smooth and relatively non-porous. Light microscopy of the hydrogel-microsphere composites (**Figure 5.5c**) confirmed that the microspheres were dispersed throughout the thickness of the hydrogel.

5.4 DISCUSSION

The first goal of this work was to characterize the release of a model protein, BSA, from GMHA and GMHA-PEG hydrogel scaffolds. These materials have previously been shown to be photocrosslinkable, biocompatible, bioactive, enzymatically degradable, porous, and highly hydrated [6,7]. We found that the release rate of BSA from the hydrogels to be rapid (>60% release within 6 h; **Figure 5.1**). This was not surprising, as the mesh size of GMHA hydrogels has been estimated to be on the order of several hundred nm [7], which is much larger than the dimensions of BSA (approximately 4.2 nm in diameter and 14.4 nm long [42]).

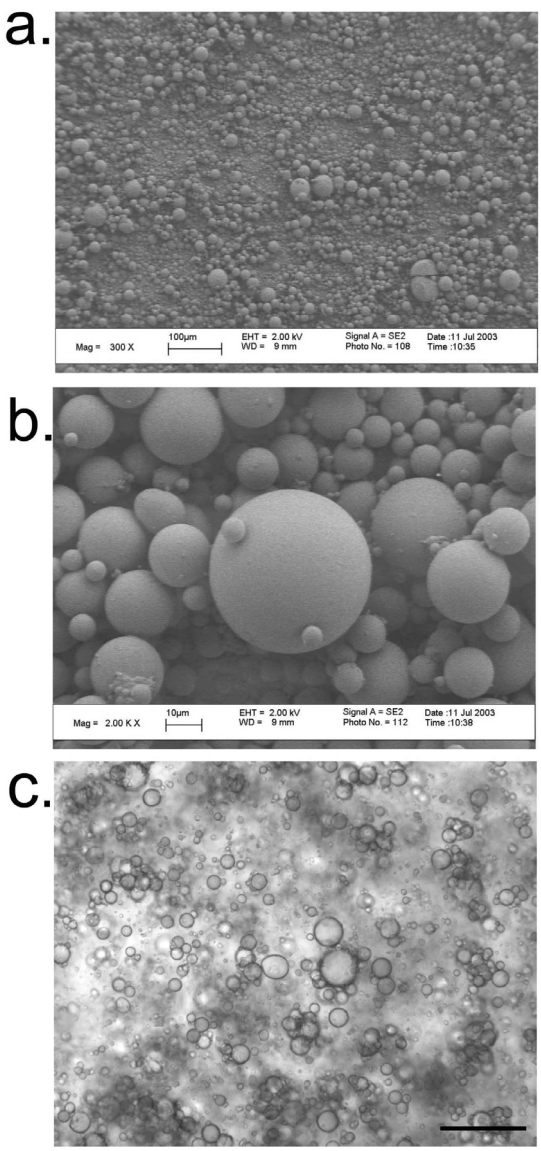

Figure 5.5 Microscopy images of BSA-PLGA microspheres alone and embedded in a GMHA hydrogel.

SEM images of dry sputter-coated BSA-PLGA microspheres were captured at (a) 300x magnification (scale bar, 100 µm) and (b) 2000x magnification (scale bar, 10 µm). (c) Light microscopy was used to image 40 mg/ml BSA-PLGA microspheres embedded in crosslinked GMHA hydrogel (scale bar, 100 µm).

Table 5.3: Comparison of D_e and D_e/D_o of BSA released from GMHA and GMHA-PEG hydrogels with literature

Matrix	Solute	Conditions	$D_e \times 10^7$ (cm^2/s)	D_e/D_o	Reference
GMHA hydrogels	BSA	37°C, in PBS	0.85 - 4.54	0.09 - 0.48	See Table 5.1
Polyvinyl alcohol membranes	BSA	37°C, in water	0.18 - 8.07	0.02 - 0.86 *	[43]
Polyacrylamide hydrogels	BSA	37°C, in PBS	~0.5 - ~2	~0.05 - ~0.2 *	[12]
PEG-diacrylate (2000 Da) hydrogels	BSA	37°C, in PBS	0.005	0.0005	[44]
PEG-diacrylate (575 Da) hydrogels	BSA	37°C, in PBS	< 0.004	<0.0005	[16]
GMHA-PHEA hydrogels	Sodium benzoate	25°C, in water	1.2 - 69.5	0.01 - 0.632	[28]

Abbreviations: Effective diffusion coefficient (D_e), diffusion coefficient in water (D_o), bovine serum albumin (BSA), glycidyl methacrylate (GM), hyaluronic acid (HA), phosphate buffered saline (PBS), polyethylene glycol (PEG), polyhydroxyethyl acrylate (PHEA)

* D_e/D_o was not reported in original references and were calculated from reported D_e and D_o = 9.41 x 10^{-7} cm^2/s for BSA at 37°C [40]

An effective method of comparing the protein release from different hydrogel materials is to calculate the effective diffusion coefficient, D_e [20]. The values of D_e for BSA released from GMHA and GMHA-PEG hydrogels ranged from 0.85 x 10^{-7} - 4.54 x 10^{-7} cm^2/s, which is within the range that is typically found for diffusion through rubbery polymers [20]. We found that there is a significant decrease in D_e for these systems compared to the infinite-dilution diffusion coefficient, D_o, for BSA in water at the same temperature (**Table 5.1**). Hydrogels with decreased hydrogel water content (increased concentrations of GMHA or PEG) were associated with lower values of D_e (**Figure 5.3**), in agreement with published work with other release systems [45]. Furthermore, the D_e/D_o values are also in general agreement with other similar release systems (examples summarized in **Table 5.3**). Notable exceptions are the remarkably low D_e/D_o values obtained for non-degradable low molecular weight PEG hydrogels [16,44]. These highly crosslinked hydrogels are ideal for the delivery of biopharmaceutic proteins; for soft tissue engineering applications, however, such materials could be associated with potential drawbacks (e.g., non-degradable, highly crosslinked structure that impedes the diffusion cellular nutrients, endogenous signaling molecules, and metabolic waste).

As the GMHA hydrogels are crosslinked in the presence of BSA, we were interested in determining whether the crosslinking agents or the exposure to UV light affects protein stability. We carried out preliminary studies to evaluate the presence of BSA aggregates in the release solutions using size exclusion chromatography. We found that the release solutions were, in fact, enriched in the

monomer form of BSA compared to the BSA standards (**Table 5.2**). Additionally, only about 53% of the BSA in the uncrosslinked gelation solutions is released from the hydrogels. We hypothesize that the hydrogels may selectively allow the release of the lower molecular weight monomer, while larger aggregates are retained. Similar effects have also been noted for PLGA microspheres [36]. However, these data do not preclude the fact that the BSA could be bound to the hydrogel matrix via reaction with the crosslinking reagents, free radical addition, or a Michael-type addition between lysine amino acids in the protein and acrylate or methacrylate groups in the polymers [16]. The BSA also could have nonspecifically adsorbed to the release vial surfaces or formed complexes with HA [46] or PEG [47]. Further investigation of the BSA structure within the hydrogel, using a technique such as fourier-transform infrared spectrometry (FTIR) [16,38], may help to clarify this issue.

The second goal of this work was to extend the duration of protein release from the GMHA hydrogels. We were particularly interested in methods that preserve the native protein structure and also provide a versatile method of fine-tuning the protein release rate. The simplest method of extending protein release is to decrease the diffusivity of the materials by decreasing the hydrophilicity [48] or diffusivity [45] of the hydrogel structure. Covalently linking the protein to the hydrogel matrix is another method to slow down protein delivery [13]. Each of these methods has been applied towards modifying HA for drug delivery applications [31], but as mentioned earlier, these methods pose drawbacks for tissue engineering applications.

A composite hydrogel-microsphere system, on the other hand, poses significant advantages for the controlled release of therapeutic proteins from a three dimensional matrix. Foremost, sustained release from microspheres is one of the most extensively studied and clinically utilized systems for delivering one-time injectable drugs or proteins [49]. Recent research focusing on protein delivery from microspheres has made great progress towards meeting this system's primary technical challenges: high protein stability and minimal rapid early release (i.e., "burst") [17,48]. In particular, work at The University of Texas at Austin by Drs. Keith P. Johnston and Robert O. Williams, III in the departments of Chemical Engineering and Pharmaceutics, have developed new methods for increasing the effectiveness of microencapsulated proteins. Two techniques in particular, a novel spray freezing into liquid (SFL) protein preparation [37,38] and an improved solid-in-oil-in-oil (s/o/o) microsphere synthesis have been used in conjunction to stabilize proteins with the virtual elimination of rapid early release [39]. These techniques circumvent air-water and water-organic interfaces, which have been linked to protein denaturation in other encapsulation techniques such as spray freeze drying of proteins [50] and the water-in-oil-in-water (w/o/o) double emulsion process [36,51,52].

To extend the duration of BSA release from the GMHA and GMHA-PEG hydrogels, BSA-PLGA microspheres were created with SFL-prepared BSA and the s/o/o encapsulation process. Magnesium hydroxide was also encapsulated in

the PLGA microspheres; this poorly water-soluble base has been demonstrated to prevent the acid denaturation associated with the acidic environment within degrading PLGA microspheres [53]. As expected, the BSA-PLGA microspheres extended the duration of release in a dose-dependent fashion (**Figure 5.4**). Hydrogel-microsphere composites with half of the BSA in the hydrogel and half in the PLGA microspheres were associated with a two phase release profile: a rapid release phase within the first day and an extended release phase lasting several weeks. Such a release profile may be advantageous for applications such as peripheral nerve regeneration that could benefit from an early release of anti-inflammatory or angiogenic factors and an extended release of a neurotrophic factor such as nerve growth factor.

In conclusion, we report a characterization of the protein release from GMHA and GMHA-PEG hydrogels as well as hydrogel-microsphere composite systems. The hydrogel release profiles were rapid, but could be controlled by varying the GMHA and PEG concentrations. Preliminary studies suggest that the BSA released from the hydrogel matrices is almost entirely released in the monomeric form, indicating that the photocrosslinking step does not contribute to high amounts of protein aggregation. However, more detailed studies will be required to confirm these results. Finally, BSA-PLGA microspheres synthesized using SFL-processed BSA and a non-aqueous s/o/o technique were shown to extend the duration of BSA release from hydrogel-microsphere composites to

several weeks. These initial studies indicate that these GMHA and GMHA-PEG hydrogels and hydrogel-microsphere composites are tunable systems for delivering stable proteins in soft tissue engineering applications. Future work will examine the effect of the microspheres on the hydrogel degradation and the in vitro cellular response to the microsphere-hydrogel composite systems releasing bioactive proteins, such as growth factors.

5.5 REFERENCES

1. Hubbell JA. Biomaterials in tissue engineering. *Biotechnology (NY)* 1995;13:565-76.
2. Ratner BD. Reducing capsular thickness and enhancing angiogenesis around implant drug release systems. *J Control Release* 2002;78:211-8.
3. Griffith LG, Naughton G. Tissue engineering--current challenges and expanding opportunities. *Science* 2002;295:1009-14.
4. Kim BS, Mooney DJ. Development of biocompatible synthetic extracellular matrices for tissue engineering. *Trends Biotechnol* 1998;16:224-30.
5. Lee KY, Mooney DJ. Hydrogels for tissue engineering. *Chem Rev* 2001;101:1869-79.
6. Baier Leach J, Bivens KA, Patrick Jr CW, Schmidt CE. Photocrosslinked hyaluronic acid hydrogels: Natural, biodegradable tissue engineering scaffolds. *Biotechnol Bioeng* 2003;82:578-89.

7. Baier Leach J, Bivens KA, Collins CN, Schmidt CE. Development of photocrosslinkable hyaluronic acid-polyethylene glycol-peptide composite hydrogels for soft tissue engineering. *J Biomed Mater Res* (submitted).
8. Baier Leach J, Schmidt CE. Hyaluronan. In: Wnek GE and Bowlin GL, Editor. *Encyclopedia of Biomaterials and Biomedical Engineering*. New York: Marcel Dekker; (in press).
9. Hern DL, Hubbell JA. Incorporation of adhesion peptides into nonadhesive hydrogels useful for tissue resurfacing. *J Biomed Mater Res* 1998;39:266-76.
10. Mann BK, West JL. Cell adhesion peptides alter smooth muscle cell adhesion, proliferation, migration, and matrix protein synthesis on modified surfaces and in polymer scaffolds. *J Biomed Mater Res* 2002;60:86-93.
11. Rowley JA, Mooney DJ. Alginate type and RGD density control myoblast phenotype. *J Biomed Mater Res* 2002;60:217-23.
12. Davis BK. Diffusion in polymer gel implants. *Proc Natl Acad Sci U S A* 1974;71:3120-3.
13. Gombotz WR, Pettit DK. Biodegradable polymers for protein and peptide drug delivery. *Bioconj Chem* 1995;6:332-351.
14. Hubbell JA. Hydrogel systems for barriers and local drug delivery in the control of wound healing. *J Control Release* 1996;39:305-313.
15. Lowman AM, Peppas NA. Solute transport analysis in pH-responsive, complexing hydrogels of poly(methacrylic acid-g-ethylene glycol). *J Biomater Sci Polym Ed* 1999;10:999-1009.

16. Mellott MB, Searcy K, Pishko MV. Release of protein from highly cross-linked hydrogels of poly(ethylene glycol) diacrylate fabricated by UV polymerization. *Biomaterials* 2001;22:929-41.
17. Cleland JL, Daugherty A, Mrsny R. Emerging protein delivery methods. *Curr Opin Biotechnol* 2001;12:212-9.
18. Bos GW, Verrijk R, Franssen O, Bezemer JM, Hennink WE, Crommelin DJA. Hydrogels for the controlled release of pharmaceutical proteins. *Pharm Technol N Am* 2001;25:110-120.
19. Hatefi A, Amsden B. Biodegradable injectable in situ forming drug delivery systems. *J Control Release* 2002;80:9-28.
20. Narasimhan B, Mallapragada SK, Peppas NA. Release kinetics, data interpretation. In: Mathiowitz E, Editor. *Encyclopedia of Controlled Drug Delivery*. New York: John Wiley & Sons; 1999. p. 921-35.
21. Saffran M, Kumar GS, Savariar C, Burnham JC, Williams F, Neckers DC. A new approach to the oral administration of insulin and other peptide drugs. *Science* 1986;233:1081-4.
22. Andrianov AK, Chen J, Payne LG. Preparation of hydrogel microspheres by coacervation of aqueous polyphosphazene solutions. *Biomaterials* 1998;19:109-15.
23. Politis MJ, Ederle K, Spencer PS. Tropism in nerve regeneration in vivo. Attraction of regenerating axons by diffusible factors derived from cells in distal nerve stumps of transected peripheral nerves. *Brain Res* 1982;253:1-12.

24. Larsen NE, Balazs EA. Drug delivery systems using hyaluronan and its derivatives. *Adv Drug Deliv Rev* 1991;7:279-93.
25. Ghezzo E, Benedetti L, Rochira M, Biviano F, Callegaro L. Hyaluronane derivative microspheres as NGF delivery devices: Preparation methods and in vitro release characterization. *Int J Pharm* 1992;87:21-9.
26. Simon LD, Stella VJ, Charman WN, Charman SA. Mechanisms controlling diffusion and release of model proteins through and from partially esterified hyaluronic acid membranes. *J Control Release* 1999;61:267-79.
27. Inukai M, Jin Y, Yomota C, Yonese M. Preparation and characterization of hyaluronate-hydroxyethyl acrylate blend hydrogel for controlled release device. *Chem Pharm Bull (Tokyo)* 2000;48:850-4.
28. Jin Y, Yamanaka J, Sato S, Miyata I, Yomota C, Yonese M. Recyclable characteristics of hyaluronate-polyhydroxyethyl acrylate blend hydrogel for controlled releases. *J Control Release* 2001;73:173-81.
29. Kim MR, Park TG. Temperature-responsive and degradable hyaluronic acid/Pluronic composite hydrogels for controlled release of human growth hormone. *J Control Release* 2002;80:69-77.
30. Kim HD, Valentini RF. Retention and activity of BMP-2 in hyaluronic acid-based scaffolds in vitro. *J Biomed Mater Res* 2002;59:573-84.
31. Vercruysse KP, Prestwich GD. Hyaluronate derivatives in drug delivery. *Crit Rev Ther Drug Carrier Syst* 1998;15:513-55.
32. Jacobsen S, Guth L. An electrophysiological study of the early stages of peripheral nerve regeneration. *Exp Neurol* 1965;11:48-60.

33. Chorny RC, Krasuk JH. Extraction for different geometries. *Ind Eng Chem Process Des Dev* 1966;5:206-208.
34. Crank J. *The Mathematics of Diffusion*. Oxford: Oxford University Press; 1975.
35. Castellanos IJ, Cuadrado WO, Griebenow K. Prevention of structural perturbations and aggregation upon encapsulation of bovine serum albumin into poly(lactide-co-glycolide) micropheres using the solid-in-oil-in water technique. *J Pharm Pharmacol* 2001;53:1099-107.
36. Perez-Rodriguez C, Montano N, Gonzalez K, Griebenow K. Stabilization of alpha-chymotrypsin at the CH(2)Cl(2)/water interface and upon water-in-oil-in-water encapsulation in PLGA microspheres. *J Control Release* 2003;89:71-85.
37. Yu Z, Rogers TL, Hu J, Johnston KP, Williams RO, 3rd. Preparation and characterization of microparticles containing peptide produced by a novel process: spray freezing into liquid. *Eur J Pharm Biopharm* 2002;54:221-8.
38. Yu Z, Garcia AS, Johnston KP, Williams RO, 3rd. Spray freezing into liquid for highly stable protein nanostuctured microparticles. (submitted).
39. Leach WT, Simpson D, Val TN, Anuta EC, Yu Z, Williams RO, 3rd, Johnston KP. Reducing burst in protein loaded PLA microspheres through protein micronization and dispersion. (submitted).
40. Han JH, Krochta JM, Hsieh YL, Kurth MJ. Mechanism and characteristics of protein release from lactitol-based cross-linked hydrogel. *J Agric Food Chem* 2000;48:5658-65.

41. Andreopoulos FM, Roberts MJ, Bentley MD, Harris JM, Beckman EJ, Russell AJ. Photoimmobilization of organophosphorus hydrolase within a PEG-based hydrogel. *Biotechnol Bioeng* 1999;65:579-88.
42. Peters T, Jr. *All About Albumin*. San Diego: Academic Press; 1996.
43. Reinhart CT, Peppas NA. Solute diffusion in swollen membranes. Part II. Influence of crosslinking on diffusive properties. *J Memb Sci* 1984;18:227-39.
44. Cruise GM, Scharp DS, Hubbell JA. Characterization of permeability and network structure of interfacially photopolymerized poly(ethylene glycol) diacrylate hydrogels. *Biomaterials* 1998;19:1287-94.
45. Amsden B. Solute Diffusion within Hydrogels. Mechanisms and Models. *Macromolecules* 1998;31:8382-8395.
46. Xu S, Yamanaka J, Sato S, Miyama I, Yonese M. Characteristics of complexes composed of sodium hyaluronate and bovine serum albumin. *Chem Pharm Bull (Tokyo)* 2000;48:779-83.
47. Azegami S, Tsuboi A, Izumi T, Hirata M, Dubin PL, Wang B, Kokufuta E. Formation of an intrapolymer complex from human serum albumin and poly(ethylene glycol). *Langmuir* 1999;15:940-947.
48. Johnson OL, Tracy MA. Peptide and protein drug delivery. In: Mathiowitz E, Editor. *Encyclopedia of Controlled Drug Delivery*. New York: John Wiley & Sons; 1999. p. 816-32.
49. Jain RA. The manufacturing techniques of various drug loaded biodegradable poly(lactide-co-glycolide) (PLGA) devices. *Biomaterials* 2000;21:2475-90.

50. Costantino HR, Firouzabadian L, Hogeland K, Wu C, Beganski C, Carrasquillo KG, Cordova M, Griebenow K, Zale SE, Tracy MA. Protein spray-freeze drying. Effect of atomization conditions on particle size and stability. *Pharm Res* 2000;17:1374-83.
51. Perez C, Castellanos IJ, Costantino HR, Al-Azzam W, Griebenow K. Recent trends in stabilizing protein structure upon encapsulation and release from bioerodible polymers. *J Pharm Pharmacol* 2002;54:301-13.
52. Kwon YM, Baudys M, Knutson K, Kim SW. In situ study of insulin aggregation induced by water-organic solvent interface. *Pharm Res* 2001;18:1754-9.
53. Zhu G, Schwendeman SP. Stabilization of proteins encapsulated in cylindrical poly(lactide-co-glycolide) implants: mechanism of stabilization by basic additives. *Pharm Res* 2000;17:351-7.

Chapter 6: Conclusions and Recommendations

6.1 SUMMARY

Ideally, rationally designed tissue engineering scaffolds should promote directed interactions with complex living systems. With this goal in mind, we sought to create a biomimetic hydrogel material to support the regeneration of soft tissues (e.g., peripheral nerve). Model implants for soft tissues should be degradable, porous, highly permeable, able to maintain a desired shape, and able to precisely modulate biological responses. Naturally derived materials are particularly suitable for these applications as they are degradable and intrinsically bioactive. Our work has made significant progress towards completing this aim through the design and characterization of crosslinked hyaluronic acid (HA) hydrogel scaffolds.

The accomplishments of this dissertation were organized into three main areas: (1) the development of a novel hydrogel tissue engineering scaffold based on photocrosslinkable glycidyl methacrylate-modified HA (GMHA), (2) the enhancement of GMHA-based hydrogels by covalently binding bioactive peptide sequences to the hydrogel matrix, and (3) the characterization of GMHA-based hydrogels and hydrogel-microsphere composite materials for controlled protein release. In summary, this work provides a new and versatile tissue engineering

scaffold designed expressly for augmenting the repair and regeneration of soft tissue injuries.

Future work, as outlined below, is recommended to further enhance these materials for specific soft tissue applications (e.g., nerve repair), to more thoroughly investigate the chemical and biological properties of GMHA and GMHA-based hydrogels, and to use the glycidyl methacrylate modification chemistry as a platform for the development of new naturally derived materials.

6.2 RECOMMENDATIONS FOR FUTURE RESEARCH

6.2.1 Development GMHA Hydrogels for Nerve Repair

The original long-term goal of this work was to use crosslinked HA materials in the study of peripheral nerve repair. However, significant hurdles in the design of the HA-based hydrogels prevented us from immediately reaching this goal. These challenges have nevertheless uncovered several potential areas of exciting research.

First, a more detailed understanding of the potential mechanisms for HA degradation in regenerating peripheral nerve is required. Currently, we do not know the local levels of hyaluronidase in nerve injury sites. Even less clear, is the availability of other means of HA degradation, such as oxygen free radicals. Without thorough knowledge about the kinetics of these processes it is exceedingly difficult to match the degradation rate of HA-based materials to the time scale of nerve regeneration.

Second, the organization and presentation of covalently bound peptides must be finely tuned to maximize the cellular responses required for directing the growth of axons. For instance, bioactive or adhesive peptide sequences could be used to support the infiltration of support cells (e.g., Schwann cells, endothelial cells) into the hydrogel scaffold. Cellular infiltration, however, is a process that relies not only on cellular adhesion and migration, but also degradation of the scaffolding material. This fact clearly emphasizes the importance of the first area of suggested research, understanding the HA-degradation mechanisms in nerve tissue. Fortunately, covalently bound peptide sequences could also be used for an additional mode of matrix degradation: proteolytically degradable crosslinks between the GMHA chains. Thus, covalently bound peptides could be used in several ways to further tune the biological properties of GMHA hydrogels.

Third, the encapsulation and delivery of bioactive proteins must be more thoroughly developed for fragile proteins such as growth factors. BSA is a well-established model for preliminarily characterizing protein delivery devices; however, it is also a relatively stable protein. Neurotrophic and angiogenic proteins (e.g., nerve growth factor and vascular endothelial growth factor) could add a potent mechanism for promoting nerve repair, but they are easily denatured and degraded by many techniques for materials synthesis. Therefore, in depth studies of the bioactivity and release rate of these growth factors are required before GMHA materials could be successfully applied for this use.

6.2.2 HA-Based Materials for Studying Biological Systems

As discussed in **Chapter 2**, HA is involved in a number of biological processes. However, the exact mechanisms by which it influences cellular behavior are not clear. Designing new functionalized forms of HA may provide a unique engineering approach for studying these systems. For example, many facets of HA's biological activity could be studied by progressively masking the carboxyl, hydroxyl, and acetamido functional groups in HA's backbone. Such changes would consequently affect receptor recognition sites or the physicochemical properties of the polymer (e.g., hydrophilicity, stiffness). Furthermore, the methods presented in this work could be used as a springboard for the development of new HA functionalization chemistries. For instance, by tagging HA with fluorescent molecules, one may conduct detailed studies of in vivo HA degradation or cellular processes such as receptor-mediated endocytosis.

6.2.3 Novel Naturally Derived Materials

One key advantage to the glycidyl methacrylate modification technique described in these studies is that one could apply the same chemistry to other glycosaminoglycans, including heparan sulfate, chondroitin sulfate, and dermatan sulfate. The biological activity and function of glycosaminoglycans are current areas of active research. It is likely that these robust bioactive polymers are also suitable foundations for hydrogel biomaterials.

Appendix A: Experimental Protocols

A.1 GLYCIDYL METHACRYLATE-HYALURONIC ACID (GMHA) HYDROGELS

- This protocol presents a two-step process for making crosslinked hyaluronic acid (HA) hydrogels. The first step is the modification of HA with glycidyl methacrylate (GM) to yield GMHA; the second step is photocrosslinking under UV light.
- Published in *Biotechnol Bioeng* 82:578-89 (2003)
- See also similar chemistries using GM and methacrylic anhydride (references below).

GMHA Conjugate Polymers

Materials

Hyaluronic acid	Collaborative Labs
Glycidyl methacrylate*	Aldrich 151238
Triethylamine*	Aldrich 471283
Tetrabutyl ammonium bromide	Fluka 86860
Acetone*	
Glass bottles with lids or Ehrlenmeyer flasks with stoppers	
Assorted beakers	
Glass rods or pipets	

* Hazardous component—be sure to read MSDS before use. Wear safety goggles, nitrile gloves and a lab coat.

Procedure for 5% Methacrylated GMHA (4-7 days depending on batch size)

1. Dissolve 0.5g HA in 50 ml dI on a stir plate in a chemical fume hood. Thorough dissolution can take several hours to overnight.
2. Add the following components separately and in the following order: 1.0 ml triethylamine, 1.0 ml glycidyl methacrylate, 1.0 g tetrabutyl ammonium bromide. Thoroughly mix before adding the next component.
3. Mix at room temperature in a sealed flask in a chemical fume hood overnight.
4. Incubate the reaction at 50-60°C for 1 h (open the flask seal slightly) and cool to room temperature.
5. Precipitate in acetone, using one part HA solution to 20 parts acetone.
   - Pour acetone into a 1L beaker and while stirring with a glass rod or pipet, slowly add the HA solution.
   - The GMHA will precipitate as a cottony white solid that should collect on the glass stirrer.
   - If the acetone starts getting cloudy and precipitation stops, start again with fresh acetone.
6. Transfer the precipitate to a small glass dish and rinse with fresh acetone.
7. Thoroughly dissolve the precipitate in about 30 ml dI (can take several hours, but should dissolve faster than unmodified HA).
8. Repeat steps 5-7 to remove all residual excess reactants.
9. Lyophilize frozen solution 24-48 hours and store with desiccant at –20 or 4°C.

7% methacrylated GMHA
Follow the procedure for 5% methacrylated GMHA, except add 1.8 ml triethylamine, 1.8 ml glycidyl methacrylate, and 1.8 g tetrabutyl ammonium bromide to the reaction.

11% methacrylated GMHA
Follow the procedure for 5% methacrylated GMHA, except add 3.6 ml triethylamine, 3.6 ml glycidyl methacrylate, and 3.6 g tetrabutyl ammonium bromide to the reaction.

^{1}NMR Analysis of Methacrylation

Materials
Deuterated water (D_2O)
NMR tubes

To verify the extent of methacrylation: make a 0.5% solution of GMHA with D_2O and submit for ^{1}H-NMR. Compare the peak heights per proton of the HA methyl peaks (at 1.82 or 1.93) and methacrylate peaks (at 5.55 and 5.24).

Crosslinking

Materials
GMHA
Phosphate buffered saline (PBS)
Irgacure 2959 (2959) — Ciba Specialty Chemicals
N-vinyl pyrrolidone (VP)* — Aldrich V340-9
UV lamp (365 nm long wave)^ — Blak-Ray Model B-100A

* Hazardous component—be sure to read MSDS before use.
^ When using the UV light, use eye protection and minimize direct exposure to skin.

- VP acts as a reaction accelerant and co-monomer.
- Although VP concentrations up to 3% produce more highly crosslinked gels with shorter UV exposures, concentrations above 0.5% have been shown to be cytotoxic. Similarly, concentrations of 2959 above 0.1% have been shown to be cytotoxic to photoencapsulated chondrocytes (*J Biomater Sci Polym Ed* 2000, 11: 439)
- The first procedure below outlines 1-3% VP gels, which may have interesting material properties; the second procedure outlines a less cytotoxic procedure with <0.3% VP and PBS as the 2959 solvent.
- Minimize the exposure of 2959 solutions to ambient light.
- Solutions of up to 1.5% GMHA can be sterile filtered through a 0.2 μm pore size syringe filter with a 0.8 μm pore size prefilter (0.8/0.2 μm Pall Gelman Supor Acrodisc PF syringe filter).

1-3% VP Gels
1. Make a 0.5-2.0% solution of GMHA in PBS and dissolve thoroughly overnight.
2. Dissolve 2959 in VP at 250 mg/ml. Store in the dark at R/T up to 1 month.

3. Add the 2959 solution** to the GMHA solution and mix well.
4. Expose the solution (up to 1-cm thick) to UV light 0.5-4 minutes** to produce a solid gel.

<0.3% VP Gels

1. Make a 1% 2959 solution in PBS. To dissolve, sonicate the solution and heat to 50°C until the 2959 is completely dissolved. Add 0.3% VP in a chemical fume hood. Store at R/T in the dark up to 1 month.
2. Make a 0.5-2.0% GMHA solution in 2959/PBS/VP solution**; allow to dissolve thoroughly in the dark.
3. Expose the solution (up to 1-cm thick) to UV light 0.5-4 minutes** to produce a solid gel.

** The amount of 2959, VP, and UV exposure needed should be determined experimentally and depends on the GMHA degree of methacrylation.

Variables to Achieve Varying Degrees of Crosslinking

Degree of methacrylation

Molar excess GM, triethylamine, tetrabutyl ammonium bromide in reaction
Reaction temperature
Length of reaction

Crosslinking

Concentration of 2959, VP, GMHA
Intensity or time of UV exposure
Addition of other components (e.g., acrylated PEG)

Additional references on similar chemistries

Glycidyl Methacrylate

Jin, et al. *J Control Release* 73: 173-81 (2001).
Trudel & Massia. *Biomaterials* 23: 3299-3307 (2002).
Park, et al. *Biomaterials* 24:578-89 (2003).

Methacrylic Anhydride

Smeds, et al. *J.M.S.—Pure Appl. Chem.* A36(7&8): 981-9 (1999).
Smeds & Grinstaff. *JBMR* 54:115-21 (2001).

A.2 SWELLING ASSAY WITH TGA

- To assess the hydrogels' degree of swelling, the equilibrium weight-swelling ratio, q, is determined. This ratio is found from the swollen gel weight (W_s) divided by the dry gel weight (W_d).
- The swelling ratios are measured using a Perkin-Elmer TGA-7 Thermogravimetric Analyzer (TGA).
- The calculated swelling ratio will allow a relative comparison of different gel chemistries. Increased crosslinking will allow less swelling, thus a lower swelling ratio, than a gel with relatively less crosslinking.

Materials

Hydrogel samples
Phosphate buffered saline (PBS)
TGA equipment

Procedure

1. Swell the hydrogel samples overnight in PBS.
2. Start the TGA equipment.
3. During the run, it is necessary to determine W_s (initial swollen weight at room temperature) as well as W_d. The gel starts to decompose above about 115°C. Setup a profile similar to the following:
   - 25-100°C ramp at 20-35°/minute
   - 100°C for 5-20 minutes
4. Cut the hydrogel sample into 8-20 mg pieces. Keep the pieces wet until testing.
5. Run the TGA profile.
6. Record the entire weight vs. temperature or only the initial weight and the plateau weight at about 100°C.
7. Calculate the swelling ratio by dividing the swollen gel weight by the dry weight.

A.3 HYDROGEL DEGRADATION STUDIES

Hydrogel degradation studies are used to determine the relative extent of gel crosslinking due to the differences in their degradation rate in hyaluronidase (hyase) solutions.

Materials

GMHA gelation solution	
Coverwell perfusion chamber molds	Sigma Z379220
Microscope slides	
No. 1 coverslips (optional)	
Teflon-coated coverslip forceps	
24-well plate	
Bovine testicular hyaluronidase (hyase)	Sigma H3506
Citrate buffer (see below)	

Procedure

1. Tear off the plastic films from both sides of the perfusion chambers. Clean off any residual adhesive with ethanol. Stick the smooth side to a microscope slide. Look at the underside of the slide to make sure that the mold is thoroughly adhered.
2. Crosslink 0.1 ml gels in the perfusion chamber molds. Peel off the perfusion chamber mold. Using a coverslip or coverslip forceps, carefully remove the gels from the slide and transfer to individual wells in a 24-well plate.
3. Soak in 0.5-1.0 ml citrate buffer overnight at R/T to allow equilibrium swelling.
4. Carefully remove the citrate buffer while trying not to disturb the gel. Remove the gel with the coverslip forceps and carefully blot to remove excess liquid. Weigh the gels individually to obtain their initial weights. A small weigh boat turned upside-down makes a good platform that can be dried off between measurements.
5. Make a fresh batch of hyase (5-500 u/ml) in citrate buffer. Add 0.5-1.0 ml hyase solution to each well and incubate at 37°C on a shaker.
6. At desired time points, remove the hyase solution, carefully weigh the gel and return to the 24-well plate. Add fresh hyase solution and return to incubator. If gels have a very low extent of crosslinking and are very weak, use one gel per time-point.
7. Plot percent degradation versus degradation time. The initial linear slope is the 'degradation rate' in percent weight loss per time.

Citrate buffer, pH 5.3

4.393 g	1.757 g	NaCl
20.113 g	8.045 g	$Na_2HPO_4 \cdot 7H_2O$
2.883 g	1.153 g	citric acid
500 ml	200 ml	Deionized water

Adjust pH to 5.3. Filter sterilize, if necessary.

A.4 HYDROGEL HAEC CYTOCOMPATIBILITY ASSAY

- This is an in vitro method for determining hydrogel compatibility with living cells. The cells are incubated in indirect contact with the hydrogel, a method adapted from published work (*Biomaterials* 2002 23:3299-3307)
- The *Promega CellTiter 96 Aqueous Non-Radioactive Cell Proliferation Assay* is a colorimetric method for determining the number of viable cells in proliferation or toxicity studies. It is a safer and simpler version of the popular MTT cell assay. In the CellTiter assay, MTS is bioreduced by cells into a formazan that absorbs at 490nm.

Materials

GMHA gelation solutions	
0.8/0.2 μm Pall Gelman Supor Acrodisc PF syringe filter	VWR 28144-009
>3 ml syringes	
Corning Costar Transwell inserts (6.5 mm, 0.4 μm pore size)	Fisher 07-200-147
Sterile 24-well TC plate	
Phosphate buffered saline (PBS)	
General tissue culture supplies	
Human aortic endothelial cells (HAECs)*	Clonetics CC2535
Endothelial Growth Medium-2 (EGM-2)	Clonetics CC3162
CellTiter 96 Aqueous Non-Radioactive Cell Proliferation Assay	Promega G5421

* Be sure to obtain biohazard safety training before handling human cells.

Methods

1. Sterile filter the GMHA gelation solutions using the Acrodisc syringe filter and a >3 ml syringe.
2. In a sterile field, crosslink 0.1 ml gels in individual Transwell inserts.
3. Wash the hydrogels for 5 minutes each in PBS and then EGM-2.
4. Seed HAECs in the 24-well plate at a density of 6250 cells in 1 ml EGM-2 per well.
5. After the cells have adhered (at least 30 minutes of incubation) add the Transwell inserts containing the hydrogels to the wells.
6. After 24 hours of incubation, determine the cell viabilities using the CellTiter proliferation assay according to the manufacturer's instructions.

A.5 HAEC PROLIFERATION ASSAY

- This protocol uses the *Promega CellTiter 96 Aqueous Non-Radioactive Cell Proliferation Assay*, which is a colorimetric method for determining the number of viable cells in proliferation or toxicity studies. It is a safer and simpler version of the popular MTT cell assay. MTS is bioreduced by cells into a formazan that is visible and absorbs at 490nm.
- This assay uses human aortic endothelial cells (HAECs), but can be adapted for use with other cell types; see the CellTiter instructions for details.

Materials

Experimental and control doses (sterile)	
Phosphate buffered saline (PBS)	
General tissue culture supplies	
Human aortic endothelial cells (HAECs)*	Clonetics CC2535
Endothelial Growth Medium-2 (EGM-2)	Clonetics CC3162
Endothelial Basal Medium-2 (EBM-2)	Clonetics CC3156
Heat-inactivated fetal bovine serum (FBS)	Hyclone SH30071.03
96-well plate	
Multi-channel pipetman	
CellTiter 96 Aqueous Non-Radioactive Cell Proliferation Assay	Promega G5421

Methods

1. Seed the wells of a 96-well plate with 10,000 HAECs per well in EGM-2.
2. After the cells have adhered (2-4 hours), starve the cells overnight in EBM-2 with 1% heat-inactivated FBS ("starvation medium").
3. The next day, dose with experimental and control doses, 0.2 - 0.3 ml/well, 3-4 wells per dose, diluted in starvation medium. Suitable positive and negative controls are EGM-2 and starvation medium, respectively.
4. After 48-72 hours of incubation, remove all but 100 µl of liquid from the wells. Add 20µl of the CellTiter MTS/PMS solution per well. Return the plate to the incubator.
5. After 1, 2, 3, 4 hours, measure the absorbance of the wells at 490 nm with a plate reader. The absorbance of the wells is proportional to numbers of viable cells. Typically, the most reliable results are obtained at the 3 hour time-point, but this should be re-determined if cell type or density is changed.

A.6 CD31 IMMUNOHISTOCHEMICAL STAIN FOR TISSUE CRYOSECTIONS

- CD31 is an endothelial cell specific marker
- This protocol is optimized for frozen cryosections and is not recommended for paraffin embedded tissues.
- Protocol adapted from Tim King, Eric Brey, and Charles Patrick at The University of Texas M.D. Anderson Cancer Research Center (Houston, TX)

Materials

Mouse anti-rat CD31 primary antibody	Serotec MCA1334G
Goat anti-mouse IgG secondary antibody conjugated with horseradish peroxidase (HRP)	Serotec STAR77
3,3-diaminobenzidinetetrahydrochloride (DAB)	Research Genetics 750118
Phosphate buffered saline (PBS)	
Horse serum	Sigma H0164
Goat serum	Sigma G6767
Methanol*	
30% hydrogen peroxide (H_2O_2)*	
Acetone*	
Brij detergent	Fisher BP345-500
Gill's #3 hematoxylin*	Sigma GHS-3-16
Universal Mount	Research Genetics 750105
PAP pen or rubber cement	

* Hazardous materials – be sure to read MSDS sheets and wear protective equipment

Brij solution: Add 20 µl Brij detergent to 50 ml distilled water. Adjust pH to 7.6.

Protein blocking solution: Freshly prepared 5% normal horse serum with 1% normal goat serum in PBS:

	50 ml	25 ml	12.5 ml
Goat:	0.5 ml	0.25 ml	0.125 ml
Horse:	2.5 ml	1.25 ml	0.625 ml
PBS:	47.0 ml	23.5 ml	11.75 ml

Endogenous peroxidases: Freshly prepared (no more than 20 min old at time of use) 3% H_2O_2 in methanol

1 ml 30% H_2O_2 in 9 ml methanol
5 ml per 20 slides

Antibody solutions: Made in protein blocking solution at recommended concentration. Prepare about 50-70 µl per section.

Method

All incubations should be performed in a humidity chamber and do not allow the sections to dry out.

Day one (approx 2-2.5 hr)

1. Fix slides in -20°C acetone for 5 min.
2. Rinse slides in PBS (3x for 3 min each).
3. Remove slides one at a time, wipe off excess PBS and circle tissue with a PAP pen or a thin band of rubber cement dispensed from a syringe (without needle).
4. Place slides in humidity chamber.
5. Block endogenous peroxidase by incubating with 3% H_2O_2 in methanol for 12 min. Add a second drop of solution at 6 min.
6. Rinse with PBS (3x for 3 min each).
7. Incubate with protein blocking solution for 20 min.
8. Remove excess fluid and incubate with primary antibody in the humidity chamber overnight at 4°C or 2 hr at room temperature.

Day two (approx. 2-2.5 hr)

9. Rinse with PBS (3x for 3 min each).
10. Incubate with protein blocking solution for 5-10 min.
11. Remove excess fluid and incubate with HRP-conjugated secondary antibody in the humidity chamber for 60 min at room temperature.
12. Rinse with PBS (3x for 3 min each).
13. Remove excess liquid and add DAB. Incubate for 5-20 min at room temperature. Check reaction under a bright-field microscope and determine when to stop reaction.
14. Rinse with distilled water.
15. Rinse with Brij solution.
16. Remove excess fluid and add a drop of Gill's hematoxylin for a few seconds.
17. Rinse with distilled water to remove excess hematoxylin.
18. Add PBS for about 1 min.
19. Rinse with distilled water and air dry slides.
20. Remove rubber cement rings, if used. Mount sections with Universal Mount and dry on a 56°C hot plate.

Notes

- Acetone:chloroform (1:1) can be used in step 1 as an additional fixation. Fix in acetone, acetone:chloroform, acetone for 5 min each.
- The primary antibody dilution is 1:100.
- The secondary antibody dilution is 1:50.

A.7 EDC-MEDIATED GMHA-PEPTIDE CONJUGATIONS

Reactions mediated by N-ethyl-N-(3-dimethylaminopropyl)carbodiimide hydrochloride (EDC) are commonly used for conjugating carboxylates and amines [1]. However, EDC reactions are highly pH-dependent and an excess of amine is required for high levels of modification [1,2]. Furthermore, EDC-mediated reactions with HA are particularly challenging, as they readily convert HA's carboxylate to an unreactive N-acylurea [2,3,4].

References:
1. *Bioconjugate Techniques* by Hermanson (1996).
2. *JBMR* (1999) 47:152-69
3. *Carbohydr Res* (1982) 105:69-85
4. *Bioconj Chem* (1991) 2:232-4

Materials

GMHA (or HA)	
Peptide in solution	
EDC* (MW 191.71)	Aldrich 16-146-2
N-hydroxysuccinimide* (NHS, MW 115.1)	Sigma H7377
1-Hydroxybenzotriazole hydrate (HOBt, MW 135.1)	Peptides International 814421
Dimethylsulfoxide (DMSO)	
2-Morpholinoethanesulfonic acid (MES, MW 195.2)	Sigma M8250
Sodium Chloride (NaCl)	
Dialysis tubing, 7000 MWCO	Pierce 68700

* Carbodiimides and succinimides are extremely unstable in the presence of water. Solutions should be freshly prepared. EDC should be stored under N_2 or Ar in a desiccator at –20°C. NHS and HOBt should be stored with desiccant.

0.1 M MES buffer, 0.3 M NaCl, pH 5.5-7.5

Dissolve 3.9 g MES and 3.5 g NaCl in 180 ml ddI. Adjust pH. Fill to 200 ml. Filter sterilize.

Conjugation reaction

1. Dissolve GMHA in MES buffer at 1 mg/ml overnight.
2. Make a 20 mg/ml solution of NHS in ddI or HOBt in 50:50 DMSO:ddI.
3. Add the NHS or HOBt to the GMHA solution at a molar ratio of 0.25 - 1.0 mol per mol of GMHA carboxylate groups. Mix at room temperature for 5 min.
4. Meanwhile, make a 20 mg/ml solution of EDC in ddI.
5. Add the EDC solution to the GMHA solution and mix at R/T for 5 min.
6. Add the peptide solution, readjust pH, and mix at room temperature 2 h.
7. Dialyze overnight against a 20-fold greater volume of ddI than the reaction volume.
8. Lyophilize and store with desiccant at –20C.
9. Use the ninhydrin assay to measure the extent of peptide conjugation.

A.8 ACRYLATED PEG-PEPTIDES

- This protocol outlines how to conjugate an acrylated polyethylene glycol (PEG) to a peptide for photoinitiated conjugation reactions.
- Adapted from *JBMR* 39:266 (1998) and *JBMR* 60:86 (2002)

Materials

Sodium bicarbonate	
Peptide	(e.g., hexaglycine, Sigma G5630)
Acryloyl-PEG-N-hydroxysuccinimide ester (Acrl-PEG-NHS)	
	Nektar Therapeutics 012A0F02
Dialysis membrane, 1000 MWCO	Spectra/Por 131090

50 mM sodium bicarbonate buffer, pH 8.5

Add 2.1 g sodium bicarbonate to 480 ml ddI. Adjust pH to 8.3. Add ddI up to 500 ml. Filter sterilize.

Hexaglycine aliquots, 10 mg/ml in 1 M HCl

1. Dissolve 100 mg hexaglycine in 10 ml 1M HCl and warm to 37-45°C to dissolve.
2. Once aliquots are frozen, the hexaglycine will precipitate out and must be redissolved at 37-45°C before use.
3. For other peptides, see their product information for dissolution and aliquoting procedures.

Methods: Conjugation reaction, makes ~0.18 g product

1. Add 2.24 ml 10 mg/ml hexaglycine stock and 2.24 ml 1M NaOH simultaneously to 15 ml sodium bicarbonate buffer. (If you add the hexaglycine stock first, the bicarbonate will react with the HCl and make fizzy CO_2 gas.)
2. Adjust pH to ~8.0 - 8.5.
3. Add 0.2 g acryl-PEG-NHS and mix immediately to dissolve.
4. Mix 2 hr at room temperature.
5. Dialyze against at least 1 L ddI overnight.
6. Can verify reaction with MALDI-MS, which is capable of measuring the molecular weight of ionizable molecules. MALDI cannot be used to measure the molecular weight of acryl-PEG-NHS; all amino acids and peptide sequences are ionizable at their termini; many amino acid side chains are also ionizable.

A.9 NINHYDRIN ASSAY

- Adapted from *Anal Biochem* (2001) 292:125-129 and *Vaccine* (1997) 15:672-8.
- The ninhydrin assay is a sensitive method for determining the amino acid concentration in a hydrolyzed sample. This method provides several advantages over the Coomassie blue assay. First, less than 5 μg of sample can be quantified (Coomassie blue can only be used for >8 μg/ml solutions). Second, low molecular weight peptides can be detected (the lower detection limit for Coomassie blue is 3000-5000 Da). Finally, insoluble proteins can also be detected (proteins must be in solution for the Coomassie blue assay).

Materials

Concentrated HCl (12 M stock) *	
Concentrated NaOH (13.5 M stock prepared) *	
BSA or other standard protein or peptide	
Stannous chloride dihydrate ($SnCl_2 \cdot 2H_2O$) *	Lancaster 9080
Ethylene glycol *,^	
Ninhydrin	Sigma N6014
96-well plate	
Sealing tape for 96-well plate	Costar 3095 or 6570

* Hazardous materials – be sure to read MSDS sheets and wear protective equipment
^ Sensitive to ambient air, store under N_2 or Ar

0.1 M citric acid buffer, pH 4.7
Dissolve 19.21 g citric acid in 0.9 L ddI. Adjust pH to 4.5. Add volume up to 1 L with ddI. Filter sterilize.

Hydrolyzed BSA or peptide standard
1. Dissolve BSA (or other standard) in 13.5M NaOH at about 1 mg/ml in an autoclave-safe glass vial.
2. Autoclave at 125°C for at least 40 minutes.
3. Measure the sample volume after autoclaving and add water if volume is less than original volume.
4. Carefully and dropwise, add concentrated HCl in equimolar amount to NaOH to neutralize the base. (A salt precipitate may form, which does not seem to affect the results.)
5. Make sure the solution is well mixed and then prepare ~10 ml of 50 μg/ml standard in citric acid buffer.
6. Check the pH to make sure it is in the range of 2-9. Adjust pH if necessary.
7. Recalculate the final concentration of standard, if necessary.
8. Prepare standard solutions to cover the range 10 – 50 μg/ml. Use citric acid buffer to prepare the dilutions.

4N acetate buffer

Dissolve 54.4 g sodium acetate in 100 ml acetic acid. Add up to 500 ml total volume with ddI. pH should be ~5.5 (assay will still work if pH is up to ~8).

Stannous chloride solution

Add 100 mg $SnCl_2 \cdot 2H_2O$ to 1 ml ethylene glycol, mix well. Solution will be cloudy or have a fine suspension. Mix well before use.

Ninhydrin reagent

1. Add 200 mg ninhydrin to 7.5 ml ethylene glycol and 2.5 ml 4N acetate buffer, mix well on stir plate.
2. Add 250 µl freshly prepared stannous chloride solution with stirring. Solution will turn dark purple and then light red. Keep on stir plate until pale red color develops (~5-10 minutes).
3. Store under N_2 or Ar at room temperature for a few days (or while still red in color).

Methods

1. Hydrolyze sample using same procedure as hydrolyzed standards.
2. Dilute samples to fall within the 10 – 50 µg/ml range.
3. Start a water bath heating to 100°C. The bath must be large enough to hold a well plate.
4. In a 96-well plate, add samples and hydrolyzed BSA standards, 80 µl per well, in triplicate.
5. Add 80 µl per well of ninhydrin reagent.
6. Cover well plate with sealing tape. This will help prevent sample spilling and evaporation while the plate is in the boiling water bath.
7. Check the water bath to make sure that the temperature is 95-100°C and that the water is not boiling rapidly. Using tongs, place the well plate in the water bath. Incubate for 10 minutes, checking the bath periodically.
8. Remove the well plate from the bath, dry the bottom, and read the absorbance of the wells at 595 nm on a plate reader.
9. Using the standards as a calibration curve, calculate the original amino acid concentration in the samples.

Bibliography

Amsden, B. Solute Diffusion within Hydrogels. Mechanisms and Models. *Macromolecules* 1998;31:8382-8395.

Andreopoulos, F. M., M. J. Roberts, et al. Photoimmobilization of organophosphorus hydrolase within a PEG-based hydrogel. *Biotechnol Bioeng* 1999;65:579-88.

Andrianov, A. K., J. Chen, et al. Preparation of hydrogel microspheres by coacervation of aqueous polyphosphazene solutions. *Biomaterials* 1998;19:109-15.

Anseth, K. S. and J. A. Burdick. New directions in photopolymerizable biomaterials. *MRS Bulletin* 2002;27:130-6.

Awad, H. A., D. L. Butler, et al. Autologous mesenchymal stem cell-mediated repair of tendon. *Tissue Eng* 1999;5:267-77.

Azegami, S., A. Tsuboi, et al. Formation of an intrapolymer complex from human serum albumin and poly(ethylene glycol). *Langmuir* 1999;15:940-947.

Baier Leach, J., K. A. Bivens, et al. Development of photocrosslinkable hyaluronic acid-polyethylene glycol-peptide composite hydrogels for soft tissue engineering. *J Biomed Mater Res* (submitted).

Baier Leach, J., K. A. Bivens, et al. Photocrosslinked hyaluronic acid hydrogels: Natural, biodegradable tissue engineering scaffolds. *Biotechnol Bioeng* 2003;82:578-89.

Baier Leach, J. and C. E. Schmidt. Hyaluronan. In: G. E. Wnek and G. L. Bowlin, Editor. *Encyclopedia of Biomaterials and Biomedical Engineering*. New York: Marcel Dekker; (in press).

Balazs, E. A., P. A. Bland, et al. Matrix engineering. *Blood Coagul Fibrinolysis* 1991;2:173-8.

Band, P. A. Hyaluronan derivatives: chemistry and clinical applications. In: T. C. Laurent, Editor. *Chemistry, Biology and Medical Applications of Hyaluronan and Its Derivatives*. London: Portland Press; 1998. p. 33-42.

Barbucci, R., A. Magnani, et al. Modification of hyaluronic acid by insertion of sulfate groups to obtain a heparin-like molecule. Part I. Characterization and behavior in aqueous solution towards H+ and Cu2+ ions. *Gazzetta Chimica Italiana* 1995;125:169-80.

Bell, E., H. P. Ehrlich, et al. Living tissue formed in vitro and accepted as skin-equivalent tissue of full thickness. *Science* 1981;211:1052-4.

Black, A. F., F. Berthod, et al. In vitro reconstruction of a human capillary-like network in a tissue-engineered skin equivalent. *Faseb J* 1998;12:1331-40.

Bohl, K. S. and J. L. West. Nitric oxide-generating polymers reduce platelet adhesion and smooth muscle cell proliferation. *Biomaterials* 2000;21:2273-8.

Borkenhagen, M., J. F. Clemence, et al. Three-dimensional extracellular matrix engineering in the nervous system. *J Biomed Mater Res* 1998;40:392-400.

Bos, G. W., R. Verrijk, et al. Hydrogels for the controlled release of pharmaceutical proteins. *Pharm Tech North Am* 2001;25:110-120.

Brey, E. M., T. W. King, et al. A technique for quantitative three-dimensional analysis of microvascular structure. *Microvasc Res* 2002;63:273-294.

Brun, P., G. Abatangelo, et al. Chondrocyte aggregation and reorganization into three-dimensional scaffolds. *J Biomed Mater Res* 1999;46:337-46.

Bryant, S. J., C. R. Nuttelman, et al. Cytocompatibility of UV and visible light photoinitiating systems on cultured NIH/3T3 fibroblasts in vitro. *J Biomater Sci Polym Ed* 2000;11:439-57.

Bulpitt, P. and D. Aeschlimann. New strategy for chemical modification of hyaluronic acid: preparation of functionalized derivatives and their use in the formation of novel biocompatible hydrogels. *J Biomed Mater Res* 1999;47:152-69.

Burczak, K., E. Gamian, et al. Long-term in vivo performance and biocompatibility of poly(vinyl alcohol) hydrogel macrocapsules for hybrid-type artificial pancreas. *Biomaterials* 1996;17:2351-6.

Business Week. The new era of regenerative medicine. July 27, 1998.

Cadee, J. A., M. J. van Luyn, et al. In vivo biocompatibility of dextran-based hydrogels. *J Biomed Mater Res* 2000;50:397-404.

Camenisch, T. D., J. A. Schroeder, et al. Heart-valve mesenchyme formation is dependent on hyaluronan-augmented activation of ErbB2-ErbB3 receptors. *Nat Med* 2002;8:850-5.

Campoccia, D., P. Doherty, et al. Semisynthetic resorbable materials from hyaluronan esterification. *Biomaterials* 1998;19:2101-27.

Cao, Y., J. P. Vacanti, et al. Generation of neo-tendon using synthetic polymers seeded with tenocytes. *Transplant Proc* 1994;26:3390-2.

Castellanos, I. J., W. O. Cuadrado, et al. Prevention of structural perturbations and aggregation upon encapsulation of bovine serum albumin into poly(lactide-co-glycolide) micropheres using the solid-in-oil-in water technique. *J Pharm Pharmacol* 2001;53:1099-107.

Ceballos, D., X. Navarro, et al. Magnetically aligned collagen gel filling a collagen nerve guide improves peripheral nerve regeneration. *Exp Neurol* 1999;158:290-300.

Chen, G., Y. Ito, et al. Photoimmobilization of sulfated hyaluronic acid for antithrombogenicity. *Bioconjug Chem* 1997;8:730-4.

Chen, W. Y. and G. Abatangelo. Functions of hyaluronan in wound repair. *Wound Repair Regen* 1999;7:79-89.

Cheng, H., Y. Cao, et al. Spinal cord repair in adult paraplegic rats: partial restoration of hind limb function. *Science* 1996;273:510-3.

Cheung, W. F., T. F. Cruz, et al. Receptor for hyaluronan-mediated motility (RHAMM), a hyaladherin that regulates cell responses to growth factors. *Biochem Soc Trans* 1999;27:135-42.

Choi, Y. S., S. R. Hong, et al. Studies on gelatin-containing artificial skin: II. Preparation and characterization of cross-linked gelatin-hyaluronate sponge. *J Biomed Mater Res* 1999;48:631-9.

Chorny, R. C. and J. H. Krasuk. Extraction for different geometries. *Ind Eng Chem Process Des Dev* 1966;5:206-208.

Cleland, J. L., A. Daugherty, et al. Emerging protein delivery methods. *Curr Opin Biotechnol* 2001;12:212-9.

Cleland, R. L. Ionic polysaccharides. IV. Free-rotation dimensions for disaccharide polymers. Comparison with experiment for hyaluronic acid. *Biopolymers* 1970;9:811-24.

Cleland, R. L. and J. L. Wang. Ionic polysaccharides. III. Dilute solution properties of hyaluronic acid fractions. *Biopolymers* 1970;9:799-810.

Collier, J. H., J. P. Camp, et al. Synthesis and characterization of polypyrrole-hyaluronic acid composite biomaterials for tissue engineering applications. *J Biomed Mater Res* 2000;50:574-84.

Constantz, B. R., I. C. Ison, et al. Skeletal repair by in situ formation of the mineral phase of bone. *Science* 1995;267:1796-9.

Cortivo, R., P. Brun, et al. Antioxidant effects of hyaluronan and its alpha-methyl-prednisolone derivative in chondrocyte and cartilage cultures. *Semin Arthritis Rheum* 1996;26:492-501.

Costantino, H. R., L. Firouzabadian, et al. Protein spray-freeze drying. Effect of atomization conditions on particle size and stability. *Pharm Res* 2000;17:1374-83.

Crank, J. *The Mathematics of Diffusion*. Oxford: Oxford University Press; 1975.

Cruise, G. M., O. D. Hegre, et al. In vitro and in vivo performance of porcine islets encapsulated in interfacially photopolymerized poly(ethylene glycol) diacrylate membranes. *Cell Transplant* 1999;8:293-306.

Cruise, G. M., D. S. Scharp, et al. Characterization of permeability and network structure of interfacially photopolymerized poly(ethylene glycol) diacrylate hydrogels. *Biomaterials* 1998;19:1287-94.

Davis, B. K. Diffusion in polymer gel implants. *Proc Natl Acad Sci U S A* 1974;71:3120-3.

de Jong, S. J., B. van Eerdenbrugh, et al. Physically crosslinked dextran hydrogels by stereocomplex formation of lactic acid oligomers: degradation and protein release behavior. *J Control Release* 2001;71:261-75.

Delpech, B., P. Bertrand, et al. An indirect enzymoimmunological assay for hyaluronidase. *J Immunol Methods* 1987;104:223-9.

Draget, K. I., G. Skjak-Braek, et al. Alginate based new materials. *Int J Biol Macromol* 1997;21:47-55.

Duranti, F., G. Salti, et al. Injectable hyaluronic acid gel for soft tissue augmentation. A clinical and histological study. *Dermatol Surg* 1998;24:1317-25.

Dvorak, H. F., V. S. Harvey, et al. Fibrin containing gels induce angiogenesis. Implications for tumor stroma generation and wound healing. *Lab Invest* 1987;57:673-86.

Eser Elcin, A., Y. M. Elcin, et al. Neural tissue engineering: adrenal chromaffin cell attachment and viability on chitosan scaffolds. *Neurol Res* 1998;20:648-54.

Fabiani, J. N., G. D. Dreyfus, et al. The autologous tissue cardiac valve: a new paradigm for heart valve replacement. *Ann Thorac Surg* 1995;60:S189-94.

Flory, P. J. *Principles of Polymer Chemistry*. Ithaca, NY: Cornell University Press; 1953.

Geiger, B., A. Bershadsky, et al. Transmembrane crosstalk between the extracellular matrix--cytoskeleton crosstalk. *Nat Rev Mol Cell Biol* 2001;2:793-805.

Gekko, K. Solution properties of dextran and its ionic derivatives. *Am Chem Soc Symp Ser* 1981;150:415-38.

Germain, L., F. A. Auger, et al. Reconstructed human cornea produced in vitro by tissue engineering. *Pathobiology* 1999;67:140-7.

Ghezzo, E., L. Benedetti, et al. Hyaluronane derivative microspheres as NGF delivery devices: Preparation methods and in vitro release characterization. *Int J Pharm* 1992;87:21-9.

Glass, J. R., K. T. Dickerson, et al. Characterization of a hyaluronic acid-Arg-Gly-Asp peptide cell attachment matrix. *Biomaterials* 1996;17:1101-8.

Gobin, A. S. and J. L. West. Cell migration through defined, synthetic ECM analogs. *FASEB J* 2002;16:751-3.

Gombotz, W. R. and D. K. Pettit. Biodegradable polymers for protein and peptide drug delivery. *Bioconjug Chem* 1995;6:332-351.

Griffith, L. G. and G. Naughton. Tissue engineering--current challenges and expanding opportunities. *Science* 2002;295:1009-14.

Gupta, R. K., A. C. Chang, et al. Determination of protein loading in biodegradable polymer microspheres containing tetanus toxoid. *Vaccine* 1997;15:672-8.

Hadlock, T., S. Singh, et al. Ocular cell monolayers cultured on biodegradable substrates. *Tissue Eng* 1999;5:187-96.

Han, J. H., J. M. Krochta, et al. Mechanism and characteristics of protein release from lactitol-based cross-linked hydrogel. *J Agric Food Chem* 2000;48:5658-65.

Hashimoto, T., Y. Suzuki, et al. Peripheral nerve regeneration through alginate gel: analysis of early outgrowth and late increase in diameter of regenerating axons. *Exp Brain Res* 2002;146:356-68.

Hatefi, A. and B. Amsden. Biodegradable injectable in situ forming drug delivery systems. *J Control Release* 2002;80:9-28.

Hench, L. L. and J. M. Polak. Third-generation biomedical materials. *Science* 2002;295:1014-7.

Hermanson, G. T. *Bioconjugate Techniques*. San Diego, CA: Academic Press, Inc.; 1996.

Hern, D. L. and J. A. Hubbell. Incorporation of adhesion peptides into nonadhesive hydrogels useful for tissue resurfacing. *J Biomed Mater Res* 1998;39:266-76.

Hill-West, J. L., S. M. Chowdhury, et al. Efficacy of a resorbable hydrogel barrier, oxidized regenerated cellulose, and hyaluronic acid in the prevention of ovarian adhesions in a rabbit model. *Fertil Steril* 1994;62:630-4.

Hill-West, J. L., S. M. Chowdhury, et al. Prevention of postoperative adhesions in the rat by in situ photopolymerization of bioresorbable hydrogel barriers. *Obstet Gynecol* 1994;83:59-64.

Hoffman, A. S. Hydrogels for biomedical applications. *Adv Drug Deliv Rev* 2002;54:3-12.

http://www.fda.gov/cdrh. (accessed Dec 2002).

http://www.glycoforum.gr.jp/science/hyaluronan/hyaluronanE.html. (accessed Dec 2002).

Hu, M., E. E. Sabelman, et al. Improvement of Schwann cell attachment and proliferation on modified hyaluronic acid strands by polylysine. *Tissue Eng* 2000;6:585-93.

Huang, D., T. R. Chang, et al. Mechanisms and dynamics of mechanical strengthening in ligament-equivalent fibroblast-populated collagen matrices. *Ann Biomed Eng* 1993;21:289-305.

Hubbell, J. A. Biomaterials in tissue engineering. *Biotechnology (NY)* 1995;13:565-76.

Hubbell, J. A. Hydrogel systems for barriers and local drug delivery in the control of wound healing. *J Control Release* 1996;39:305-313.

Hubbell, J. A. Bioactive biomaterials. *Curr Opin Biotechnol* 1999;10:123-9.

Huglin, M. B., M. M. Rehab, et al. Thermodynamic interactions in copolymeric hydrogels. *Macromolecules* 1986;19:2986-91.

Hutmacher, D. W., J. C. Goh, et al. An introduction to biodegradable materials for tissue engineering applications. *Ann Acad Med Singapore* 2001;30:183-91.

Huynh, T., G. Abraham, et al. Remodeling of an acellular collagen graft into a physiologically responsive neovessel. *Nat Biotechnol* 1999;17:1083-6.

Inukai, M., Y. Jin, et al. Preparation and characterization of hyaluronate-hydroxyethyl acrylate blend hydrogel for controlled release device. *Chem Pharm Bull (Tokyo)* 2000;48:850-4.

Isacke, C. M. and H. Yarwood. The hyaluronan receptor, CD44. *Int J Biochem Cell Biol* 2002;34:718-21.

Jacobsen, S. and L. Guth. An electrophysiological study of the early stages of peripheral nerve regeneration. *Exp Neurol* 1965;11:48-60.

Jain, R. A. The manufacturing techniques of various drug loaded biodegradable poly(lactide-co-glycolide) (PLGA) devices. *Biomaterials* 2000;21:2475-90.

Jin, Y., J. Yamanaka, et al. Recyclable characteristics of hyaluronate-polyhydroxyethyl acrylate blend hydrogel for controlled releases. *J Control Release* 2001;73:173-81.

Johnson, O. L. and M. A. Tracy. Peptide and protein drug delivery. In: E. Mathiowitz, Editor. *Encyclopedia of Controlled Drug Delivery*. New York: John Wiley & Sons; 1999. p. 816-32.

Joly, A., J. F. Desjardins, et al. Survival, proliferation, and functions of porcine hepatocytes encapsulated in coated alginate beads: a step toward a reliable bioartificial liver. *Transplantation* 1997;63:795-803.

Kim, B. S. and D. J. Mooney. Development of biocompatible synthetic extracellular matrices for tissue engineering. *Trends Biotechnol* 1998;16:224-30.

Kim, H. D. and R. F. Valentini. Retention and activity of BMP-2 in hyaluronic acid-based scaffolds in vitro. *J Biomed Mater Res* 2002;59:573-84.

Kim, M. R. and T. G. Park. Temperature-responsive and degradable hyaluronic acid/Pluronic composite hydrogels for controlled release of human growth hormone. *J Control Release* 2002;80:69-77.

King, T. W., E. M. Brey, et al. Quantification of vascular density using a semiautomated technique for immunostained specimens. *Anal Quant Cytol Histol* 2002;24:39-48.

Kirker, K. R., Y. Luo, et al. Glycosaminoglycan hydrogel films as bio-interactive dressings for wound healing. *Biomaterials* 2002;23:3661-71.

Kito, H. and T. Matsuda. Biocompatible coatings for luminal and outer surfaces of small-caliber artificial grafts. *J Biomed Mater Res* 1996;30:321-30.

Kuo, J.-W., D. A. Swann, et al. Chemical modification of hyaluronic acid by carbodiimides. *Bioconjug Chem* 1991;2:232-241.

Kuroyanagi, Y., M. Kenmochi, et al. A cultured skin substitute composed of fibroblasts and keratinocytes with a collagen matrix: preliminary results of clinical trials. *Ann Plast Surg* 1993;31:340-9.

Kusama, K., W. L. Donegan, et al. An investigation of colon cancer associated with urinary diversion. *Dis Colon Rectum* 1989;32:694-7.

Kwon, Y. M., M. Baudys, et al. In situ study of insulin aggregation induced by water-organic solvent interface. *Pharm Res* 2001;18:1754-9.

Langer, R. and J. P. Vacanti. Tissue engineering. *Science* 1993;260:920-6.

Lapcik, L., Jr., L. Lapcik, et al. Hyaluronan: Preparation, Structure, Properties, and Applications. *Chem Rev* 1998;98:2663-2684.

Larsen, N. E. and E. A. Balazs. Drug delivery systems using hyaluronan and its derivatives. *Adv Drug Deliv Rev* 1991;7:279-93.

Laurent, T. C. and J. R. Fraser. Hyaluronan. *Faseb J* 1992;6:2397-404.

Laurent, T. C., K. Hellsing, et al. Crosslinked gels of hyaluronic acid. *Acta Chem Scand* 1964;18:274-5.

Leach, W. T., D. Simpson, et al. Reducing burst in protein loaded PLA microspheres through protein micronization and dispersion. (submitted).

Lee, C. H., A. Singla, et al. Biomedical applications of collagen. *Int J Pharm* 2001;221:1-22.

Lee, J. Y. and A. P. Spicer. Hyaluronan: a multifunctional, megaDalton, stealth molecule. *Curr Opin Cell Biol* 2000;12:581-6.

Lee, K. Y. and D. J. Mooney. Hydrogels for tissue engineering. *Chem Rev* 2001;101:1869-79.

Lindvall, O., P. Brundin, et al. Grafts of fetal dopamine neurons survive and improve motor function in Parkinson's disease. *Science* 1990;247:574-7.

Lowman, A. M. and N. A. Peppas. Hydrogels. In: E. Mathiowitz, Editor. *Encyclopedia of Controlled Drug Delivery*. NY: John Wiley and Sons, Inc.; 1999. p. 397-418.

Lowman, A. M. and N. A. Peppas. Solute transport analysis in pH-responsive, complexing hydrogels of poly(methacrylic acid-g-ethylene glycol). *J Biomater Sci Polym Ed* 1999;10:999-1009.

Mackinnon, S. E. and A. L. Dellon. *Surgery of the Peripheral Nerve*. New York: Thieme Medical Publishers; 1988.

Magnani, A., A. Albanese, et al. Blood-interaction performance of differently sulphated hyaluronic acids. *Thromb Res* 1996;81:383-95.

Mann, B. K. and J. L. West. Cell adhesion peptides alter smooth muscle cell adhesion, proliferation, migration, and matrix protein synthesis on modified surfaces and in polymer scaffolds. *J Biomed Mater Res* 2002;60:86-93.

Marler, J. J., A. Guha, et al. Soft-tissue augmentation with injectable alginate and syngeneic fibroblasts. *Plast Reconstr Surg* 2000;105:2049-58.

Marsano, E., S. Gagliardi, et al. Behavior of gels based on (hydroxypropyl) cellulose methacrylate. *Polymer* 2000;41:7691-7698.

Masters, K. S., S. J. Leibovich, et al. Effects of nitric oxide releasing poly(vinyl alcohol) hydrogel dressings on dermal wound healing in diabetic mice. *Wound Repair Regen* 2002;10:286-94.

Matsuda, T. and T. Magoshi. Preparation of vinylated polysaccharides and photofabrication of tubular scaffolds as potential use in tissue engineering. *Biomacromolecules* 2002;3:942-50.

Matsuda, T., M. J. Moghaddam, et al. Photoinduced prevention of tissue adhesion. *Asaio J* 1992;38:M154-7.

Mellott, M. B., K. Searcy, et al. Release of protein from highly cross-linked hydrogels of poly(ethylene glycol) diacrylate fabricated by UV polymerization. *Biomaterials* 2001;22:929-41.

Metters, A. T., K. S. Anseth, et al. Fundamental studies of biodegradable hydrogels as cartilage replacement materials. *Biomed Sci Instrum* 1999;35:33-8.

Moseley, R., M. Leaver, et al. Comparison of the antioxidant properties of HYAFF-11p75, AQUACEL and hyaluronan towards reactive oxygen species in vitro. *Biomaterials* 2002;23:2255-64.

Muzzarelli, R. A., C. Zucchini, et al. Osteoconductive properties of methylpyrrolidinone chitosan in an animal model. *Biomaterials* 1993;14:925-9.

Narasimhan, B., S. K. Mallapragada, et al. Release kinetics, data interpretation. In: E. Mathiowitz, Editor. *Encyclopedia of Controlled Drug Delivery*. New York: John Wiley & Sons; 1999. p. 921-35.

Nehls, V. and W. Hayen. Are hyaluronan receptors involved in three-dimensional cell migration? *Histol Histopathol* 2000;15:629-36.

Nerem, R. M. Cellular engineering. *Ann Biomed Eng* 1991;19:529-45.

Niklason, L. E., J. Gao, et al. Functional arteries grown in vitro. *Science* 1999;284:489-93.

Noble, P. W. Hyaluronan and its catabolic products in tissue injury and repair. *Matrix Biol* 2002;21:25-9.

Oberpenning, F., J. Meng, et al. De novo reconstitution of a functional mammalian urinary bladder by tissue engineering. *Nat Biotechnol* 1999;17:149-55.

Ogamo, A., K. Matsuzaki, et al. Preparation and properties of fluorescent glycosaminoglycuronans labeled with 5-aminofluorescein. *Carbohydrate Research* 1982;105:69-85.

Ohya, S., Y. Nakayama, et al. Thermoresponsive artificial extracellular matrix for tissue engineering: hyaluronic acid bioconjugated with poly(N-isopropylacrylamide) grafts. *Biomacromolecules* 2001;2:856-63.

Pandit, A. S., D. S. Feldman, et al. In vivo wound healing response to a modified degradable fibrin scaffold. *J Biomater Appl* 1998;12:222-36.

Park, Y. D., N. Tirelli, et al. Photopolymerized hyaluronic acid-based hydrogels and interpenetrating networks. *Biomaterials* 2003;24:893-900.

Pathak, C. P., A. S. Sawhney, et al. Rapid photopolymerization of immunoprotective gels in contact with cells and tissue. *J Am Chem Soc* 1992;114:8311-12.

Pavesio, A., D. Renier, et al. Anti-adhesive surfaces through hyaluronan coatings. *Med Device Technol* 1997;8:20-1, 24-7.

Pelham, R. J., Jr. and Y. Wang. Cell locomotion and focal adhesions are regulated by substrate flexibility. *Proc Natl Acad Sci U S A* 1997;94:13661-5.

Perez, C., I. J. Castellanos, et al. Recent trends in stabilizing protein structure upon encapsulation and release from bioerodible polymers. *J Pharm Pharmacol* 2002;54:301-13.

Perez-Rodriguez, C., N. Montano, et al. Stabilization of alpha-chymotrypsin at the CH(2)Cl(2)/water interface and upon water-in-oil-in-water encapsulation in PLGA microspheres. *J Control Release* 2003;89:71-85.

Peters, T., Jr. *All About Albumin*. San Diego: Academic Press; 1996.

Peyron, J. G. A new approach to the treatment of osteoarthritis: viscosupplementation. *Osteoarthritis Cartilage* 1993;1:85-7.

Politis, M. J., K. Ederle, et al. Tropism in nerve regeneration in vivo. Attraction of regenerating axons by diffusible factors derived from cells in distal nerve stumps of transected peripheral nerves. *Brain Res* 1982;253:1-12.

Pouyani, T. and G. D. Prestwich. Functionalized derivatives of hyaluronic acid oligosaccharides: drug carriers and novel biomaterials. *Bioconjug Chem* 1994;5:339-47.

Pozo, M. A., E. A. Balazs, et al. Reduction of sensory responses to passive movements of inflamed knee joints by hylan, a hyaluronan derivative. *Exp Brain Res* 1997;116:3-9.

Ratner, B. D. The engineering of biomaterials exhibiting recognition and specificity. *J Mol Recognit* 1996;9:617-25.

Ratner, B. D. Reducing capsular thickness and enhancing angiogenesis around implant drug release systems. *J Control Release* 2002;78:211-8.

Reinhart, C. T. and N. A. Peppas. Solute diffusion in swollen membranes. Part II. Influence of crosslinking on diffusive properties. *J Memb Sci* 1984;18:227-39.

Roden, L., P. Campbell, et al. Enzymic pathways of hyaluronan catabolism. *Ciba Found Symp* 1989;143:60-76.

Rowley, J. A., G. Madlambayan, et al. Alginate hydrogels as synthetic extracellular matrix materials. *Biomaterials* 1999;20:45-53.

Rowley, J. A. and D. J. Mooney. Alginate type and RGD density control myoblast phenotype. *J Biomed Mater Res* 2002;60:217-23.

Saffran, M., G. S. Kumar, et al. A new approach to the oral administration of insulin and other peptide drugs. *Science* 1986;233:1081-4.

Schreiber, R. E., B. M. Ilten-Kirby, et al. Repair of osteochondral defects with allogeneic tissue engineered cartilage implants. *Clin Orthop* 1999;S382-95.

Seckel, B. R., D. Jones, et al. Hyaluronic acid through a new injectable nerve guide delivery system enhances peripheral nerve regeneration in the rat. *J Neurosci Res* 1995;40:318-24.

Shin, H., S. Jo, et al. Modulation of marrow stromal osteoblast adhesion on biomimetic oligo[poly(ethylene glycol) fumarate] hydrogels modified with Arg-Gly-Asp peptides and a poly(ethyleneglycol) spacer. *J Biomed Mater Res* 2002;61:169-79.

Simon, L. D., V. J. Stella, et al. Mechanisms controlling diffusion and release of model proteins through and from partially esterified hyaluronic acid membranes. *J Control Release* 1999;61:267-79.

Skalak, R. and C. F. Fox, Eds. *Tissue Engineering*. 1988, Liss: New York.

Smeds, K. A., A. Pfister-Serres, et al. Synthesis of a novel polysaccharide hydrogel. *J Macromolec Sci Pure Appl Chem* 1999;A36:981-989.

Solchaga, L. A., J. E. Dennis, et al. Hyaluronic acid-based polymers as cell carriers for tissue-engineered repair of bone and cartilage. *J Orthop Res* 1999;17:205-13.

Soon-Shiong, P., R. E. Heintz, et al. Insulin independence in a type 1 diabetic patient after encapsulated islet transplantation. *Lancet* 1994;343:950-1.

Stading, M. and R. Langer. Mechanical shear properties of cell-polymer cartilage constructs. *Tissue Eng* 1999;5:241-50.

Starcher, B. A ninhydrin-based assay to quantitate the total protein content of tissue samples. *Anal Biochem* 2001;292:125-9.

Stocum, D. L. Regenerative biology and engineering: strategies for tissue restoration. *Wound Repair Regen* 1998;6:276-90.

Suh, J. K. and H. W. Matthew. Application of chitosan-based polysaccharide biomaterials in cartilage tissue engineering: a review. *Biomaterials* 2000;21:2589-98.

Taguchi, T., A. Kishida, et al. Apatite formation on/in hydrogel matrices using an alternate soaking process: II. Effect of swelling ratios of poly(vinyl alcohol) hydrogel matrices on apatite formation. *J Biomater Sci Polym Ed* 1999;10:331-9.

Tomer, R., D. Dimitrijevic, et al. Electrically controlled release of macromolecules from cross-linked hyaluronic acid hydrogels. *J Control Release* 1995;33:405-13.

Tomihata, K. and Y. Ikada. Crosslinking of hyaluronic acid with glutaraldehyde. *J Polym Sci A: Polym Chem* 1997;35:3553-3559.

Tomihata, K. and Y. Ikada. Crosslinking of hyaluronic acid with water-soluble carbodiimide. *J Biomed Mater Res* 1997;37:243-51.

Toole, B. P. Hyaluronan in morphogenesis. *Semin Cell Dev Biol* 2001;12:79-87.

Toole, B. P., T. N. Wight, et al. Hyaluronan-cell interactions in cancer and vascular disease. *J Biol Chem* 2002;277:4593-6.

Trudel, J. and S. P. Massia. Assessment of the cytotoxicity of photocrosslinked dextran and hyaluronan-based hydrogels to vascular smooth muscle cells. *Biomaterials* 2002;23:3299-3307.

Tung, J. S., G. E. Mark, et al. A microplate assay for hyaluronidase and hyaluronidase inhibitors. *Anal Biochem* 1994;223:149-52.

van Dijk-Wolthuis, W. N. E., J. J. Kettenes-van den Bosch, et al. Reaction of dextran with glycidyl methacrylate: an unexpected transesterification. *Macromolecules* 1997;30:3411-3413.

Vercruysse, K. P., D. M. Marecak, et al. Synthesis and in vitro degradation of new polyvalent hydrazide cross-linked hydrogels of hyaluronic acid. *Bioconjug Chem* 1997;8:686-94.

Vercruysse, K. P. and G. D. Prestwich. Hyaluronate derivatives in drug delivery. *Crit Rev Ther Drug Carrier Syst* 1998;15:513-55.

Weisser, J., B. Rahfoth, et al. Role of growth factors in rabbit articular cartilage repair by chondrocytes in agarose. *Osteoarthritis Cartilage* 2001;9:S48-54.

West, D. C. and T.-P. D. Fan. Hyaluronan oligosaccharides promote wound repair. In: T.-P. D. Fan and E. C. Kohn, Editor. *The New Angiotherapy*. Totowa, N. J.: Humana Press; 2002. p. 177-88.

West, D. C. and S. Kumar. The effect of hyaluronate and its oligosaccharides on endothelial cell proliferation and monolayer integrity. *Exp Cell Res* 1989;183:179-96.

West, J. L. Wound healing. In: C. W. Patrick Jr., A. G. Mikos and L. V. McIntire, Editor. *Frontiers in Tissue Engineering*. NY: Elsevier Science, Inc.; 1998. p. 138-51.

West, J. L. and J. A. Hubbell. Separation of the arterial wall from blood contact using hydrogel barriers reduces intimal thickening after balloon injury in the rat: the roles of medial and luminal factors in arterial healing. *Proc Natl Acad Sci U S A* 1996;93:13188-93.

Woerly, S., E. Pinet, et al. Heterogeneous PHPMA hydrogels for tissue repair and axonal regeneration in the injured spinal cord. *J Biomater Sci Polym Ed* 1998;9:681-711.

Woerly, S., E. Pinet, et al. Spinal cord repair with PHPMA hydrogel containing RGD peptides (NeuroGel). *Biomaterials* 2001;22:1095-111.

Xu, S., J. Yamanaka, et al. Characteristics of complexes composed of sodium hyaluronate and bovine serum albumin. *Chem Pharm Bull (Tokyo)* 2000;48:779-83.

Yagi, K., N. Michibayashi, et al. Effectiveness of fructose-modified chitosan as a scaffold for hepatocyte attachment. *Biol Pharm Bull* 1997;20:1290-4.

Yu, Z., A. S. Garcia, et al. Spray freezing into liquid for highly stable protein nanostuctured microparticles. (submitted).

Yu, Z., T. L. Rogers, et al. Preparation and characterization of microparticles containing peptide produced by a novel process: spray freezing into liquid. *Eur J Pharm Biopharm* 2002;54:221-8.

Yui, N., T. Okano, et al. Inflammation responsive degradation of crosslinked hyaluronic acid gels. *J Control Release* 1992;22:105-16.

Zhao, X. B., J. E. Fraser, et al. Synthesis and characterization of a novel double crosslinked hyaluronan hydrogel. *J Mater Sci Mater Med* 2002;13:11-6.

Zhu, G. and S. P. Schwendeman. Stabilization of proteins encapsulated in cylindrical poly(lactide-co-glycolide) implants: mechanism of stabilization by basic additives. *Pharm Res* 2000;17:351-7.

Vita

Jennie Melinda Baier was born to Kathleen Grieshop Baier and Kenneth Edwin Baier in Cincinnati, Ohio on May 30, 1975. She received her high school education from Oldenburg Academy in Oldenburg, Indiana. From 1993-1998, Jennie attended Rensselaer Polytechnic Institute in Troy, New York, where she obtained a Bachelor's of Science degree in Chemical Engineering with a minor in Biology. Her interest in research began while she was as an undergraduate research assistant with Drs. Georges Belfort and Todd Przybycien. She completed a two-semester co-op and a summer internship at W.L. Gore & Associates, in Elkton, Maryland. Jennie also swam with the Rensselaer Varsity Swimming Team, where she was a captain for two years, and an assistant coach for one year.

For her doctoral studies in Chemical Engineering, Jennie attended The University of Texas at Austin (UT) in Austin, Texas (1998-2003). During this time, she completed an internship at Sulzer Biologics in Austin, Texas, where worked with Drs. Rama Akella and C.P. Pathak. Jennie presented work at the 2001 and 2002 annual meetings of the American Institute for Chemical Engineers and the Biomedical Engineering Society. She wrote five first-author publications and was a contributor to four other articles. While in Austin, Jennie also met and married a fellow UT PhD chemical engineer, Tom Leach.

Permanent address: 3660 Hanley Road; Cincinnati, Ohio 45247

This dissertation was typed by the author.